

Universiteit
Leiden
The Netherlands

Nanosized blood microparticles

Yuana, Y.

Citation
Yuana, Y. (2011, October 27). *Nanosized blood microparticles*. Retrieved from https://hdl.handle.net/1887/17987

Version:	Corrected Publisher's Version
License:	Licence agreement concerning inclusion of doctoral thesis in the Institutional Repository of the University of Leiden
Downloaded from:	https://hdl.handle.net/1887/17987

Note: To cite this publication please use the final published version (if applicable).

NANOSIZED BLOOD MICROPARTICLES

Yuana

NANOSIZED BLOOD MICROPARTICLES

PROEFSCHRIFT

ter verkrijging van
de graad van Doctor aan de Universiteit Leiden,
op gezag van de Rector Magnificus prof. mr. P.F. van der Heijden,
volgens besluit van het College voor Promoties
te verdedigen op donderdag 27 oktober 2011
klokke 11:15 uur

door

Yuana

geboren te Jakarta, Indonesië
in 1976

Promotiecommissie

Promotores:	Prof. dr. S. Osanto Prof. dr. R.M. Bertina
Overige leden:	Prof. dr. H.J. Tanke Prof. dr. A.F. Cohen Dr. P. Harrison (Oxford Haemophilia and Thrombosis Centre, Churchill Hospital, Oxford, United Kingdom)

The research presented in this thesis was performed in the Department of Clinical Oncology and Einthoven Laboratory of the Leiden University Medical Center, The Netherlands.

The studies published in this thesis were supported by a grant of the Dutch Cancer Society (KWF UL 2006-3618).

Financial support for the printing of this thesis was obtained from the Department of Clinical Oncology of the Leiden University Medical Centre and from Beckman Coulter Nederland B.V.

Cover photo and design: Beach on Terschelling by Yuana and M.J.W. Dignum

Printed by: Uitgeverij BOXPress, Oisterwijk

© 2011, Yuana
ISBN: 978-90-8891-325-9

Rejoice in the Lord always. I will say it again: Rejoice!
(Philippians 4:4)

In memoriam of

Tiromsa Sinaga (1976-2006)
Lidyawati (1956-2007)

Table of contents

		Page
Chapter 1	General Introduction	7
Chapter 2	Pre-analytical and analytical issues in the analysis of blood microparticles	19
Chapter 3	Atomic Force Microscopy: A novel approach to detect nanosized blood microparticles	49
Chapter 4	The detection of tissue factor bearing-microparticles by atomic force microscopy	69
Chapter 5	Determination of the size distribution of blood microparticles directly in plasma using atomic force microscopy and microfluidics	81
Chapter 6	Cryo-electron microscopy of submicron particles in plasma	101
Chapter 7	Use of immuno-magnetic beads for direct capture of nanosized blood microparticles from plasma	121
Chapter 8	Microparticle-associated tissue factor activity and venous thrombosis in multiple myeloma	139
Chapter 9	Summary and General Discussion	155
Nederlandse samenvatting		167
Curriculum vitae		177
List of publications		179
Acknowledgments		181

CHAPTER 1

General Introduction

Yuana Yuana

Background

The association between cancer and venous thromboembolism (VTE) is bidirectional. Starting with the observations of Bouillaud (1) and Trousseau (2), it was discovered that cancer patients are more prone to develop thrombosis, whereas thrombosis may be the harbinger of the presence of cancer. Epidemiological studies by Sorensen (3) and Blom (4) indicated that the incidence of cancer is increased among patients diagnosed with acute VTE. About 10% of patients with an episode of idiopathic VTE will develop cancer within a few years after the diagnosis (5;6). Cancer patients who developed thrombosis also have a poor survival compared to those who did not develop thrombosis (7).

Microparticles

Microparticles (MPs) are nanosized membrane vesicles, also named microvesicles, which are formed by budding of cell membranes upon activation or apoptosis and released into body fluids, such as blood, urine and synovial fluid. In the past, they have been considered to be inert cell debris (“platelet dust”) (8).

MPs still bear antigens derived from their parental cells. By using specific antibodies it was shown that the majority of MPs detected in blood originates from platelets (9;10). Other blood cells such as leucocytes, erythrocytes, endothelial cells and also malignant cells all may shed MPs (11). MPs have been shown to contain DNA, RNA, and recently also miRNA (12;13).

Most MPs expose the negatively charged phosphatidylserine (PS) on their membrane surface as a result of plasma membrane remodeling during formation from their parental cells (11;14;15). The exposure of PS on MPs provides a catalytic surface which promotes the assembly of procoagulant proteins and stimulates coagulation reactions (16;17). The PS content of MPs may vary according to their cellular origin, the mechanism by which they have been formed, and several pre-analytical conditions (18;19).

The presence of MPs in the blood of healthy persons is well documented, and elevated numbers of specific subsets of MPs have been reported in vascular disorders, cancer, and auto-immune diseases (11;16;20). In recent years, there has been a growing interest to study the role of MPs in physiology and pathology. However, individual studies use a wide variation of pre-analytical and analytical procedures, which all may affect the outcome of the MP measurement (21;22).

Procoagulant microparticles in cancer-associated thrombosis

Several studies have been conducted to identify the mechanism underlying the association between cancer and thrombosis (23-25). In various studies, an association between (active) tissue factor (TF)-bearing MPs and thrombosis in cancer patients has been found. This suggests that perhaps the release of MPs bearing TF by tumor cells and host cells into the blood may trigger thrombosis (9;26-28). TF has a major role in the initiation of blood coagulation. TF is found predominantly in the adventitial and much less in the medial layers surrounding blood vessels. Fibroblasts, adipocytes, and pericytes have also been shown to constitutively express TF. Normally, TF is not expressed by cells within the vasculature. However, after *in vitro* or *in vivo* stimulation by various agonists smooth muscle cells, endothelial cells, and peripheral blood mononuclear cells (monocytes and neutrophils) can express TF. TF binds to coagulation factor VII/VIIa (fVII/VIIa) to form a bimolecular complex that functions as the primary initiator of blood coagulation *in vivo*. In the presence of calcium ions (Ca^{2+}) and negatively charged phospholipids (PL), the TF/fVIIa complex activates fX into fXa which subsequently leads to the formation of thrombin and insoluble fibrin. Thrombin also activates platelets which together with fibrin form a stable clot (29).

One of the processes of tumor metastasis is the invasion of tumour cells through the vessel wall into the blood. This invasion of tumour cells causes vascular damage which triggers the expression of TF on cells within the vasculature leading to exposure of TF to the blood (30). The presence of a tumour may also elicit a host response that leads to induction of TF expression in monocytes and possibly endothelial cells and to the shedding of MPs bearing TF (31). In addition, some tumour cells express TF themselves (32) and these cells may shed MPs bearing TF (33;34). Figure 1 illustrates this hypothetical explanation of the role of MPs bearing TF in cancer-associated thrombosis.

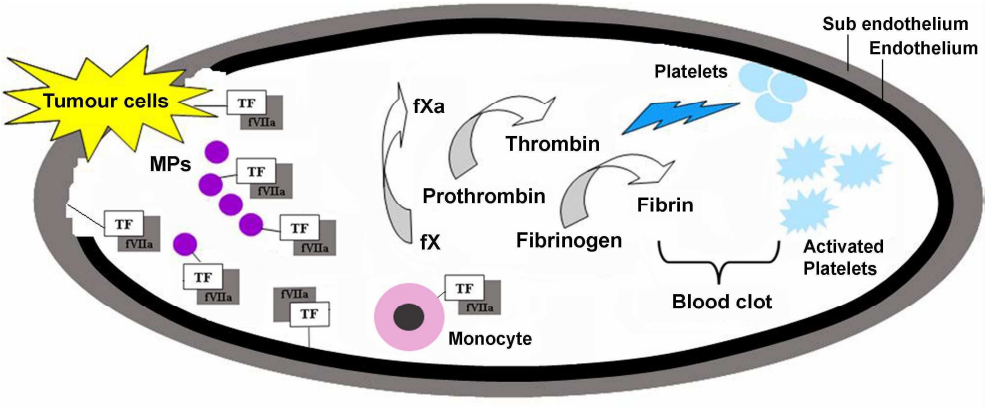


Figure 1. Hypothesis of the role of MPs bearing TF in cancer-associated thrombosis

Not all TF antigen is able to initiate the coagulation process (35;36). TF with reduced procoagulant activity has been referred to as encrypted. To date, little is known about the encryption status of cell- or MP-bound TF *in vivo*. Interestingly, in the cohorts studied by Tesselaar et al (9), cancer patients with elevated MP-associated TF activity and poor prognosis also had a small fraction of MUC-1-positive MP in their pool of blood MP suggesting tumour MPs bearing active TF as a link between cancer and thrombosis. In addition to its procoagulant activity, TF has cell signaling properties. Formation of the TF/fVIIa complex may activate signal transduction pathways via de proteolytic cleavage of protein-activated receptor 2 (PAR2) promoting tumor growth and tumor angiogenesis (31;37).

Measurement of microparticles

The choice of anticoagulant used for blood collection, the centrifugation speeds used for the preparation of plasma and the isolation of MPs, and the storage of blood and plasma samples are important pre-analytical variables which all may affect the outcome of MP measurements. Blood can be collected in sodium citrate, ethylenediaminetetraacetic acid (EDTA), and citrate theophylline adenosine dipyridamole (CTAD) anticoagulants, but more information is needed on the relative stability of MPs in these anticoagulants (38). After blood withdrawal, blood should be immediately centrifuged to isolate plasma (39). The centrifugation speed applied should remove platelets from plasma to avoid cellular activation of platelets leading to inadvertent production of platelet MPs (PMPs). A direct measurement of MPs in fresh plasma is preferred to reduce MP loss and to preserve MP characteristics (21). When frozen-thawed plasma is used, especially PMP and annexin V-positive MP counts should be interpreted with caution (39-41). For certain MP assays (e.g. fluorescence or electron microscopy, proteomic analysis and some functional MP assays), MPs are isolated from plasma to reduce the plasma protein content and to increase the MP concentration. Nevertheless, isolation procedures include multiple washing steps and will inevitably cause loss of some MPs. Most importantly, it is not known which centrifugation force is optimal to pellet plasma MPs (42).

Different analytical methods and combinations of these have been used to measure the number, concentration, and functional properties of MPs. Flow cytometry, capture-based assays, and functional assays are commonly used methods to measure MPs.

Since flow cytometry uses laser light which typically excites at a wavelength of 488 nm and MPs vary in size below 1 µm in diameter, using flow cytometry the enumeration of MPs with a size of less than 0.5 µm is inaccurate (43;44). To

standardize PMP measurements by flow cytomety in multi-centre studies, the ISTH SSC Working Group on Vascular Biology proposed the use of calibrated beads with sizes of 0.5, 0.9 and 3 µm (Megamix beads) to adjust the instrument settings and increase the resolution of the flow cytometer (45). Recently, a new generation of flow cytometers has been developed (e.g. Gallios from Beckman Coulter, Influx from Becton Dickinson, and Apogee A50 from Apogee Flow System) which seem to have improved scatter performances in terms of resolution and background as they can detect and resolve beads with sizes between 0.3 and 0.5 µm (46). However, plastic beads remain an imperfect model for size calibration of MPs. The scattering intensity of MPs depends on the characteristics of MPs such as shape, refractive index, and absorption which are different from those of the calibration beads (44).

Flow cytometry allows fast enumeration of total MPs by using annexin V. This method is based on the assumption that all blood MPs carry PS on their membrane. However, not all MPs expose PS. For example, in vitro stimulation of endothelial cells by TNF-α generated MPs with low PS exposure (47), platelets treated with thrombin receptor-activating peptide (TRAP) generated both PS-positive and -negative MPs (48), and a human monocytic cell line (THP-1) stimulated with soluble P-selectin-Ig chimera (P-sel-Ig) generated more PS-negative MPs (~60%) than PS-positive MPs (49). Furthermore, the binding of annexin V to MPs is influenced by the calcium concentration and the membrane PS content (50). Therefore, the use of other fluorescent dyes or proteins (e.g. calcein AM, lactadherin, SYTO13) might increase the accuracy of enumeration of total MPs (46).

Specific antibodies conjugated with different fluorochromes are used in flow cytometry measurements to identify and accurately count subsets of MPs. A list of antibodies to distinguish MPs derived from platelets, leucocytes, erythrocytes, and endothelial cells can be found in the publication of the Forum “Measuring circulating cell derived microparticles” (21) and some recent reviews (11;22). Additionally, MPs derived from malignant cells have been detected by the use of antibodies such as MUC1 for breast and pancreatic cancer cells (9;25), FasL for melanoma cells (51), EGFRvIII for glioblastoma cells (52), and CXCR-4 for leukemic cells (53).

Recently, quantum dots, nanocrystals of inorganic semiconductors with a diameter of 2–8 nm (200–10000 atoms), have opened new possibilities for antibody labelling (54;55). Quantum dots have significant advantages over common fluorochromes (for example, fluoroscein, phycoerythrin or allophycocyanin), such as brighter fluorescence and resistance to photobleaching (54). Additionally, quantum dots

have relatively narrow emission spectra giving less spectral overlap in standard multicolor immunophenotyping by flow cytometry (55). In the near future, the use of quantum dots-labeled specific antibodies may improve the sensitivity of flow cytometry detection of MP subsets (44).

Capture-based assays for MP measurement rely on an antibody or annexin V which specifically binds a subset of MPs from plasma. Captured MPs can then be quantified/characterized by using a second probe (e.g., peroxidase conjugated-antibody) (56) or by the measurement of the concentration of negatively charged phospholipids supporting prothrombinase activity (57;58). These capture-based assays enable a high-throughput measurement of subsets of MPs but do not provide direct enumeration of total MPs in plasma. Other disadvantages are interference by soluble antigens and lack of information on the size distribution of MPs (59).

The measurement of functional properties of plasma MP is limited at the moment to the measurement of MP-associated TF activity. Such assays are based on the fVII-dependent fXa generation in isolated MPs (9;27). The TF activity of MP (MP-TF activity) is defined as the fVII dependent and anti-TF sensitive formation of fXa. The assay provides information on MPs bearing active TF. A commercial two-stage chromogenic assay (Actichrome® TF from American Diagnostica) has also been used to measure TF activity in plasma (58;60). However, the observed fXa generation was found to be independent of exogenously added fVIIa and/or TF, and not inhibited by anti-fVIIa (61). Although the measurement of MP-associated TF activity provides information on MPs bearing active TF, it still fails to identify the cellular origin(s) of these MPs.

Aims of this thesis

MPs have important physiological and pathological roles in blood coagulation, inflammation and tumor progression (11;16). In recent years MPs also have been recognized to participate in important biological processes (15), such as in signaling and in the horizontal transfer of their membrane and/or cargo molecules, which are enriched in specific proteins and mRNAs. However, studies of MPs have been hampered by the lack of methods for the sensitive detection and accurate quantification of MPs. Furthermore, there is no method available to asses the origin of MPs bearing active TF in plasma. Thus, one of the aims in this thesis was to develop a new methodology for the sensitive detection and accurate quantification of MPs (MP subsets). Preferentially, such a method would also allow the determination of the size distribution of these MPs in their native state. In addition, efforts have been made to develop a method for analyzing subsets of MPs bearing

active TF. Finally, TF activity was measured in MPs isolated from plasma of multiple myeloma patients and its possible association with the development of VTE was investigated.

Outline of this thesis

Chapter 2 is a literature based review of pre-analytical and analytical issues in the analysis of blood microparticles. This review discusses pre-analytical variables related to plasma and MP preparation which may affect the outcome of MP measurements. In addition, several analytical issues in commonly used MP assays and some novel approaches for the detection and characterization of MPs are briefly discussed.

In Chapter 3 atomic force microscopy (AFM) is proposed as a new methodology for MP measurement. The use of AFM operated in fluid tapping mode is compared with the widely used conventional flow cytometry to quantify the number of CD41-positive MPs isolated from fresh plasma and to determine their size distribution. Finally, it was investigated whether this new methodology also can be used to detect MPs bearing TF antigen (Chapter 4).

To prevent loss of MPs during the isolation procedure, it would be preferable to use blood plasma directly for the MP measurements. Therefore, the use of microfluidics in combination with AFM was explored for the direct detection, quantification, and size determination of CD41-positive MPs in plasma. Results of this study are reported in Chapter 5.

Although conventional transmission electron microscopy (TEM) has been used in the past to study the morphology and membrane composition of MPs, this method requires steps such as dehydration, chemical fixation, and staining of specimens which all may affect MP morphology. This method is also not suitable for direct detection of MPs in plasma. For that reason, the use of cryo-TEM for visualization of submicron particles (MPs and exosomes) directly in plasma was studied. Chapter 6 deals with the results of cryo-TEM imaging of platelet-rich, platelet-poor, and platelet-free plasma isolated from citrate and EDTA anticoagulated-blood. Results are compared with images of submicron particles isolated from plasma and in the supernatant of thrombin activated-isolated platelets.

Up till now the cellular origin of MPs bearing active TF in blood is unknown. Chapter 7 presents the development of an immuno-magnetic beads method to directly capture/deplete selected subsets of MPs from plasma. By using biotinylated antibody and streptavidin coated magnetic beads, CD41- and CD14-

positive MPs were captured from plasma. Fractions containing captured and depleted CD41-/CD14-positive MPs were analysed for MP-associated TF activity.

Multiple myeloma (MM) is one of the malignancies associated with an increased risk of VTE complications. Chapter 8 reports the results of MP-TF activity measurements in patients with newly diagnosed MM before and after chemotherapy and discusses whether MP-TF activity levels found in these patients are associated with VTE.

All results presented in this thesis are summarized and discussed in Chapter 9.

References

(1) Bouillaud. De l'Obliteration des veines et de son influence sur la formation des hydropisies partielles: consideration sur la hydropisies passive et general. Arch Intern Med 1823;1 :188-204.

(2) Trousseau A. Phlegmasia alba dolens. Clinique medicale de l' Hôtel-dieu de Paris. London: JB Ballière et Fils ; 1865 ; tome troisieme:654-712.

(3) Sorensen HT, Mellemkjaer L, Steffensen FH, Olsen JH, Nielsen GL. The risk of a diagnosis of cancer after primary deep venous thrombosis or pulmonary embolism. N Engl J Med 1998;338:1169-1173.

(4) Blom JW, Doggen CJ, Osanto S, Rosendaal FR. Malignancies, prothrombotic mutations, and the risk of venous thrombosis. JAMA 2005;293:715-722.

(5) Prandoni P, Lensing AW, Buller HR, Cogo A, Prins MH, Cattelan AM, et al. Deep-vein thrombosis and the incidence of subsequent symptomatic cancer. N Engl J Med 1992;327:1128-1133.

(6) Murchison JT, Wylie L, Stockton DL. Excess risk of cancer in patients with primary venous thromboembolism: a national, population-based cohort study. Br J Cancer 2004;91:92-95.

(7) Sorensen HT, Mellemkjaer L, Olsen JH, Baron JA. Prognosis of cancers associated with venous thromboembolism. N Engl J Med 2000;343:1846-1850.

(8) Wolf P. The nature and significance of platelet products in human plasma. Br J Haematol 1967;13:269-288.

(9) Tesselaar ME, Romijn FP, van der Linden IK, Prins FA, Bertina RM, Osanto S. Microparticle-associated tissue factor activity: a link between cancer and thrombosis? J Thromb Haemost 2007;5:520-527.

(10) Nieuwland R, Berckmans RJ, Rotteveel-Eijkman RC, Maquelin KN, Roozendaal KJ, Jansen PG, et al. Cell-derived microparticles generated in patients during cardiopulmonary bypass are highly procoagulant. Circulation 1997;96:3534-3541.

(11) Burnier L, Fontana P, Kwak BR, Angelillo-Scherrer A. Cell-derived microparticles in haemostasis and vascular medicine. Thromb Haemost 2009;101:439-451.

(12) Hunter MP, Ismail N, Zhang X, Aguda BD, Lee EJ, Yu L, et al. Detection of microRNA expression in human peripheral blood microvesicles. PLoS ONE 2008;3:1-11.

(13) Chen TS, Lai RC, Lee MM, Choo AB, Lee CN, Lim SK. Mesenchymal stem cell secretes microparticles enriched in pre-microRNAs. Nucleic Acids Res 2010;38:215-224.

(14) Zwaal RF, Comfurius P, Bevers EM. Surface exposure of phosphatidylserine in pathological cells. Cell Mol Life Sci 2005;62:971-988.

(15) Cocucci E, Racchetti G, Meldolesi J. Shedding microvesicles: artefacts no more. Trends Cell Biol 2009;19:43-51.

(16) Piccin A, Murphy WG, Smith OP. Circulating microparticles: pathophysiology and clinical implications. Blood Rev 2007;21:157-171.
(17) Castellana D, Kunzelmann C, Freyssinet JM. Pathophysiologic significance of procoagulant microvesicles in cancer disease and progression. Hamostaseologie 2009;29:51-57.
(18) Morel O, Jesel L, Freyssinet JM, Toti F. Cellular mechanisms underlying the formation of circulating microparticles. Arterioscler Thromb Vasc Biol 2011;31:15-26.
(19) Yuana Y, Bertina RM, Osanto S. Pre-analytical and analytical issues in the analysis of blood microparticles. Thromb Haemost 2010;105:396-408.
(20) Anderson HC, Mulhall D, Garimella R. Role of extracellular membrane vesicles in the pathogenesis of various diseases, including cancer, renal diseases, atherosclerosis, and arthritis. Lab Invest 2010;90:1549-1557.
(21) Jy W, Horstman LL, Jimenez JJ, Ahn YS, Biro E, Nieuwland R, et al. Measuring circulating cell-derived microparticles. J Thromb Haemost 2004;2:1842-1843.
(22) Enjeti AK, Lincz LF, Seldon M. Detection and measurement of microparticles: an evolving research tool for vascular biology. Semin Thromb Hemost 2007;33:771-779.
(23) Furie B, Furie BC. Mechanisms of thrombus formation. N Engl J Med 2008;359:938-949.
(24) Sousou T, Khorana AA. New insights into cancer-associated thrombosis. Arterioscler Thromb Vasc Biol 2009;29:316-320.
(25) Zwicker JI, Liebman HA, Neuberg D, Lacroix R, Bauer KA, Furie BC, et al. Tumor-derived tissue factor-bearing microparticles are associated with venous thromboembolic events in malignancy. Clin Cancer Res 2009;15:6830-6840.
(26) Tesselaar ME, Romijn FP, van dL, I, Bertina RM, Osanto S. Microparticle-associated tissue factor activity in cancer patients with and without thrombosis. J Thromb Haemost 2009;7:1421-1423.
(27) Manly DA, Wang J, Glover SL, Kasthuri R, Liebman HA, Key NS, et al. Increased microparticle tissue factor activity in cancer patients with Venous Thromboembolism. Thromb Res 2010;125:511-512.
(28) Tilley RE, Holscher T, Belani R, Nieva J, Mackman N. Tissue factor activity is increased in a combined platelet and microparticle sample from cancer patients. Thromb Res 2008;122:604-609.
(29) Bertina RM. The role of procoagulants and anticoagulants in the development of venous thromboembolism. Thromb Res 2009;123 Suppl 4:S41-S45.
(30) Drake TA, Morrissey JH, Edgington TS. Selective cellular expression of tissue factor in human tissues. Implications for disorders of hemostasis and thrombosis. Am J Pathol 1989;134:1087-1097.
(31) Kasthuri RS, Taubman MB, Mackman N. Role of tissue factor in cancer. J Clin Oncol 2009;27:4834-4838.
(32) Rickles FR, Patierno S, Fernandez PM. Tissue factor, thrombin, and cancer. Chest 2003;124:58S-68S.
(33) Thomas GM, Panicot-Dubois L, Lacroix R, gnat-George F, Lombardo D, Dubois C. Cancer cell-derived microparticles bearing P-selectin glycoprotein ligand 1 accelerate thrombus formation in vivo. J Exp Med 2009;206:1913-1927.
(34) Dvorak HF, Van DL, Bitzer AM, Dvorak AM, Anderson D, Harvey VS, et al. Procoagulant activity associated with plasma membrane vesicles shed by cultured tumor cells. Cancer Res 1983;43:4434-4442.
(35) Bach RR. Tissue factor encryption. Arterioscler Thromb Vasc Biol 2006;26:456-461.
(36) Versteeg HH, Ruf W. Tissue factor coagulant function is enhanced by protein-disulfide isomerase independent of oxidoreductase activity. J Biol Chem 2007;282:25416-25424.
(37) Versteeg HH, Schaffner F, Kerver M, Petersen HH, Ahamed J, Felding-Habermann B, et al. Inhibition of tissue factor signaling suppresses tumor growth. Blood 2008;111:190-199.

(38) Shah MD, Bergeron AL, Dong JF, Lopez JA. Flow cytometric measurement of microparticles: pitfalls and protocol modifications. Platelets 2008;19:365-372.

(39) Ayers L, Kohler M, Harrison P, Sargent I, Dragovic R, Schaap M, et al. Measurement of circulating cell-derived microparticles by flow cytometry: Sources of variability within the assay. Thromb Res 2011;127:370-377.

(40) Weber H, Kollars M, Kyrle PA, Weltermann A. Comparison of different methods for isolation and storage of microparticles from human blood. J Thromb Haemost 5[supplement 2]. 2007;5(suppl 2):P-M-445.

(41) Mobarrez F, Antovic J, Egberg N, Hansson M, Jorneskog G, Hultenby K, et al. A multicolor flow cytometric assay for measurement of platelet-derived microparticles. Thromb Res 2010;125:e110-e116.

(42) Shet AS. Characterizing blood microparticles: technical aspects and challenges. Vasc Health Risk Manag 2008;4:769-774.

(43) Furie B, Furie BC. Cancer-associated thrombosis. Blood Cells Mol Dis 2006;36:177-181.

(44) Van Der Pol E, Hoekstra AG, Sturk A, Otto C, Van Leeuwen TG, Nieuwland R. Optical and non-optical methods for detection and characterization of microparticles and exosomes. J Thromb Haemost 2010;8:2596-2607.

(45) Lacroix R, Robert S, Poncelet P, Kasthuri RS, Key NS, Dignat-George F. Standardization of platelet-derived microparticle enumeration by flow cytometry using calibrated beads: results of ISTH SSC collaborative workshop. J Thromb Haemost 2010;8:2571-2574.

(46) Lacroix R, Robert S, Poncelet P, Dignat-George F. Overcoming limitations of microparticle measurement by flow cytometry. Semin Thromb Hemost 2010;36:807-818.

(47) Jimenez JJ, Jy W, Mauro LM, Soderland C, Horstman LL, Ahn YS. Endothelial cells release phenotypically and quantitatively distinct microparticles in activation and apoptosis. Thromb Res 2003;109:175-180.

(48) Perez-Pujol S, Marker PH, Key NS. Platelet microparticles are heterogeneous and highly dependent on the activation mechanism: studies using a new digital flow cytometer. Cytometry A 2007;71:38-45.

(49) Bernimoulin M, Waters EK, Foy M, Steele BM, Sullivan M, Falet H, et al. Differential stimulation of monocytic cells results in distinct populations of microparticles. J Thromb Haemost 2009;7:1019-1028.

(50) Connor DE, Exner T, Ma DD, Joseph JE. The majority of circulating platelet-derived microparticles fail to bind annexin V, lack phospholipid-dependent procoagulant activity and demonstrate greater expression of glycoprotein Ib. Thromb Haemost 2010;103:1044-1052.

(51) Andreola G, Rivoltini L, Castelli C, Huber V, Perego P, Deho P, et al. Induction of lymphocyte apoptosis by tumor cell secretion of FasL-bearing microvesicles. J Exp Med 2002;195:1303-1316.

(52) Al Nedawi K, Meehan B, Micallef J, Lhotak V, May L, Guha A, et al. Intercellular transfer of the oncogenic receptor EGFRvIII by microvesicles derived from tumour cells. Nat Cell Biol 2008;10:619-624.

(53) Kalinkovich A, Tavor S, Avigdor A, Kahn J, Brill A, Petit I, et al. Functional CXCR4-expressing microparticles and SDF-1 correlate with circulating acute myelogenous leukemia cells. Cancer Res 2006;66:11013-11020.

(54) Ibanez-Peral R, Bergquist PL, Walter MR, Gibbs M, Goldys EM, Ferrari B. Potential use of quantum dots in flow cytometry. Int J Mol Sci 2008;9:2622-2638.

(55) Chattopadhyay PK, Price DA, Harper TF, Betts MR, Yu J, Gostick E, et al. Quantum dot semiconductor nanocrystals for immunophenotyping by polychromatic flow cytometry. Nat Med 2006;12:972-977.

(56) Nomura S, Shouzu A, Taomoto K, Togane Y, Goto S, Ozaki Y, et al. Assessment of an ELISA kit for platelet-derived microparticles by joint research at many institutes in Japan. J Atheroscler Thromb 2009;16:878-887.

(57) Aupeix K, Hugel B, Martin T, Bischoff P, Lill H, Pasquali JL, et al. The significance of shed membrane particles during programmed cell death in vitro, and in vivo, in HIV-1 infection. J Clin Invest 1997;99:1546-1554.

(58) Steppich BA, Braun SL, Stein A, Demetz G, Groha P, Schomig A, et al. Plasma TF activity predicts cardiovascular mortality in patients with acute myocardial infarction. Thromb J 2009;7:1-9.

(59) Horstman LL, Jy W, Jimenez JJ, Bidot C, Ahn YS. New horizons in the analysis of circulating cell-derived microparticles. Keio J Med 2004;53:210-230.

(60) Funderburg NT, Mayne E, Sieg SF, Asaad R, Jiang W, Kalinowska M, et al. Increased tissue factor expression on circulating monocytes in chronic HIV infection: relationship to in vivo coagulation and immune activation. Blood 2010;115:161-167.

(61) Bogdanov VY, Cimmino G, Tardos JG, Tunstead JR, Badimon JJ. Assessment of plasma tissue factor activity in patients presenting with coronary artery disease: limitations of a commercial assay. J Thromb Haemost 2009;7:894-897.

CHAPTER 2

Pre-analytical and analytical issues in the analysis of blood microparticles

Yuana Yuana, Rogier M. Bertina and Susanne Osanto

Thrombosis Haemostasis 2010 Dec 21;105(3):396-408

Abstract

Results of plasma microparticles (MPs) measurements reported in the literature vary widely. This is clearly not only related to the lack of well-standardized MP assays, but also to variations in pre-analytical conditions. In this review we will discuss the pre-analytical variables related to plasma and MP preparation which may affect MP analysis. Additionally we will address several analytical issues in commonly used MP assays and briefly discuss some novel approaches for the detection and characterization of MPs.

Ideally MP measurements should be performed in plasma, freshly prepared directly after blood withdrawal. As platelet contamination seems to be one of the major pre-analytical problems in processing plasma for MP measurement, the use of platelet-free plasma may be preferred. When frozen-thawed plasma is used, especially PMP and annexinV-positive MP counts should be interpreted with caution.

When flow cytometry is chosen as a method for quantification of MPs, some analytical conditions should be standardized, e.g. settings of the flow cytometer, quality of the antibodies, and use of counting beads. Fluorescence-nanoparticle tracking analysis and atomic force microscopy can accurately count nanosized MPs, but unfortunately the operational procedures of both methods are still time consuming and they give no information on the functional properties of MPs. The MP-TF activity assay provides information on MPs carrying active TF, regardless of their parental origin.

Ultimately, standardisation of pre-analytical procedures and the introduction of reliable and rapid methods for the measurement of MPs are urgently needed to facilitate their use as biomarker in the pathophysiology of diseases.

Introduction

Since Wolf in 1967 (1) showed that platelet shedding results in the formation of 'platelet-dust', the shedding of microparticles (MPs) in blood has been recognized as a regulated process during cell activation and early apoptosis (2;3). MPs formed by membrane vesiculation of cells are generally heterogeneous in size (<1 µm). They differ from exosomes with respect to their origin, protein content, and size distribution. Exosomes originate from multivesicular bodies and are usually more homogeneous and smaller in size (<0.1 µm) (4-7). However, there is no consensus on the precise cut off in the size distributions of these two populations. This is not only due to limitations of the methods used for the characterization of these nanoparticles, but also by pre-analytical variables like anticoagulant, centrifugation, and storage.

The large majority of MPs detected in blood originates from platelets, but other blood cells such as leucocytes, erythrocytes, endothelial cells and even malignant cells also may shed MPs. These MPs still bear antigens of their parental cells so that their origin can be determined by using specific antibodies against these antigens (4;8). Furthermore, blood MPs may carry the negatively charged phosphatidylserine (PS) on their surface as a result of plasma membrane remodeling during their formation from their parental cells (2;4;5). The exposure of PS on MPs provides a catalytic surface which promotes the assembly of procoagulant proteins and stimulates coagulation reactions (2;9-11). The PS content of MPs may vary according to their cellular origin, the mechanism by which they have been formed and several pre-analytical conditions (9-14).

The presence of MPs in the blood of healthy persons is well documented and elevated numbers of specific subsets of MPs have been reported in vascular disorders, cancer, and auto-immune diseases. Therefore, there is a growing interest to study the role of MPs in physiology and pathology (for recent reviews see (4;9;12-16)). However, individual studies use a wide variation of pre-analytical and analytical procedures, which all may affect the outcome of the MP measurement (17) (Table 1). Therefore, the Vascular Biology group of the Scientific and Standardization Committee (SSC) of the International Society on Thrombosis and Haemostasis (ISTH) decided during their meeting in 2003, to address issues related to the detection, measurement, function, and clinical significance of membrane MPs derived from blood and vascular cells.

At present, standardization of pre-analytical and analytical methods for the measurement of MPs remains a challenge. In this review we will discuss the pre-analytical variables related to plasma and MP preparation which may affect the

characterization and enumeration of MPs. In addition we will address several analytical issues in commonly used MP assays and briefly discuss some novel approaches for the detection and characterization of MPs. Finally, we will make some general recommendations on pre-analytical and analytical conditions in MP assays.

Pre-analytical conditions

Blood collection

Needles ranging from 19 to 22 Gauge (G) are commonly used for venepuncture in haemostasis laboratories (18). Prolonged placement of a tourniquet is avoided during venepuncture (19). Theoretically, when a small-diameter needle (high G number) is connected to an evacuated tube, the vacuum force applied to the blood is large. Such shear stress and excessive pressure on the vein during blood withdrawal might cause *in vitro* haemolysis (20) and possibly formation of erythrocyte MPs (ErMPs) (21). A system using a small-diameter butterfly needle is commonly used on small children and patients with difficult venous access (22). This system reduces the blood flow and consequently increases the risk of platelet activation (18). During blood collection, the first 3-7.5 mL of blood is discarded to avoid the effects of the vascular damage caused by the venepuncture (23;24).

Several anticoagulants are used to collect blood for MP analysis (Table 1). It is important to consider how these anticoagulants may help to limit platelet activation during blood collection and plasma preparation, because platelet activation will result in release of alpha and dense granules and platelet MPs (PMPs) (25-27). Sodium citrate with a concentration of 0.105 or 0.129 mol/L (3.2% or 3.8%) is the most widely used anticoagulant (8). Other anticoagulants that have been used are Acid-Citrate-Dextrose (ACD) (28-30), ethylenediaminetetraacetic acid (EDTA) (8;31-33), a strong chelator of calcium ions, and heparin (34-36), which will preserve extracellular calcium. However, blood collected in heparin gave significantly higher levels of annexin V-positive MPs than blood collected in sodium citrate (37). Connor et al (38) reported that the number of annexin V-positive MP and the concentration of procoagulant phospholipid increased more strongly over a 60 min period following blood collection in sodium citrate-anticoagulated samples than in EDTA-anticoagulated samples. They suggested that when blood is not immediately processed, MP measurement should be performed on EDTA-anticoagulated samples. Use of citrate theophylline adenosine dipyridamole (CTAD) has been shown to inhibit *in vitro* platelet activation by increasing the cytosolic AMP concentration without affecting platelet function (18;25;39). During a period of 3 hours after blood collection PMPs counts increased 2-fold in plasma

from citrated blood but were relatively stable in plasma isolated from CTAD-blood (40). Unfortunately, there is no study which directly compares the effects of citrate, CTAD and EDTA on plasma MP counts.

Plasma isolation

Platelets need to be removed from the plasma in order to avoid cellular activation leading to inadvertent production of MPs. For this purpose, a proper centrifugal speed should be applied for plasma preparation. According to the Clinical and Laboratory Standards Institute (CLSI) (41), plasma with a platelet count less than $10x10^9$/L is obtained by centrifuging the blood at 1,500g for 15 minutes at room temperature (RT). To obtain platelet-poor plasma (PPP) CLSI recommends re-centrifuging the plasma for another 10 minutes at 1,500g. We observed that PPP isolated by centrifuging blood once at 1,550g for 20 minutes still contained $2.8x10^9$/L platelets. However, when the same blood sample was used to isolate PPP by performing a two-step centrifugation, each at 2,000g for 10 minutes, there were only $6.1x10^8$/L platelets present in the plasma.

Platelet-free plasma (PFP) can be isolated by a centrifugation using 1,500g for 20 minutes followed by a high speed centrifugation at 13,000g for 2 minutes (8). Some studies (23;42;43) where flow cytometry was used to measure MPs, indicate that MP counts are lower in PFP than in PPP. The reason is still unclear. Probably, the last centrifugation step used in the preparation of PFP is vigorous and depletes platelets and also some MPs.

Cold activation of citrated blood samples has been reported to result in falsely elevated levels of (activated) factor VII (FVII) and factor VIII (FVIII) (44;44). Therefore, the temperature is generally kept at RT (20-25℃) for centrifuging citrated blood (8). However, the effect of centrifugation temperature on MPs has not yet been thoroughly investigated.

Furthermore, during centrifugation the use of breaks should be avoided as much as possible and plasma should be carefully collected without disturbing the platelet layer to prevent remixing of the plasma with the platelets.

Storage

Ideally, plasma is prepared immediately after blood collection. To avoid changes in MP number and characteristics the use of freshly isolated plasma is recommended for MP measurements (8). However, the logistic of blood sampling, transport time

to the in-house laboratory or even to laboratories elsewhere are all variables which are difficult to control and keep uniform across different centres.

According to CLSI guidelines (41) storage of uncentrifuged blood on ice is not recommended because of the possibility of cold activation of FVII and FVIII, loss of von Willebrand Factor (vWF), and platelet disruption (45). During storage blood samples should be maintained at room temperature while mechanical agitation is avoided (46).

In multi-centre studies and prospective trials it is often inevitable to freeze and store the plasma samples before performing the assay. However, validated protocols are not yet available for freezing and thawing of plasma to be used for MP analysis (47). In some publications it is described that plasma is first snap frozen in liquid nitrogen before it is stored at -80°C (23;47-50) while others directly freeze the plasma directly at -80°C (51-53).

Frozen-thawed PPP prepared by single centrifugation at 2,000g for 30 minutes contained 10-fold more PMPs counted by flow cytometry than fresh PPP (54). Conversely, PMP and annexin V-positive counts were not increased in frozen-thawed PFP prepared by a two-step centrifugation procedure (1,500g for 20 minutes and 13,000g for 2 minutes) (48). Probably some platelets present in PPP are fragmented during freezing and thawing leading to an increase in the number of PMPs and annexin V-positive MPs. Weber et al reported in an abstract that methods applied for cryopreservation of MPs, even by using established chemicals for cell cryo-conservation such as DMSO, trehalose, and paraformaldehyde, could not prevent the 10-fold increase in the number of annexin V-positive MPs caused by freezing and thawing (43).

However, most studies which investigated the effect of storage on MPs used flow cytometry for the measurement of MPs. A conventional flow cytometer uses a 488-nm laser and as MPs are heterogeneous and can have sizes below 488 nm, the sizing and identification of MPs is not accurate ((55), see also section ‘Flow cytometry’ for a more detailed discussion).

MPs isolation

Direct measurement of MPs in plasma is preferred to prevent loss of MPs during the isolation procedure and to preserve their morphology (51). For this purpose, flow cytometry and capture-based assays can be employed (31;32;51-53;56;57). Other methods require a MP isolation step prior to the MP measurements, such as fluorescence or electron microscopy, proteomic analysis and some functional MP

assays (29;34;49;58;59). In the next section these analytical methods will be discussed.

The advantages of using isolated MPs are less interference of plasma proteins and an increase in MP concentration. On the other hand, isolation procedures will cause inevitably loss of some MPs, especially when multiple washing steps are included. Most importantly, it is not known which centrifugation speed is optimal to pellet (all) plasma MPs.

Table 2 compares the results of several studies using different centrifugation protocols to prepare plasma and MPs for the measurement of PMPs by flow cytometry. Results are those obtained for citrated blood of healthy subjects. It seems that when fresh plasma is used, more PMPs can be detected directly in plasma than in the isolated MP fraction. Furthermore, the number of PMPs is about 3-10-fold higher in MPs isolated from frozen-thawed PPP than in MPs isolated from fresh PPP, especially when single-centrifuged PPP has been used.

Recommendations

During blood collection, it is necessary to prevent *ex vivo* activation of blood leading to inadvertent production of ErMPs or PMPs. Therefore, blood should be withdrawn by using a large diameter needle, for example a 21-G needle, and a tourniquet is only applied for locating the vein. In general, sodium citrate, EDTA, and CTAD anticoagulants can be used for blood collection. However, more information is needed on the relative stability of MP in blood collected in these anticoagulants.

After blood withdrawal, blood should be immediately centrifuged to isolate plasma. The centrifugation speed applied is crucial for the removal of platelets from plasma. Because PPP still contains some platelets, use of PFP may be preferred. However, it should be considered that some MPs might be lost during the high-speed centrifugation step. MPs measurements should be performed preferably directly in fresh plasma to reduce MP loss and to preserve MP characteristics. When frozen-thawed plasma is used for MP measurements, especially PMP and annexin V-positive MP counts should be interpreted with caution.

Ultimately, it is important to set up guidelines for preparing samples for MP measurements which include the choice of anticoagulant used for blood collection, the centrifugation speed to isolate plasma and MPs, and the preferred storage of plasma.

Table 1. Pre analytical variables and analytical methods to detect and characterize MPs.

Blood collection			Plasma preparation			Storage	MP isolation			Detection method	Ref.
Needle (G)	Anticoagulant	Type	Speed(g)	Time(min)	T (°C)	(°C)	Speed (g)	Time (min)	T (°C)		
19	EDTA	PFP	1st: 1,200 2nd: 12,000	15 12	20 20	-70	2x100,000	60	20	• Flow cytometry • EM • 1B10 antibody capture assay combined with MP-TF assay	(34)
21	Citrate	PPP	2,600	15	4	-	-	-	-	▪ Flow cytometry	(33)
n.s.	Citrate	PPP	1,550	20	20	-80	18,890	30	20	▪ Flow cytometry ▪ MP-TF assay ▪ Fluorescence confocal microscopy	(49)
21	Citrate	PFP	1st. 1,500 2nd: 13,000	15 2	RT RT	-80	-	-	-	▪ Flow cytometry	(51)
19 (butterfly needle)	Citrate	PPP	3,000	15	n.s.	-40	20,000	30	n.s.	▪ Flow cytometry ▪ EM ▪ Prothrombinase assay	(80)
n.s.	Citrate	PPP	2,000	15	8	-80	-	-	-	▪ TF-ELISA ▪ MP-TF assay	(52)
21	Citrate	PFP	1st: 200 2nd: 20,000	15 15	20 20	-80	-	-	-	▪ EM ▪ MP-TF assay	(86)
n.s.	Citrate	PFP	1st: 1,500 2nd: 13,400	15 2	n.s.	-80	-	-	-	▪ Annexin V-capture assay	(53)
21	EDTA-ACD	PPP	8,000	5	RT	-40	-	-	-	▪ PMP-capture assay	(31)
21	ACD	[a]PPP [b]PFP	[a] 2x 1,550 [b] 1st: 2x 1,550 2nd: 10,000	20 20 10	n.s.	-80	-	-	-	▪ Flow cytometry	(23)
n.s	Citrate	PPP	2x 2,100	20	n.s.	-80	-	-	-	▪ Impedance-based flow cytometry	(75)
21	Citrate	PPP	2x 2,000	10	20	-	18,890	30	20	▪ Flow cytometry ▪ AFM	(58)

-: not done; n.s: not specified; RT: room temperature

Table 2. The effect of different centrifugation steps and storage on flow cytometry detection of PMP in citrated plasma of healthy subjects. MPs were measured either directly in plasma or after an additional centrifugation step to isolate the MPs from plasma (fresh or frozen/thawed).

Healthy Volunteers		Plasma Preparation				Frozen* / Thawing	MP Isolation			PMP/10^6 L		Ref.
N	Sex	Type	Speed (g)	Time (min)	T (°C)		Speed (g)	Time (min)	T (°C)	Mean	Range	
10	ns	PPP	1,550	15	RT	-	-	-	-	922	(365-1,802)	(40)
15	m: 15	PPP	1,550	20	20	-	17,570	30	20	237	(116-565)	(110)
7	m, f: 7	PPP	2x2,000	2x10	20	-	18,890	30	20	141	(63-291)	(58)
60	m: 30 f: 30	PFP	1st: 1,500 2nd: 13,000	15 2	RT RT	-80°C/37°C	-	-	-	656 1,775	(407–962) (1,014–3,039)	(51)
47	m: 18 f: 29	PFP	1st: 1,500 2nd: 13,000	15 2	RT RT	-80°C/n.s.	-	-	-	625 ± 493		(111)
45	m: 29 f: 16	PPP	2x3,000	2x15	RT	-80°C/37°C	-	-	-	945	(659–1,393)	(112)
20	m: 4 f: 16	PPP	2x2,000	2x30	4	-70°C/n.s.	20,800	45	10	517 ± 72		(113)
37	m: 16 f: 21	PPP	1,550	20	20	-80°C/on melting ice	18,890	30	20	1,500	(700-7,100)	(49)
20	m: 16 f: 4	PPP	1,550	20	20	-80°C/on melting ice	17,570	30	20		~4,500-6,250	(50)
10	m: 4 f: 6	PPP	1,550	20	20	-80°C/on melting ice	18,890	30	20	3,200	(2,500-4,100)	(21)

-: not done; n.s. : not specified; RT: room temperature; m: male; f: female; *: storage

Analytical methods for MP measurements

Common MP assays

Flow cytometry

Flow cytometry is commonly used for the measurement of MPs. It is fast and allows both the enumeration of MPs and the assessment of their cellular origin (4;8). MPs pass a laser in a flowing sample stream and are counted by flow cytometer. The enumeration of MPs is based on the light that is scattered by each MP in forward direction (roughly proportional to their size) and in side direction (dependent on to granularity and structural complexity). However, the laser used by the flow cytometer excites at 488 nm. As MPs are heterogeneous and can have sizes below 488 nm, this wavelength is not suitable as a trigger or discriminator for MP detection (55;58;60).

To provide the concentration or absolute count of MPs in a sample, counting beads of a known concentration are used. These are calibrated microsphere-polypropylene/latex beads (mean diameter 7-9 or ~10 µm) that are brightly fluorescent across a wide range of excitation and emission wavelengths. When they are used as internal standard, the beads are added to each sample before the flow cytometry measurement. When used as external standard, the counting beads are processed as a sample at the same flow cytometry settings/conditions used for the samples. The flow cytometer counts the number of beads and/or MPs in the sample until the acquisition time is reached. With these numbers, the concentration of MPs in plasma can be calculated (50;51;58;61). As to the flow cytometry settings, the MP population is defined by using size calibration beads. Beads of 1 µm diameter are used to define the upper limit of the MP population and to discriminate the MP population from platelets (34;40). Another possibility is to use a mixture of fluorescent beads with diameters of 0.5, 0.9, and 3 µm (Megamix beads) to cover the MP (0.5 and 0.9 µm) and platelet populations (0.9 and 3 µm) ranges (51;62). However, as the refractive index of the plastic beads is different than that of MPs, also these beads remain an imperfect model for defining the cut-off of MP population.

The cellular origin of MP can be assessed by staining MPs with fluorescently labelled antibodies. In a flow cytometer, the fluorescent light passes a series of filters and appropriate fluorescence detectors allowing the simultaneous detection of more than two antigens on one MP (63). The correlation of the fluorescence signal to the light scatter of all measured events is used to identify and count a certain subset of MPs. The downside of this approach is that the fluorescence

signal depends on the specificity and affinity of the antibody to the target antigen and on the number of antigens present on the MP surface.

Although not all MPs expose PS (34;61;64-67), fluorescently labelled annexin V is commonly used to measure the total number of MPs with flow cytometry. The binding of annexin V to MPs is influenced by the calcium concentration and the membrane PS content (64;68). Consequently, the concentration of calcium in the buffer should be titrated for optimal staining of MPs in citrate- and EDTA-anticoagulated plasma samples. Staining with lactadherin, a milk-derived protein that also binds PS, has been shown to give similar results as obtained with annexin V staining (69). Lactadherin has been claimed to be more sensitive to small changes in PS expression than annexin V (66) and it detects PS-positive MPs in a calcium-free environment, such as citrate- or EDTA-anticoagulated plasma samples. Other markers such as bio-maleimide, phalloidin, and calcein acetoxymethyl ester (calcein AM) have been recently used to improve the detection of MPs. The staining with bio-maleimide, a thiol-reactive probe with spectral characteristics very similar to fluorescein, was found to give similar results as staining with annexin V (70). Staining with phalloidin and calcein AM seems to be useful to avoid false positive counts related to platelet or other cellular fragments. Phalloidin, a cyclic peptide which binds f-actin with high affinity, only stains platelet fragments discriminating these from PMPs (54). Calcein AM, a non-fluorescent marker that becomes fluorescent upon cleavage by cytosolic esterases only stains intact MP/cells and is not reactive with cellular fragments (65;71;72)

Flow cytometry uses fluorescently labelled specific antibodies to identify the cellular origin of MPs. These antibodies can distinguish MPs derived from platelets, leucocytes, erythrocytes, and endothelial cells. A list of such antibodies can be found in the publication of the Forum “Measuring circulating cell derived microparticles” (8) and some recent reviews (4;73;74). In addition, there are antibodies that have been used for the detection of MPs derived from malignant cells such as MUC1 for breast and pancreatic cancer cells (49;75), FasL for melanoma cells (76), EGFRvIII for glioblastoma cells (77), and CXCR-4 for leukemic cells (78).

The results of flow cytometry measurements depend on the type of instrument, instrument settings, and resolution. Recently, the ISTH SSC Working Group on Vascular Biology proposed the use of calibrated beads with sizes of 0.5, 0.9 and 3 µm (Megamix beads) to adjust the instrument setting and increase the resolution of the flow cytometer. The primary goal was to standardize the enumeration of PMPs >0.5 µm by using flow cytometry (51). Forty laboratories from 14 countries participated in the study. Firstly, these laboratories had to establish the resolution

and the level of background noise of their cytometers and to set the window of MP analysis by using the same batch of Megamix beads. Secondly, to define the inter-instrument reproducibility they received the same frozen PFP with three different concentrations of PMPs and used the same batch of phycoerythrin-labelled anti-CD41/IgG1 and fluorescein isothiocyanate-labelled annexin V from BioCytex (Marseille, France) for PMP staining. Several types of flow cytometer were used by these laboratories, such as FACSCalibur, FACSCanto II, and LSRII (all from Becton Dickinson) and EPICS XL, Gallios and FC500 (all from Beckman Coulter). The results of this study have been reported recently (62). Among 59 registered instruments from 40 laboratories, 49 were tested and 33 (67%) from 29 laboratories were qualified for subsequent analysis of PMP samples indicating that the strategy of using calibrated megamix beads is useful for the standardisation of PMP measurements by flow cytomety in multi-centre studies.

The enumeration of MPs by flow cytometer will not only be influenced by the analytical factors (e.g. laser, antibody, type of instrument, instrument calibration), but also on factors related to the sample preparation and storage (see Table 2). Especially the presence of residual platelets, storage of the blood/plasma, freezing/thawing of the plasma and centrifugation can influence MP counts.

Electron and fluorescence confocal laser scan microscopy

Electron microscopy (EM) can be used to study the morphology and membrane composition of MPs. In addition information on the antigenic composition of isolated MPs can be obtained by using immunogold-labelled antibodies (34;65;79). Heijnen et al (79) firstly reported that there were two types of membrane particles released by platelets after stimulation with thrombin receptor agonist peptide (TRAP). They concluded that the larger particles (diameters of 0.1-1 µm) were MPs because these particles were positively stained by immunogold-labelled antibodies against annexin V, GPIb, Pecam-1, integrins αIIb-β3, and two tetraspanins, Peta-3 and CD9. In contrast, from the smaller particles (diameters of 40-100 nm and defined as exosomes) less than 30% were stained by these antibodies, while about 50% were stained by gold labelled anti-CD63. Aras et al (34) performed EM imaging of MPs (diameters of 0.1-0.5 µm) isolated from PFP of a volunteer receiving endotoxin and showed that MPs have vesicular structures, but no cellular organelles. Interestingly, some of these MPs expressed CD14 and/or TF antigen as shown by immunogold labelling. By using EM, Bernimoulin et al. (65) demonstrated that MPs derived from THP-1 cells contain cytoskeletal proteins organized into a complex cytoskeletal network. As to the enumeration of MPs, EM can be used to make a rough estimate of the relative number of MPs in preparations subjected to flow cytometric analysis (54;80).

EM operational procedures require a vacuum environment and dehydration of the sample. These conditions may affect particle/MP morphology and are also not suitable for direct detection of MPs in plasma. The standard diameter of EM grids, 3.05 mm, can only hold a small sample volume (~2-4 µL). The sample material used to perform a conventional on-grid negative staining by using uranyl acetate preferably contains 0.1 to 1.0 mg protein/mL in aqueous solution (81). Therefore, plasma MPs need to be isolated and concentrated by centrifugation. In addition, EM produces a two-dimensional image of a sample, which gives an inaccurate estimation of the MP size.

Prior to detection by confocal laser microscopy, MPs are stained with fluorescently labelled antibodies to enable the identification of subsets of MPs based on their antigen expression. Confocal laser microscopy has been used by Dale et al (82) to characterize PMPs. These PMPs were 0.3–0.5 µm in diameter and positive for glycoprotein IIb/IIIa, glycoprotein Ib, CD9, and PS, but negative for fibrinogen and thrombospondin. Interestingly, confocal laser microscopy also can be used to identify fusion particles. For instance, Tesselaar et al (49) used fluorescence confocal laser microscopy to demonstrate that part of the MUC1-positive MPs isolated from the plasma of a metastatic breast carcinoma patient, co-expressed the platelet specific antigen, CD61. The fluorescence intensity profiles of these MPs corresponded with a MP diameter of approximately 0.15-0.2 µm. However, this estimation of MP diameter was based on a two-dimensional image and therefore inaccurate. Unfortunately it is not possible to use this method directly in plasma because of the high background caused by the interference of plasma proteins.

Like other optical methods that are based on the detection of a fluorescence signal, the results obtained by confocal laser microscopy also depend on the specificity and affinity of the antibody to the target antigen and on the density of the antigens on the MP surface.

EM and fluorescence confocal laser scan microscopy give information on morphological features of MPs (e.g. size, membrane structure, cytoskeleton). The operation of both methods requires several hours and they are not suitable for direct detection and quantification of MPs in plasma. However, they are useful for visualizing MPs and for validation of other MP measurements.

Capture-based assays

For capture-based assays, wells are coated with a probe (antibody or annexin V) that specifically binds a subset of MPs from plasma. Captured MPs can then be

quantified/characterized by using a second probe (e.g., peroxidase conjugated-antibody) (31;32) or by using a functional property of the captured microparticles (e.g. their procoagulant activity) (53;56;57;83). At present there is limited experience with this type of approach, while there are still many questions related to the kinetics of MP capture. Nevertheless, we will briefly describe some of the test designs that have been proposed in the literature. A clear advantage of these assays is that they will allow the measurement of MPs directly in plasma.

Nomura et al (32) and Ueba et al (31) described a method to measure the number of PMPs in EDTA-ACD PPP. Wells were coated with a monoclonal antibody against glycoprotein CD42a, while anti-CD42b, conjugated to a peroxidase, was used as secondary antibody. The concentration of PMPs is reported as U/mL where one U/mL is defined as the number of PMPs obtained from 24,000 solubilised platelets/mL.

Aupeix et al (84) first reported the use of annexin V-coated wells for the quantification of procoagulant MPs. The immobilized annexin V captures PS containing MPs from recalcified PFP. The procoagulant surface of these MPs is then quantified by measuring the prothrombinase activity after adding excess FXa-FVa. A direct relationship exists between the procoagulant phospholipid concentration and the amount of thrombin generated. Hugel et al (8) described this assay in detail in a publication of the Forum “Measuring circulating cell derived microparticles”. Liposomes of known concentration containing 33% PS/67% PC (mol/mol) were used as reference material. The MP concentration is reported as nM PS equivalent.

Meanwhile two commercially available variants of this assay are available (Actichrome® MP activity from American Diagnostica, Connecticut, USA and Zymuphen MP activity from Hyphen Biomed, Neuville-sur-Oise, France). These assays use a washed and lysed platelet concentrate as calibrator. Results are reported as nM PS.

Annexin V captures PS containing MPs in the presence of calcium ions. Therefore, the free calcium concentration in (diluted) plasma is an important determinant, which may influence the capture efficiency. As PFP is used for these measurement, the type of anticoagulant (EDTA, 3.2% citrate, 3.8% citrate) used for blood collection may influence the test result. The need to recalcify the plasma also raises the possibility of activation of the clotting system. This should be prevented by adding specific inhibitors to the (diluted) plasma. A final analytical issue is that the calculation of the MP concentration in plasma is based on comparison with a calibrator which does not have the same characteristics/behaviour as plasma MPs.

A limitation of this approach is the need to use fresh plasma, because freezing thawing will result in an increase in the number of annexin V-positive MPs (43;47)

Instead of biotinylated annexin V, biotinylated antibodies (e.g. anti-CD42b for platelets, anti-CD31 and anti-CD105 for endothelial cells, anti-CD3 and/or CD4 for T lymphocytes and anti-CD11a for leucocytes) have been used to capture specific subsets of MPs and then measure the prothrombinase activity as in the annexin V capture-based assay (8;83). As a control, irrelevant IgG is used for capturing MPs. The MP concentration in this antibody capture-based assay is expressed in nM PS as in the annexin V capture-based assays. A problem with the interpretation of the results of these tests is that part of the captured MPs might not express PS and that the specificity of the antibodies is broader than generally assumed (e.g., anti CD31 and anti CD105).

Aras et al (34) described the use of an immunoglobulin M monocolonal mouse anti human fibroblast surface protein (1B10) to capture MPs from PFP. Captured MPs were analysed for the presence of active TF using a two-step chromogenic assay. The TF-dependent FXa generation (pM/hour) was determined after subtracting the amount of FXa generated in the presence of polyclonal anti-human TF antibody prior to addition of FVIIa and FX. The 1B10 antibody apparently recognizes antigens on the surface of monocytes, granulocytes, endothelial cells, smooth muscle cells and fibroblasts, but not on platelets and epithelial cells. Consequently, MPs originating from platelets and epithelial cells are most likely not measured in this assay.

These capture-based assays enable a high-throughput measurement of subsets of MPs but will give no information on the size and total number of these MPs in plasma. Specific problems related to the antibody capture-based assays are not only the eventual presence of soluble antigen together with MP bound-antigen (42), but also the specificity and affinity of the antibody for the target antigen, and the amount of antibody coated on the well. Together they will determine the number of MPs captured in the assay.

Apart from the analytical factors that influence the capture-based assays, pre-analytical steps such as blood collection, plasma isolation and sample storage are also important. Although frozen-thawed plasma is frequently used in capture-based assays, there is not much information on how freezing and thawing of plasma will affect the concentration of MP in these assays.

Functional assays on isolated MPs

The analysis of certain functional properties of MPs can be achieved by separating MPs from the plasma proteins. An example of this is the measurement of TF activity in isolated MPs. The isolated MPs are supplemented with excess FVII(a) and FX in the presence of calcium, after which the formation of FXa is measured with a specific chromogenic substrate using either a one-stage (49;85) or two-stage approach (86;87). The TF activity of MP (MP-TF activity) is defined as the FVII dependent and anti-TF sensitive formation of FXa. MP-TF activity and has been expressed as fM Xa/min (no external calibrator) or as pg/mL (using relipidated recombinant human TF as a calibrator). The one-stage assay uses excess negatively charged phospholipids in the assay (49;85;88), while the users of the two-stage assay do not add phospholipids. In our own experience the presence of these phospholipids does not importantly affects the TF activity of isolated MPs. Interestingly no difference in MP-TF activity was observed between MPs isolated from fresh plasma and MPs isolated from frozen thawed plasma (49). A commercial two-stage chromogenic assay (Actichrome® TF, American Diagnostica, CT, USA) has also been used to quantify TF activity in the isolated MP fraction. Although this assay has also been used to measure TF activity in plasma (57;89), the observed FXa generation was found to be independent of exogenously added FVIIa and/or TF, and not inhibited by anti-FVIIa (90).

One limitation of all available TF-dependent FXa generation assays is the lack of an accepted standard for TF. For this reason, a working group on TF standardization in cancer was presented by the SSC at ISTH 2005. This group aimed and proposed to compare measurement of TF with a variety of methods in different laboratories and to improve intra- and inter-laboratory reproducibility by developing standardized protocols, appropriate reagents, and reference materials.

New approaches in MP assays

Proteomics analysis

Mass spectrometry (MS)-based proteomic analysis provides an opportunity to characterize the protein composition of MPs. Generally this method requires extraction, separation, trypsin digestion, MS analysis, and identification of proteins. Cell-surface antigens are generally of high molecular weight and hydrophobic (91;92). Therefore, an ionic/non-ionic detergent (e.g. sodium dodecyl sulfate, Triton X-100, NP-40) or a high-pH solvent (sodium carbonate pH 11) is used for the extraction of the membrane proteins prior to the gel separation and MS analysis

(92;93). Finally, each MS spectrum is used to search the protein database for matched peptides (91;94).

Proteomic analysis has been used by several groups to investigate the protein content of PMPs (29;30). For instance, PMPs isolated from the supernatant of ADP stimulated-platelets contained membrane surface proteins derived from platelets (GPIIIa, GPIIb, and P-selectin), chemokine ligand 4 (CXCL4), pro-platelet basic protein (CXCL7), and RANTES (CCL5). Proteins from the alpha granules (fibrinogen, vWF, FV and FXIII, thrombospondin, and protein S) were also found (30). In a different study (29), several proteins were detected in MPs isolated from plasma that were not found in PMPs isolated from the supernatant of ADP stimulated-platelets. These included proteins associated with apoptosis (CD5-like antigen, galectin 3-binding protein, and several complement components), iron transport (transferrin, transferrin receptor, haptoglobin), immune response (immunoglobulin J and Kappa chains), and blood coagulation (protein S and FVII). Some of these might represent contamination of the MP with plasma proteins.

The supernatant of TRAP-induced platelets contains mainly proteins from alpha granules (28). Some proteins potentially involved in angiogenesis, such as platelet-derived endothelial cells growth factor (PD-ECGF), angiopoietin-1, and galectin-3 binding protein are also found in this fraction. Importantly, four different isoforms of protein disulfide isomerase (PDIA3, P4HB, PDIA4 and PDIA6) were found, proteins that have been identified as critical mediators of wound healing (95) and assist in the de-encryption of an inactive form of TF into its active form (96;97). Recently, the presence of PDI on the surface of PMPs was also reported (98).

Proteomic analysis allows identification of various proteins in a complex mixture. However, quantification of proteins is difficult. The contamination of MPs with abundant plasma proteins like albumin and immunoglobulins might affect the results of proteomic analysis (94).

Impedance-based flow cytometry

Unlike the conventional flow cytometer, impedance-based flow cytometry is based on the Coulter principle to detect changes in electrical impedance produced by particles in suspension. These changes can be measured as a voltage pulse or a current pulse. The pulse height is proportional to the volume of the sensed particles (99). For MP measurement, this system is calibrated using fluorescent polystyrene microspheres of uniform size. Subsequently, MPs can be detected directly in PPP by using fluorescently labelled antibodies.

Zwicker et al. (75) have compared the measurement of PMPs, calibrated microspheres (0.78 µm), and platelets in frozen-thawed PPP, both by impedance- and light scatter-based flow cytometry. The size of platelets and PMPs is poorly characterized by the light-scatter based flow cytometry and both populations overlap with the 0.78 µm-microspheres. Conversely, the impedance-based flow cytometer could resolve the populations of PMPs, calibrated microspheres, and platelets. The same group (75) used impedance-based flow cytometry to measure the number of TF-bearing MPs in PPP of pancreatic cancer patients and found 3 to 4 orders of magnitude more MPs than previously reported by Tesselaar et al (49) who used light scatter-based flow cytometry. This might confirm that light scattering is not suitable for the enumeration of TF-bearing MPs. Impedance-based flow cytometry is presently used to quantify TF bearing MPs in the MicroTEC study, a randomized, multi-centre trial to evaluate the benefit of primary thrombophylaxis in cancer patients with high levels of TF bearing MPs (100).

In impedance-based flow cytometry, the size detection limit of the measurement depends on the diameter of the flow cell. Postmarket installation of smaller flow cells with diameters of 25 and 40 µm is required to analyze particles between 0.3 and 1.0 µm in diameter (75). Thus, MPs below 0.3 µm in diameter might not be detected by using these flow cells. Using fluorescently labelled antibody, the size distribution of MPs can theoretically be determined from the amplitude of the fluorescent signal under the assumption that the signal is either proportional to the volume or the surface of the particles (in the case of surface labeling). In addition the size distribution is calculated assuming a spherical shape. In the case of fluorescent labeling one generally assumes that the labeling efficiency is independent of the particle shape and (surface) composition.

Dynamic light scattering (DLS) and Nanoparticle tracking analysis (NTA)

Dynamic light scattering (DLS) and nanoparticle tracking analysis (NTA) measure Brownian motion of MPs in liquid suspension and from this movement the particle size can be calculated using the Stokes-Einstein equation (101). NTA measures the movement of each particle through image tracking analysis, whereas DLS measures all particles at the same time and produces an average particle size.

Two DLS systems, the Zetasizer Nano S (Malvern Instruments Ltd, Worcestershire, UK) and the N5 Submicron Particle Size Analyser (Beckman Coulter, CA, USA) were used to examine the size distribution of MPs in frozen-thawed plasma (102). It was found that MPs with sizes ranging from 50-1000 nm could be detected by the N5 instrument utilizing a 30.1° angle of measurement, whereas the Zetasizer detected some particles considerably larger than those

identified by the N5. The main disadvantage of DLS for measuring MPs is that it performs best in studying monodisperse particles while cell-derived MPs are clearly polydisperse. This makes that the size distribution of MPs measured by DLS is biased towards the presence of small numbers of large particles or contaminants as they scatter light more intensely than the smaller particles. The Zetasizer Nano S uses the back scattered light to increase the sensitivity of the method, while the N5 system can use up to 6 different scattering angles. The scattering angles of both instruments do not overlap.

This problem seems not to occur with the NTA approach because a microscope and a CCD camera track and visualize the individual particles by using particle tracking image analysis software. Harrison, et al. (103) used an NTA system, known as Nanosight LM10 (Nanosight, Amesbury, UK) to measure MP distributions in isolated MPs and in PPP diluted in PBS (1:40-1:60). They found that MPs have a polydisperse distribution up to 1,000 nm, but with a predominant population from lower than 50 nm to above 300 nm. They estimated that PPP contains ~200-260x10^9 MPs/L which is 1,000-fold higher than previous estimates based on using flow cytometry.

As mentioned before, NTA can accurately size particles in a sample, but unfortunately the presence of a few larger particles will reduce the number of small particles detected by the software. This has been demonstrated by Filipe et al (104) by mixing 60-nm/100-nm beads in a 4:1 ratio. The NTA analysis of this mixture showed two distinct size populations, but it detected more 100-nm beads than 60-nm beads due to the masking effect of the larger beads over the smaller beads.

For MP measurements the NTA approach has some disadvantages when compared to the DLS approach. The operation of NTA is not yet as user friendly as that of DLS. This is due to the fact that several parameters need to be adjusted carefully by a skilled operator prior to the NTA measurement. These parameters include the settings for the video capture and analysis, which are essential to obtain accurate and reproducible measurement results. As the Brownian motion of a particle in a solution depends on the viscosity and temperature of the solution, these parameters should also be defined prior to MP measurement in (diluted) plasma.

NTA and DLS may be unable to differentiate MPs from other particles present in plasma like (lipids/lipoproteins). Recently, Nanosight has launched a fluorescence-NTA, the NS500. This instrument enables the detection of individual quantum dots, fluorescent nanoparticles with a diameter of 2-10 nm, with minimal background

interference of other particles in the solution. This will hopefully enable the detection of specific subsets of MPs, for example by using quantum dot-labelled antibodies.

Atomic force microscopy

Scanning probe microscopy, especially atomic force microscopy (AFM), has opened new perspectives in biomedical research for the investigation of (bio)particles (105). AFM probes the surface of a sample with an ultra-sharp tip, a couple of microns long and often less than 100 Å in diameter. The tip is located at the free end of a cantilever which is 100-200 µm long. The interaction force between the tip and the sample depends on their distance. A detector, often with the use of a laser beam, measures the cantilever deflection when the tip moves across the sample or when the sample is moved under the tip. The measured cantilever deflections allow a computer to generate a three dimensional (3D)-surface topography (x, y and z dimensions) (106). The detection is so sensitive that forces can be detected as small as a few picoNewton. The advantage of employing AFM in the study of MP is that AFM can be operated in fluid tapping mode. The AFM tip is oscillated in liquid to create intermittent contact with the sample surface allowing the preservation of sample properties in their physiological state (Figure 1). A flat surface is needed for MP attachment, in order to distinguish individual MPs from the roughness of the supporting surface. Muscovite mica is a commonly used surface for AFM imaging because this non conductive mineral consists of layers which can be easily cleaved to produce clean and atomically flat surfaces (107). After cleaving, the mica surface can be modified to covalently attach a protein or antibody.

Recently, Yuana et al (58) have used AFM operated in fluid tapping mode for the sensitive detection of a defined subset of MPs isolated from double-centrifuged PPP. Using AFM and mica-coupled anti-CD41 1,000-fold more CD41-positive MPs were detected than by using conventional flow cytometry. These MPs have sizes ranging between 10-475 nm with a peak at 67.5 nm which is clearly below the detection limit of conventional flow cytometry. After freezing and thawing a decrease in the number of CD41-positive MPs was found by AFM, but the size distribution of these MPs remained the same. AFM also was employed to investigate the formation of PMPs by Siedlecki et al. (108). PMPs were generated by using surface-activated and thrombin-stimulated platelets deposited on glass and were found to have a similar size distribution as reported by Yuana et al (58). Siedlecki's group also showed that PMPs are clustered in close proximity to adherent platelets and localized in the platelet periphery and in some cases appeared to originate from platelet pseudopodia.

Baran et al (109) used AFM to detect MPs from frozen-thawed PFP isolated from EDTA blood of gastric cancer patients. AFM detected MPs mainly with sizes around 10 nm. This result was confirmed by using other techniques such as transmission EM and DLS. However, they did not operate AFM in fluid, so the characteristic of MPs might have changed.

AFM can be operated in fluid to detect MPs with a minimal force, thereby preserving their natural state, but it also enables the detection of the individual MP and simultaneously measures the 3D-size of MPs. Furthermore, the numbers of MPs attached to the surface can be quantified by using image processing software. When a specific antibody is used to coat a surface, a specific subset of MPs can be captured (58). However, as MPs need to be isolated from plasma and concentrated prior to AFM measurement, the isolation step might influence the morphology and the number of MPs. At present, the detection of MPs by AFM is low-throughput (typically 2 hours per sample). Therefore, modifications that will allow faster detection of specific populations of MPs in plasma will be essential.

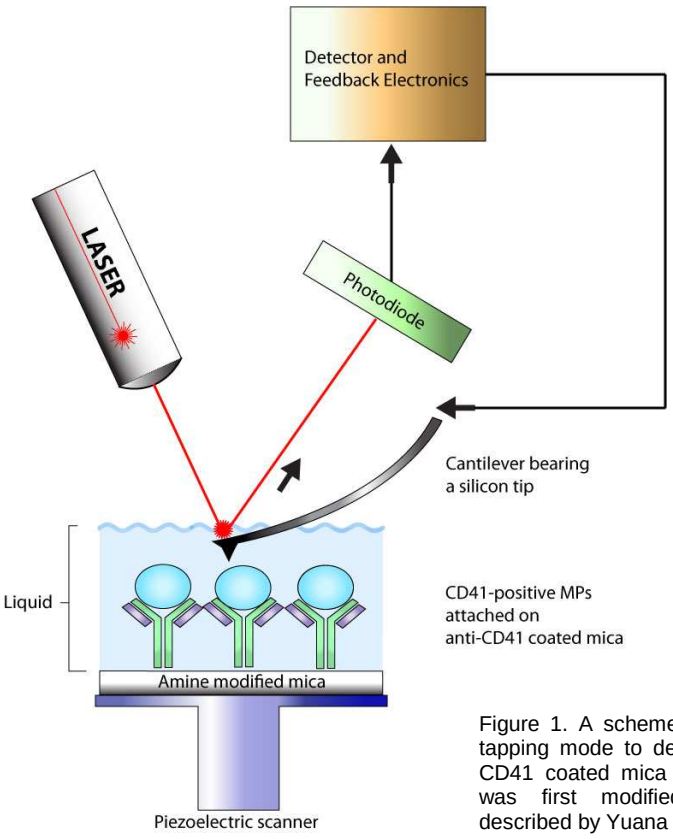


Figure 1. A scheme showing AFM operated in tapping mode to detect MPs attached on anti-CD41 coated mica surface. This mica surface was first modified with ethanolamine as described by Yuana et al. (58).

Recommendations

Results of plasma MP measurements reported in the literature vary widely. This is clearly not only related to the lack of well-standardized high-throughput MP assays, but also to variations in pre-analytical conditions. Some examples of these variations are listed in Table 1. Therefore, standardisation of both pre-analytical procedures and assay protocols is urgently needed.

When flow cytometry is chosen as a method for quantification of MPs, some analytical conditions should be standardized. Before measurement of the samples, the setting of the flow cytometer should be adjusted by using calibrated size standard beads, for example Megamix beads, to define the threshold (>0.5 µm and <0.9 µm) of MP detection. Counting beads should be used to measure the concentration or absolute count of MPs in a sample. For the characterization and enumeration of subsets of MPs the choice of antibody for labelling and capturing MPs is crucial. The antibody should be specific and have a high affinity for the target antigen.

Since not all plasma MPs expose annexin V and the percentage of annexin V-positive MPs can differ importantly depending on preanalytical conditions, the total number of MPs should not only be determined by binding of annexin V to MPs. In flow cytometry measurements and annexin V-capture assays binding of annexin V to MPs is influenced by the calcium concentration and the membrane PS content. Thus, it is important to find/develop a marker for direct detection of total number of MPs in a calcium-free environment.

Fluorescence-NTA and AFM can accurately count the nanosized MPs, but unfortunately both do not give information on the functional properties of MPs. Before employed in the clinic these methods need to be further validated. Similar like other methods which rely on the use of an antibody for the detection of MPs, specific and high affinity antibodies are required for the fluorescence-NTA and AFM.

Remaining Issues

Ideally MP measurements should be performed in plasma, freshly prepared directly after blood withdrawal. Platelet contamination seems to be one of the major pre-analytical problems in processing plasma for MP measurement. Platelets might be activated and/or fragmented resulting in an increase in the number of PMPs. Therefore, the choice of the anticoagulant used for blood collection and the centrifugation speed used for plasma preparation is critical. Freezing/thawing of

PPP unfortunately results in changes in the number of PMPs and in the number of PS-exposing MPs. There is therefore a great need for internationally accepted recommendations for the preparation and storage of plasma for MP measurements and for the isolation of MP from plasma. In addition, standardization of protocols, including the use of appropriate reagents and reference materials, is needed to improve intra- and inter-laboratory reproducibility in MP measurements.

At this moment we still have very limited information on what type of MPs (e.g. origin, protein content, and morphology) play a role in the development and progression of vascular disorders, cancer, and auto-immuno diseases. This is mostly due to the limitations of the methodology presently used for the enumeration of specific subsets of plasma MP. Some new methods (Impedance-based flow cytometry, DLS, NTA, and AFM) have been developed in the past years that might enable the accurate measurement of these nanosized MPs, but unfortunately these methods do not give information on the functional properties of MPs. Moreover, at this moment these methods are impractical for use in the clinic as they are low throughput and labour-intensive.

Acknowledgments

This work is supported by the Dutch Cancer Society (KWF UL 2006-3618). The authors thank Dr. T.H. Oosterkamp and Dr. M.E. Kuil for their critical reading of the manuscript.

References

(1) Wolf P. The nature and significance of platelet products in human plasma. Br J Haematol 1967;13:269-288.

(2) Zwaal RF, Comfurius P, Bevers EM. Surface exposure of phosphatidylserine in pathological cells. Cell Mol Life Sci 2005;62:971-988.

(3) Nieuwland R, Sturk A. Why do cells release vesicles? Thromb Res 2010;125 Suppl 1:S49-S51.

(4) Burnier L, Fontana P, Kwak BR, Angelillo-Scherrer A. Cell-derived microparticles in haemostasis and vascular medicine. Thromb Haemost 2009;101:439-451.

(5) Cocucci E, Racchetti G, Meldolesi J. Shedding microvesicles: artefacts no more. Trends Cell Biol 2009;19:43-51.

(6) Toth B, Lok CA, Boing A, Diamant M, van der Post JA, Friese K, et al. Microparticles and exosomes: impact on normal and complicated pregnancy. Am J Reprod Immunol 2007;58:389-402.

(7) Thery C, Ostrowski M, Segura E. Membrane vesicles as conveyors of immune responses. Nat Rev Immunol 2009;9:581-593.

(8) Jy W, Horstman LL, Jimenez JJ, Ahn YS, Biro E, Nieuwland R, et al. Measuring circulating cell-derived microparticles. J Thromb Haemost 2004;2:1842-1843.

(9) Castellana D, Kunzelmann C, Freyssinet JM. Pathophysiologic significance of procoagulant microvesicles in cancer disease and progression. Hamostaseologie 2009;29:51-57.

(10) Piccin A, Murphy WG, Smith OP. Circulating microparticles: pathophysiology and clinical implications. Blood Rev 2007;21:157-171.
(11) Martinez MC, Kunzelmann C, Freyssinet JM. Phosphatidylserine and signal transduction: who needs whom? Sci STKE 2006;2006:e3.
(12) Redman CW, Sargent IL. Circulating microparticles in normal pregnancy and pre-eclampsia. Placenta 2008;29 Suppl A:S73-S77.
(13) Nomura S, Ozaki Y, Ikeda Y. Function and role of microparticles in various clinical settings. Thromb Res 2008;123:8-23.
(14) George FD. Microparticles in vascular diseases. Thrombosis Research 2008;122:S55-S59.
(15) Pap E, Pallinger E, Pasztoi M, Falus A. Highlights of a new type of intercellular communication: microvesicle-based information transfer. Inflamm Res 2009;58:1-8.
(16) Azevedo LC, Pedro MA, Laurindo FR. Circulating microparticles as therapeutic targets in cardiovascular diseases. Recent Patents Cardiovasc Drug Discov 2007;2:41-51.
(17) Ahn YS. Cell-derived microparticles: 'Miniature envoys with many faces'. J Thromb Haemost 2005;3:884-887.
(18) Polack B, Schved JF, Boneu B. Preanalytical recommendations of the 'Groupe d'Etude sur l'Hemostase et la Thrombose' (GEHT) for venous blood testing in hemostasis laboratories. Haemostasis 2001;31:61-68.
(19) Lippi G, Salvagno GL, Montagnana M, Franchini M, Guidi GC. Venous stasis and routine hematologic testing. Clin Lab Haematol 2006;28:332-337.
(20) Lippi G, Franchini M, Montagnana M, Salvagno GL, Poli G, Guidi GC. Quality and reliability of routine coagulation testing: can we trust that sample? Blood Coagul Fibrinolysis 2006;17:513-519.
(21) van Beers EJ, Schaap MC, Berckmans RJ, Nieuwland R, Sturk A, van Doormaal FF, et al. Circulating erythrocyte-derived microparticles are associated with coagulation activation in sickle cell disease. Haematologica 2009;94:1513-1519.
(22) Hefler L, Grimm C, Leodolter S, Tempfer C. To butterfly or to needle: the pilot phase. Ann Intern Med 2004;140:935-936.
(23) van Ierssel SH, Van Craenenbroeck EM, Conraads VM, Van T, V, Vrints CJ, Jorens PG, et al. Flow cytometric detection of endothelial microparticles (EMP): effects of centrifugation and storage alter with the phenotype studied. Thromb Res 2010;125:332-339.
(24) Woywodt A, Blann AD, Kirsch T, Erdbruegger U, Banzet N, Haubitz M, et al. Isolation and enumeration of circulating endothelial cells by immunomagnetic isolation: proposal of a definition and a consensus protocol. J Thromb Haemost 2006;4:671-677.
(25) Ahnadi CE, Sabrinah CE, Lepine M, Okrongly D, Pujol-Moix N, Hernandez A, et al. Assessment of platelet activation in several different anticoagulants by the Advia 120 Hematology System, fluorescence flow cytometry, and electron microscopy. Thromb Haemost 2003;90:940-948.
(26) Macey M, Azam U, McCarthy D, Webb L, Chapman ES, Okrongly D, et al. Evaluation of the anticoagulants EDTA and citrate, theophylline, adenosine, and dipyridamole (CTAD) for assessing platelet activation on the ADVIA 120 hematology system. Clin Chem 2002;48:891-899.
(27) Neufeld M, Nowak-Gottl U, Junker R. Citrate-theophylline-adenine-dipyridamol buffer is preferable to citrate buffer as an anticoagulant for flow cytometric measurement of platelet activation. Clin Chem 1999;45:2030-2033.
(28) Piersma SR, Broxterman HJ, Kapci M, de Haas RR, Hoekman K, Verheul HM, et al. Proteomics of the TRAP-induced platelet releasate. J Proteomics 2009;72:91-109.
(29) Smalley DM, Root KE, Cho H, Ross MM, Ley K. Proteomic discovery of 21 proteins expressed in human plasma-derived but not platelet-derived microparticles. Thromb Haemost 2007;97:67-80.
(30) Garcia BA, Smalley DM, Cho H, Shabanowitz J, Ley K, Hunt DF. The platelet microparticle proteome. J Proteome Res 2005;4:1516-1521.

(31) Ueba T, Haze T, Sugiyama M, Higuchi M, Asayama H, Karitani Y, et al. Level, distribution and correlates of platelet-derived microparticles in healthy individuals with special reference to the metabolic syndrome. Thromb Haemost 2008;100:280-285.

(32) Nomura S, Shouzu A, Taomoto K, Togane Y, Goto S, Ozaki Y, et al. Assessment of an ELISA kit for platelet-derived microparticles by joint research at many institutes in Japan. J Atheroscler Thromb 2009;16:878-887.

(33) Hron G, Kollars M, Weber H, Sagaster V, Quehenberger P, Eichinger S, et al. Tissue factor-positive microparticles: Cellular origin and association with coagulation activation in patients with colorectal cancer. Thromb Haemost 2007;97:119-123.

(34) Aras O, Shet A, Bach RR, Hysjulien JL, Slungaard A, Hebbel RP, et al. Induction of microparticle- and cell-associated intravascular tissue factor in human endotoxemia. Blood 2004;103:4545-4553.

(35) Breimo ES, Osterud B. Generation of tissue factor-rich microparticles in an ex vivo whole blood model. Blood Coagul Fibrinolysis 2005;16:399-405.

(36) Brunialti MK, Kallas EG, Freudenberg M, Galanos C, Salomao R. Influence of EDTA and heparin on lipopolysaccharide binding and cell activation, evaluated at single-cell level in whole blood. Cytometry 2002;50:14-18.

(37) Shah MD, Bergeron AL, Dong JF, Lopez JA. Flow cytometric measurement of microparticles: pitfalls and protocol modifications. Platelets 2008;19:365-372.

(38) Connor DE, Exner T, Ma DD, Joseph JE. Detection of the procoagulant activity of microparticle-associated phosphatidylserine using XACT. Blood Coagul Fibrinolysis 2009;20:558-564.

(39) Contant G, Gouault-Heilmann M, Martinoli JL. Heparin inactivation during blood storage: its prevention by blood collection in citric acid, theophylline, adenosine, dipyridamole-C.T.A.D. mixture. Thromb Res 1983;31:365-374.

(40) Kim HK, Song KS, Lee ES, Lee YJ, Park YS, Lee KR, et al. Optimized flow cytometric assay for the measurement of platelet microparticles in plasma: pre-analytic and analytic considerations. Blood Coagul Fibrinolysis 2002;13:393-397.

(41) CLSI. Collection, Transport, and Processing of Blood Specimens for Testing Plasma-Based Coagulation Assays and Molecular Hemostasis Assays; Approved Guideline-Fifth Edition. CLSI document H21-A5. 2008. Wayne, PA: Clinical and Laboratory Standards Institute.

(42) Horstman LL, Jy W, Jimenez JJ, Bidot C, Ahn YS. New horizons in the analysis of circulating cell-derived microparticles. Keio J Med 2004;53:210-230.

(43) Weber H, Kollars M, Kyrle PA, Weltermann A. Comparison of different methods for isolation and storage of microparticles from human blood. J Thromb Haemost 2007;5(suppl 2):P-M-445.

(44) Favaloro EJ, Soltani S, McDonald J. Potential laboratory misdiagnosis of hemophilia and von Willebrand disorder owing to cold activation of blood samples for testing. Am J Clin Pathol 2004;122:686-692.

(45) Bohm M, Taschner S, Kretzschmar E, Gerlach R, Favaloro EJ, Scharrer I. Cold storage of citrated whole blood induces drastic time-dependent losses in factor VIII and von Willebrand factor: potential for misdiagnosis of haemophilia and von Willebrand disease. Blood Coagul Fibrinolysis 2006;17:39-45.

(46) van Geest-Daalderop JH, Mulder AB, Boonman-de Winter LJ, Hoekstra MM, van den Besselaar AM. Preanalytical variables and off-site blood collection: influences on the results of the prothrombin time/international normalized ratio test and implications for monitoring of oral anticoagulant therapy. Clin Chem 2005;51:561-568.

(47) Gelderman MP, Simak J. Flow cytometric analysis of cell membrane microparticles. Methods Mol Biol 2008;484:79-93.

(48) Trummer A, De Rop C, Tiede A, Ganser A, Eisert R. Recovery and composition of microparticles after snap-freezing depends on thawing temperature. Blood Coagulation & Fibrinolysis 2009;20:52-56.

(49) Tesselaar ME, Romijn FP, van der Linden IK, Prins FA, Bertina RM, Osanto S. Microparticle-associated tissue factor activity: a link between cancer and thrombosis? J Thromb Haemost 2007;5:520-527.

(50) van der Zee PM, Biro E, Ko Y, de Winter RJ, Hack CE, Sturk A, et al. P-selectin- and CD63-exposing platelet microparticles reflect platelet activation in peripheral arterial disease and myocardial infarction. Clin Chem 2006;52:657-664.

(51) Robert S, Poncelet P, Lacroix R, Arnaud L, Giraudo L, Hauchard A, et al. Standardization of platelet-derived microparticle counting using calibrated beads and a Cytomics FC500 routine flow cytometer: a first step towards multicenter studies? J Thromb Haemost 2009;7:190-197.

(52) Khorana AA, Francis CW, Menzies KE, Wang JG, Hyrien O, Hathcock J, et al. Plasma tissue factor may be predictive of venous thromboembolism in pancreatic cancer. J Thromb Haemost 2008;6:1983-1985.

(53) Ay C, Freyssinet JM, Sailer T, Vormittag R, Pabinger I. Circulating procoagulant microparticles in patients with venous thromboembolism. Thromb Res 2009;123:724-726.

(54) Mobarrez F, Antovic J, Egberg N, Hansson M, Jorneskog G, Hultenby K, et al. A multicolor flow cytometric assay for measurement of platelet-derived microparticles. Thromb Res 2010;125:e110-e116.

(55) Furie B, Furie BC. Cancer-associated thrombosis. Blood Cells Mol Dis 2006;36:177-181.

(56) Bal L, Ederhy S, Di AE, Toti F, Zobairi F, Dufaitre G, et al. Circulating procoagulant microparticles in acute pulmonary embolism: A case-control study. Int J Cardiol 2010;145:321-322.

(57) Steppich BA, Braun SL, Stein A, Demetz G, Groha P, Schomig A, et al. Plasma TF activity predicts cardiovascular mortality in patients with acute myocardial infarction. Thromb J 2009;7:11.

(58) Yuana Y, Oosterkamp TH, Bahatyrova S, Ashcroft B, Garcia RP, Bertina RM, et al. Atomic force microscopy: a novel approach to the detection of nanosized blood microparticles. J Thromb Haemost 2010;8:315-323.

(59) Miguet L, Pacaud K, Felden C, Hugel B, Martinez MC, Freyssinet JM, et al. Proteomic analysis of malignant lymphocyte membrane microparticles using double ionization coverage optimization. Proteomics 2006;6:153-171.

(60) Van Der Pol E, Hoekstra AG, Sturk A, Otto C, Van Leeuwen TG, Nieuwland R. Optical and non-optical methods for detection and characterisation of microparticles and exosomes. J Thromb Haemost 2010;8:2596-2607.

(61) Shet AS, Aras O, Gupta K, Hass MJ, Rausch DJ, Saba N, et al. Sickle blood contains tissue factor-positive microparticles derived from endothelial cells and monocytes. Blood 2003;102:2678-2683.

(62) Lacroix R, Robert S, Poncelet P, Kasthuri RS, Key NS, Dignat-George F; on behalf of the ISTH SSC Workshop. Standardization of platelet-derived microparticle enumeration by flow cytometry using calibrated beads: results of ISTH SSC collaborative workshop. J Thromb Haemost 2010;8:2571-2574.

(63) Carter NP, Ormerod MG. Introduction to the principles of flow cytometry. In: Flow cytometry: a pratical approach. 3rd ed. Oxford University Press; 2000. pp. 1-22.

(64) Connor DE, Exner T, Ma DD, Joseph JE. The majority of circulating platelet-derived microparticles fail to bind annexin V, lack phospholipid-dependent procoagulant activity and demonstrate greater expression of glycoprotein Ib. Thromb Haemost 2010;103:1044-1052.

(65) Bernimoulin M, Waters EK, Foy M, Steele BM, Sullivan M, Falet H, et al. Differential stimulation of monocytic cells results in distinct populations of microparticles. J Thromb Haemost 2009;7:1019-1028.

(66) Perez-Pujol S, Marker PH, Key NS. Platelet microparticles are heterogeneous and highly dependent on the activation mechanism: studies using a new digital flow cytometer. Cytometry A 2007;71:38-45.

(67) Jimenez JJ, Jy W, Mauro LM, Soderland C, Horstman LL, Ahn YS. Endothelial cells release phenotypically and quantitatively distinct microparticles in activation and apoptosis. Thromb Res 2003;109:175-180.

(68) Tait JF, Gibson D. Phospholipid binding of annexin V: effects of calcium and membrane phosphatidylserine content. Arch Biochem Biophys 1992;298:187-191.

(69) Shi J, Heegaard CW, Rasmussen JT, Gilbert GE. Lactadherin binds selectively to membranes containing phosphatidyl-L-serine and increased curvature. Biochim Biophys Acta 2004;1667:82-90.

(70) Enjeti AK, Lincz L, Seldon M. Bio-maleimide as a generic stain for detection and quantitation of microparticles. Int J Lab Hematol 2008;30:196-199.

(71) Bratosin D, Mitrofan L, Palii C, Estaquier J, Montreuil J. Novel fluorescence assay using calcein-AM for the determination of human erythrocyte viability and aging. Cytometry A 2005;66:78-84.

(72) Falati S, Liu Q, Gross P, Merrill-Skoloff G, Chou J, Vandendries E, et al. Accumulation of tissue factor into developing thrombi in vivo is dependent upon microparticle P-selectin glycoprotein ligand 1 and platelet P-selectin. J Exp Med 2003;197:1585-1598.

(73) Enjeti AK, Lincz LF, Seldon M. Detection and measurement of microparticles: an evolving research tool for vascular biology. Semin Thromb Hemost 2007;33:771-779.

(74) Horstman LL, Jy W, Minagar A, Bidot CJ, Jimenez JJ, Alexander JS, et al. Cell-derived microparticles and exosomes in neuroinflammatory disorders. Int Rev Neurobiol 2007;79:227-268.

(75) Zwicker JI, Liebman HA, Neuberg D, Lacroix R, Bauer KA, Furie BC, et al. Tumor-derived tissue factor-bearing microparticles are associated with venous thromboembolic events in malignancy. Clin Cancer Res 2009;15:6830-6840.

(76) Andreola G, Rivoltini L, Castelli C, Huber V, Perego P, Deho P, et al. Induction of lymphocyte apoptosis by tumor cell secretion of FasL-bearing microvesicles. J Exp Med 2002;195:1303-1316.

(77) Al Nedawi K, Meehan B, Micallef J, Lhotak V, May L, Guha A, et al. Intercellular transfer of the oncogenic receptor EGFRvIII by microvesicles derived from tumour cells. Nat Cell Biol 2008;10:619-624.

(78) Kalinkovich A, Tavor S, Avigdor A, Kahn J, Brill A, Petit I, et al. Functional CXCR4-expressing microparticles and SDF-1 correlate with circulating acute myelogenous leukemia cells. Cancer Res 2006;66:11013-11020.

(79) Heijnen HF, Schiel AE, Fijnheer R, Geuze HJ, Sixma JJ. Activated platelets release two types of membrane vesicles: microvesicles by surface shedding and exosomes derived from exocytosis of multivesicular bodies and alpha-granules. Blood 1999;94:3791-3799.

(80) Jayachandran M, Litwiller RD, Owen WG, Heit JA, Behrenbeck T, Mulvagh SL, et al. Characterization of blood borne microparticles as markers of premature coronary calcification in newly menopausal women. Am J Physiol Heart Circ Physiol 2008;295:H931-H938.

(81) Harris JR. Negative Staining of Thinly Spread Biological Samples. In: Methods in Molecular Biology. Humana Press Inc.; 2007. pp. 107-142.

(82) Dale GL, Remenyi G, Friese P. Quantitation of microparticles released from coated-platelets. J Thromb Haemost 2005;3:2081-2088.

(83) Habib A, Kunzelmann C, Shamseddeen W, Zobairi F, Freyssinet JM, Taher A. Elevated levels of circulating procoagulant microparticles in patients with beta-thalassemia intermedia. Haematologica 2008;93:941-942.

(84) Aupeix K, Hugel B, Martin T, Bischoff P, Lill H, Pasquali JL, et al. The significance of shed membrane particles during programmed cell death in vitro, and in vivo, in HIV-1 infection. J Clin Invest 1997;99:1546-1554.

(85) Tesselaar ME, Romijn FP, van dL, I, Bertina RM, Osanto S. Microparticle-associated tissue factor activity in cancer patients with and without thrombosis. J Thromb Haemost 2009;7:1421-1423.

(86) Tilley RE, Holscher T, Belani R, Nieva J, Mackman N. Tissue factor activity is increased in a combined platelet and microparticle sample from cancer patients. Thromb Res 2008;122:604-609.

(87) Manly DA, Wang J, Glover SL, Kasthuri R, Liebman HA, Key NS, et al. Increased microparticle tissue factor activity in cancer patients with Venous Thromboembolism. Thromb Res 2010;125:511-512.

(88) Garcia RP, Eikenboom HC, Tesselaar ME, Huisman MV, Nijkeuter M, Osanto S, et al. Plasma levels of microparticle-associated tissue factor activity in patients with clinically suspected pulmonary embolism. Thromb Res 2010;126:345-349.

(89) Funderburg NT, Mayne E, Sieg SF, Asaad R, Jiang W, Kalinowska M, et al. Increased tissue factor expression on circulating monocytes in chronic HIV infection: relationship to in vivo coagulation and immune activation. Blood 2010;115:161-167.

(90) Bogdanov VY, Cimmino G, Tardos JG, Tunstead JR, Badimon JJ. Assessment of plasma tissue factor activity in patients presenting with coronary artery disease: limitations of a commercial assay. J Thromb Haemost 2009;7:894-897.

(91) Miguet L, Sanglier S, Schaeffer C, Potier N, Mauvieux L, Van DA. Microparticles: a new tool for plasma membrane sub-cellular proteomic. Subcell Biochem 2007;43:21-34.

(92) Josic D, Clifton JG. Mammalian plasma membrane proteomics. Proteomics 2007;7:3010-3029.

(93) Wu CC, MacCoss MJ, Howell KE, Yates JR, III. A method for the comprehensive proteomic analysis of membrane proteins. Nat Biotechnol 2003;21:532-538.

(94) Smalley DM, Ley K. Plasma-derived microparticles for biomarker discovery. Clin Lab 2008;54:67-79.

(95) Cho J, Furie BC, Coughlin SR, Furie B. A critical role for extracellular protein disulfide isomerase during thrombus formation in mice. J Clin Invest 2008;118:1123-1131.

(96) Reinhardt C, von Bruhl ML, Manukyan D, Grahl L, Lorenz M, Altmann B, et al. Protein disulfide isomerase acts as an injury response signal that enhances fibrin generation via tissue factor activation. J Clin Invest 2008;118:1110-1122.

(97) Versteeg HH, Ruf W. Tissue factor coagulant function is enhanced by protein-disulfide isomerase independent of oxidoreductase activity. J Biol Chem 2007;282:25416-25424.

(98) Raturi A, Miersch S, Hudson JW, Mutus B. Platelet microparticle-associated protein disulfide isomerase promotes platelet aggregation and inactivates insulin. Biochim Biophys Acta 2008;1778:2790-2796.

(99) Hoffman RA, Johnson TS, Britt WB. Flow cytometric electronic direct current volume and radiofrequency impedance measurements of single cells and particles. Cytometry 1981;1:377-384.

(100) Zwicker JI. Predictive value of tissue factor bearing microparticles in cancer associated thrombosis. Thromb Res 2010;125 Suppl 2:S89-S91.

(101) Kaszuba M, McKnight D, Connah MT, Neil-Watson FK, Nobbmann U. Measuring sub nanometre sizes using dynamic light scattering. Journal of Nanoparticle Research 2008;10:823-829.

(102) Lawrie AS, Albanyan A, Cardigan RA, Mackie IJ, Harrison P. Microparticle sizing by dynamic light scattering in fresh-frozen plasma. Vox Sang 2009;96:206-212.

(103) Harrison P, Dragovic R, Albanyan A, Lawrie AS, Murphy M, Sargent I. Application of dynamic light scattering to the measurement of microparticles. J Thromb Haemost 2009;7(Suppl):OC-TU-056.

(104) Filipe V, Hawe A, Jiskoot W. Critical evaluation of Nanoparticle Tracking Analysis (NTA) by NanoSight for the measurement of nanoparticles and protein aggregates. Pharm Res 2010;27:796-810.

(105) Parot P, Dufrene YF, Hinterdorfer P, Le Grimellec C, Navajas D, Pellequer JL, et al. Past, present and future of atomic force microscopy in life sciences and medicine. J Mol Recognit 2007;20:418-431.

(106) Ricci D, Braga PC. How the Atomic Force Microscopy Works. In: Methods in Molecular Biology: Biomedical Methods and Applications. Humana Press Inc; 2004. pp. 3-12.

(107) Muller DJ, Amrein M, Engel A. Adsorption of biological molecules to a solid support for scanning probe microscopy. J Struct Biol 1997;119:172-188.

(108) Siedlecki CA, Wang IW, Higashi JM, Kottke-Marchant K, Marchant RE. Platelet-derived microparticles on synthetic surfaces observed by atomic force microscopy and fluorescence microscopy. Biomaterials 1999;20:1521-1529.

(109) Baran J, Baj-Krzyworzeka M, Weglarczyk K, Szatanek R, Zembala M, Barbasz J, et al. Circulating tumour-derived microvesicles in plasma of gastric cancer patients. Cancer Immunol Immunother 2010;59:841-850.

(110) Berckmans RJ, Neiuwland R, Boing AN, Romijn FP, Hack CE, Sturk A. Cell-derived microparticles circulate in healthy humans and support low grade thrombin generation. Thromb Haemost 2001;85:639-646.

(111) Sabatier F, Darmon P, Hugel B, Combes V, Sanmarco M, Velut JG, et al. Type 1 and type 2 diabetic patients display different patterns of cellular microparticles. Diabetes 2002;51:2840-2845.

(112) Enjeti AK, Lincz LF, Scorgie FE, Seldon M. Circulating microparticles are elevated in carriers of Factor V Leiden. Thromb Res 2010;126:250-253.

(113) Pereira J, Alfaro G, Goycoolea M, Quiroga T, Ocqueteau M, Massardo L, et al. Circulating platelet-derived microparticles in systemic lupus erythematosus. Association with increased thrombin generation and procoagulant state. Thromb Haemost 2006;95:94-99.

CHAPTER 3

Atomic force microscopy: a novel approach to the detection of nanosized blood microparticles

Yuana Yuana, Tjerk H. Oosterkamp, Svetlana Bahatyrova, Brian Ashcroft, Patricia Garcia Rodriguez, Rogier M. Bertina and Susanne Osanto

Journal of Thrombosis and Haemostasis 2010; 8(2): 315-323

Abstract

Background: Microparticles (MPs) are small vesicles released from cells of different origin, bearing surface antigens from parental cells. Elevated numbers of blood MPs have been reported in (cardio)vascular disorders and cancer. Most of these MPs are derived from platelets.

Objectives: To investigate whether atomic force microscopy (AFM) can be used to detect platelet-derived MPs and to define their size distribution.

Methods: Blood MPs isolated from seven blood donors and three cancer patients were immobilized on a modified mica surface coated with an antibody against CD41 prior to AFM imaging. AFM was performed in liquid-tapping mode to detect CD41-positive MPs. In parallel, numbers of CD41-positive MPs were measured using flow cytometry. Mouse IgG1 isotype control was used as a negative control.

Results: AFM topography measurements of the number of CD41-positive MPs were reproducible (coefficient of variation = 16%). Assuming a spherical shape of unbound MPs, the calculated diameter of CD41-positive MPs ($d$sph) ranged from 10 to 475 nm (mean: 67.5 ± 26.5 nm) and from 5 to 204 nm (mean: 51.4 ± 14.9 nm) in blood donors and cancer patients, respectively. Numbers of CD41-positive MPs were 1,000-fold higher than those measured by flow cytometry (3-702 x 10^9/L plasma vs. 11-626 x 10^6/L plasma). After filtration of isolated MPs through a 0.22-µm filter, CD41-positive MPs were still detectable in the filtrate by AFM (mean $d$sph: 37.2 ± 11.6 nm), but not by flow cytometry.

Conclusions: AFM provides a novel method for the sensitive detection of defined subsets of MPs in the nanosize range, far below the lower limit of what can be measured by conventional flow cytometry.

Introduction

Microparticles (MPs) or microvesicles are small cellular fragments (vesicles) that were initially considered to be 'cell dust', but were later shown to be released from cells upon activation and apoptosis (1,2). The majority of MPs found in blood plasma are platelet-derived MPs (PMPs), as defined by the presence of CD41 and CD61 on their surface (3,4). Several studies point to a role of blood MPs in processes such as angiogenesis, cancer, and thrombosis (4-7).

The precise mechanism by which MPs are released has not yet been elucidated; however, an increase in cytosolic calcium concentration appears to be necessary to trigger vesicle release (8). Some specific enzymes (floppase and scramblase) are thought to assist in remodeling the plasma membrane by inducing the translocation of anionic phospholipids, such as phosphatidylserine (PS), from the inner membrane to the outer membrane (9). This event is followed by MP release and cytoskeletal degradation by calcium-dependent proteolysis (10).

In recent years, blood MPs have increasingly received attention as potential biomarkers in the diagnosis and prognosis of disease. However, such studies have been hampered by the lack of accurate methods for the detection and quantification of MPs. Different methods and combinations of methods have been used, including enzyme-linked immunosorbent assays (ELISAs), capturing MPs with immobilized annexin V or cell-specific antibodies (7,11), and flow cytometry (4,5,12). The advantage of ELISAs is that these can be easily developed into user-friendly diagnostic/screening assays for analysis of large numbers of samples. Captured MPs are quantified via measurement of the concentration of negatively charged phospholipids supporting prothrombinase activity. The drawback of using this method is that MPs do need to expose accessible PS on their surfaces, and that the method does not give information on the number of MPs (12). Other disadvantages of ELISAs are interference by soluble antigens and lack of information on size distribution. An advantage of flow cytometry is that it can be used for the simultaneous detection of two or more antigens on MPs by using antibodies conjugated with different chromophores. However, the laser light employed in flow cytometers, which excites at a wavelength of 488 nm, makes the measurement of the smaller MPs by flow cytometry unreliable (13). Standardization of PMP detection with flow cytometry in the size range 500-1,000 nm by using calibrated beads was recently proposed (14).

Scanning probe microscopy, especially atomic force microscopy (AFM), has opened new perspectives in biomedical research for the investigation of (bio)particles (15). With AFM, high-resolution topography imaging of particles can

be obtained with a resolution down to the subnanometer range. Moreover, the ability of AFM to image biological samples in aqueous fluids enables the preservation of sample properties in their physiological state (16,17). We chose AFM as a method for the detection of CD41-positive MPs. Muscovite mica, a non-conducting layered mineral that can easily be cleaved and has an atomically flat surface (18), was modified and used to immobilize anti-CD41 antibody. This modified mica was then used for capturing MPs. AFM in fluid/liquid tapping mode, where the probe is oscillated in liquid to create intermittent contact with the sample surface, was used to detect the MPs. We report that AFM detects 1,000-fold more CD41-positive MPs than flow cytometry, and that the size of the majority of these MPs is below the detection limit of conventional flow cytometry. We propose AFM as a suitable method for studying the size, antigenic properties and numbers of defined subsets of MPs.

Materials and methods

Blood collection and plasma preparation

After giving their informed consent, seven blood donors were sampled between 08.00 h and 10.00 h. Venous blood was drawn by using a 21-gauge needle (BD Vacutainer; Becton Dickinson, San Jose, CA, USA) and minimal stasis. After discarding of the first 4 mL of blood, blood was collected in a 1/10 volume of sodium citrate (3.2%, 0.105 M) using a 4.5-mL BD Vacutainer tube (Becton Dickinson). Within 10-15 minutes of withdrawal, blood was centrifuged at 2,000g for 10 minutes at 20°C, without brake. Plasma was carefully collected and centrifuged again at 2,000g for 10 minutes at 20°C, without brake, to obtain platelet-poor plasma (PPP). PPP was aliquoted in 250-µL portions. For the isolation of MPs from fresh PPP, PPP was directly subjected to the next centrifugation steps. Otherwise, PPP was snap frozen in liquid N_2 and stored at -80°C until used for MP isolation. In addition, blood was collected from three patients with cancer (metastatic colorectal, pancreatic and renal cell carcinoma) after informed consent had been obtained.

Isolation of MPs

For AFM measurement, 750 µL of PPP was pooled and centrifuged at 18,890g and 20°C for 30 minutes, with minimum brake. The supernatant was removed carefully, except for 25 µL containing the MP pellet. This pellet was resuspended in 1 mL of Hepes buffer [10 mM Hepes (Merck, Darmstad, Germany), 137 mM NaCl (Merck), 4 mM KCl (Merck), 0.1 mM Pefabloc SC (Fluka, Munich, Germany), pH 7.4],

vortexed, and centrifuged as before. The supernatant was removed, leaving a volume of 25 µL containing the MP pellet. This 25 µL was vortexed and then used for AFM.

For flow cytometry, 250 µL of PPP was centrifuged at 18,890 g and 20°C for 30 minutes, with minimum brake, and the supernatant was then carefully removed, leaving a volume of 25 µL containing the pellet. To wash the MPs, 225 µL of Hepes buffer was added, and this mixture was then centrifuged again at 18,890g and 20°C for 30 minutes, with minimum brake. The supernatant (225 µL) was removed, and the residual 25 µL was diluted to 100 µL with Hepes buffer. This MP preparation was directly used for staining with antibodies.

Modification of mica for immobilization of mouse anti-human CD41 antibody

The surface of mica was modified as follows. A solution was made containing 55% (w/v) ethanolamine (Sigma Aldrich, Munich, Germany) in dimethylsulfoxide (DMSO) (99.7% purity; Biosolve BV, Dordrecht, the Netherlands). Molecular sieve beads (0.3 nm; Sigma Aldrich) were added to adsorb the water formed later during the amine reaction on the mica surface. This solution was heated at 70°C until the ethanolamine was completely dissolved. Next, freshly cleaved muscovite mica sheets (Electron Microscopy Sciences, Hatfield, PA, USA), with a diameter of 10 mm, were incubated overnight in the ethanolamine solution.

Subsequently, mica sheets were rinsed twice in DMSO (99.7% purity, 70 °C) and twice in absolute ethanol (Biosolve BV) at room temperature (RT). These mica sheets were dried under N_2. At this point, the amine-modified mica can be used immediately for the next modification step or stored in a desiccator for up to several weeks. Prior to protein coupling, the modified mica was incubated for 3 hours with 1 mg/mL EGTA (Sigma Aldrich) in chloroform (Merck) containing 0.5% (v/v) triethylamine (Merck). The mica sheets were then washed in chloroform, dried under N_2, and glued onto a steel disk (diameter of 12 mm) with a silicon-based glue (Rhodia Silicon, Leverkusen, Germany). Fifty microliters of mouse anti-human CD41 antibody clone P2 (Beckman Coulter, Fullerton, CA, USA) (0.01 mg/mL) was applied to the modified mica and incubated for 30 minutes at RT. Excess of anti-CD41 was removed by washing with Hepes buffer. As a negative control, mouse IgG1 pure clone X40 (Becton Dickinson) was used (0.01 mg/mL).

AFM analysis of CD41-positive microparticles

Twenty microliters of the MP fraction was applied to the anti-CD41-coated mica surface and incubated for 30 minutes to allow the binding of MPs to anti-CD41. To remove unbound MPs, the mica was washed twice with Hepes buffer. During the incubation step and before imaging, the mica surface was kept in a closed container.

Before use, the AFM glass fluid cell (Veeco, New York, NY, USA) was sonicated for 5 minutes in sodium dodecylsulfate (Serva Electrophoresis, Heidelberg, Germany), rinsed with distilled water, and allowed to dry under N_2. A microcantilever silicon tip (Olympus, Tokyo, Japan), with a spring constant of 2 N/m and 70-kHz resonant frequency, was attached to the fluid cell. After mounting of the steel disk containing the sample on the piezoelectric scanner of the atomic force microscope, 80 µL of imaging buffer containing 20 mM Tris (Roche, Basel, Switzerland) and 150 mM KCl (pH 7.4) was added. The fluid cell with the cantilever attached was then seated against the sample. An atomic force microscope (Veeco) operated in fluid-tapping mode was used to scan the topography of the mica and attached MPs, thus providing three dimensional images of the MPs. With an imaging rate of 1.5 Hz, the surface was scanned at different positions to obtain four to 10 images with a scan size of 100 μm^2 per image. Images were captured and recorded using NANOSCOPE software version 5.30r2 (Veeco).

AFM data were analyzed using SPMEDIATOR version 6.1 (courtesy of S. J. T. van Noort, Leiden University, Leiden, the Netherlands) that evaluates the center of mass of particles in comparison with the surface background. This software automatically calculates the volume (V) and height (z) of MPs. From the MP volume, the MP diameter ($d_{sph} = \sqrt[3]{6V/\pi}$) was calculated, assuming a spherical shape for the MP when not bound to the mica.

To calculate the number of CD41-positive MPs/L PPP detected by AFM, the following formula was used: (10^6/750) x (25/20) x (78.5 x 10^6/100) x N_{AFM}, in which 750 (µL) is the original volume of PPP used for MP isolation, 25 (µL) is the volume of MP suspension, 20 (µL) is the volume of the MP suspension applied to the mica surface, 78.5 x 10^6 (μm^2) is the surface area of the mica, 100 (μm^2) is the surface area of an AFM image, and N_{AFM} is the mean of the total number of CD41-positive MPs per image after correction for the number of MPs found on IgG1 control-coated mica.

Flow cytometry analysis of CD41-positive MPs

Flow cytometry analysis was performed using a FACS Calibur flow cytometer with CELLQUEST PRO software (Becton Dickinson). The FACS Calibur used can detect polystyrene beads of 0.2, 0.5 and 1 µm (Fluka) if they are analyzed separately, but is unable to resolve these particles when they are analyzed as a mixture (data not shown).

Five microliters of the MP fraction was incubated with 5 µL of phycoerythrin (PE)-labeled mouse anti-human CD41 clone P2 (1:100 dilution) (Beckman Coulter) in 40 µL of Hepes buffer for 30 minutes at RT in the dark. Then, 200 µL of Hepes buffer was added, and the MP suspension was centrifuged at 18,890g and 20°C for 30 minutes, with minimum brake. The supernatant was removed carefully, and the residual 50 µL was diluted to 350 µL with Hepes buffer. As negative control, mouse IgG1 PE clone X40 (Becton Dickinson) was used at the same concentration as the anti-CD41 antibody. For counting absolute numbers of CD41-positiveMPs per liter, we used flow cytometry absolute count standard beads with a mean diameter of 7.58 µm per bead and a known concentration (C_{beads}) (Bang Laboratories, Fishers, IN, USA) as an external standard. Two hundred microliters of these beads (V_{beads}) was mixed with Hepes buffer to a volume of 600 µL (V_{tot}) and then measured in triplicate (N_{beads}). For measurement of counting beads as well as MPs, the flow cytometer was programmed to count events in 1 minute. To calculate the volume (Z) measured by flow cytometry, the following formula was used: V_{tot}/V_{beads} x (N_{beads}/C_{beads}). The amount of CD41-positive MPs/L PPP detected by flow cytometry was calculated as (350/Z) x (100/5) x 10^6/250 x N_{FACS}, in which 350 (µL) is the total volume of MPs before analysis, 100 (µL) is the total volume of the original MP suspension, 5 (µL) is the volume of MPs used for antibody labeling, 250 (µL) is the original volume of PPP used for MP isolation, and N_{FACS} is the mean number of CD41-positive events counted by flow cytometry, after correction for IgG1 control background events.

Statistical analysis

Statistical evaluation was performed using SPSS 14.0. Correlation of the amount of MPs in PPP measured by AFM and flow cytometry was tested with the Pearson and Spearman correlation tests.

Results

AFM

The surface of cleaved mica scanned with an atomic force microscope operated in fluid-tapping mode was flat, with an apparent height of ~ 0.1 nm (Figure 1A). After modification of this surface, the surface topography was still nearly flat, with a measured height of ~ 0.2 nm (Figure 1B). Following the immobilization of mouse anti-human CD41 antibody on the modified mica, an apparent height of 2.3 ± 1.17 nm of the anti-CD41 antibody was detected (Figure 1C). As a negative control, a mouse IgG1 isotype control was immobilized on the modified mica, and from the surface topography scan, an apparent height of 2.3 ± 1.50 nm was determined (Figure 1D). The number of anti-CD41 and IgG1 molecules on the surface (100 μm^2) was~ 2,000/100 μm^2 and, on the basis of the surface topography scan, they were homogeneously bound.

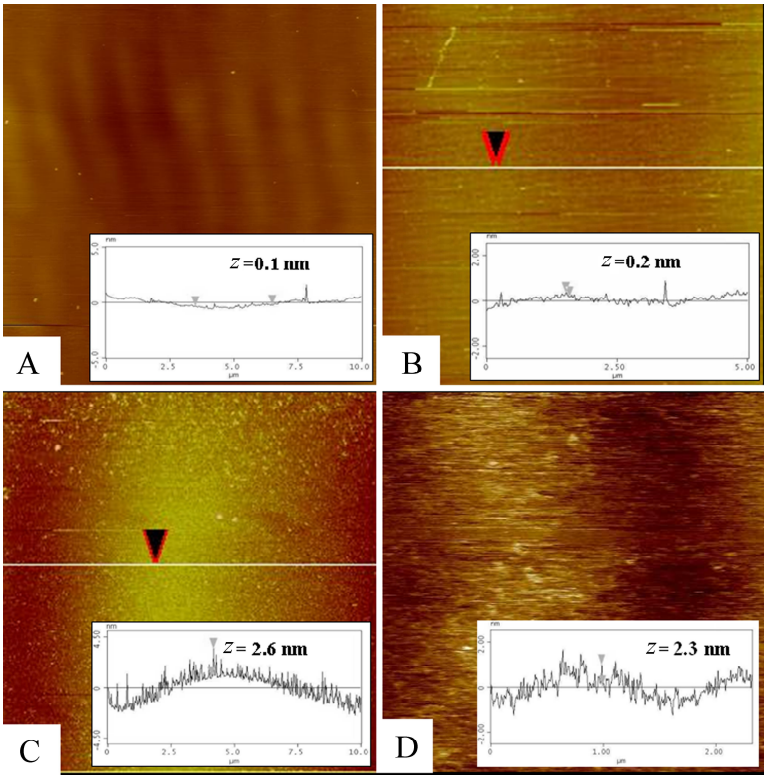


Figure 1. Atomic force microscopy image showing the three-dimensional surface topography of mica (A), modified mica (B), anti-CD41 antibody-coated mica (C), and IgG1 isotype control-coated mica (D). Inserts show the results of the height analysis (z) of the surfaces.

Imaging with AFM demonstrated specific binding of MPs isolated from fresh PPP to anti-CD41-coated mica. The three-dimensional AFM topography showed that there were particles, defined as MPs, attached to the anti-CD41-coated mica, whereas these were virtually absent on the IgG1 isotype control-coated mica (Figure 2A, B). The IgG1 isotype control was used to control for non-specific MPs binding to the modified mica. Cleaved mica itself was unable to immobilize MPs (data not shown).

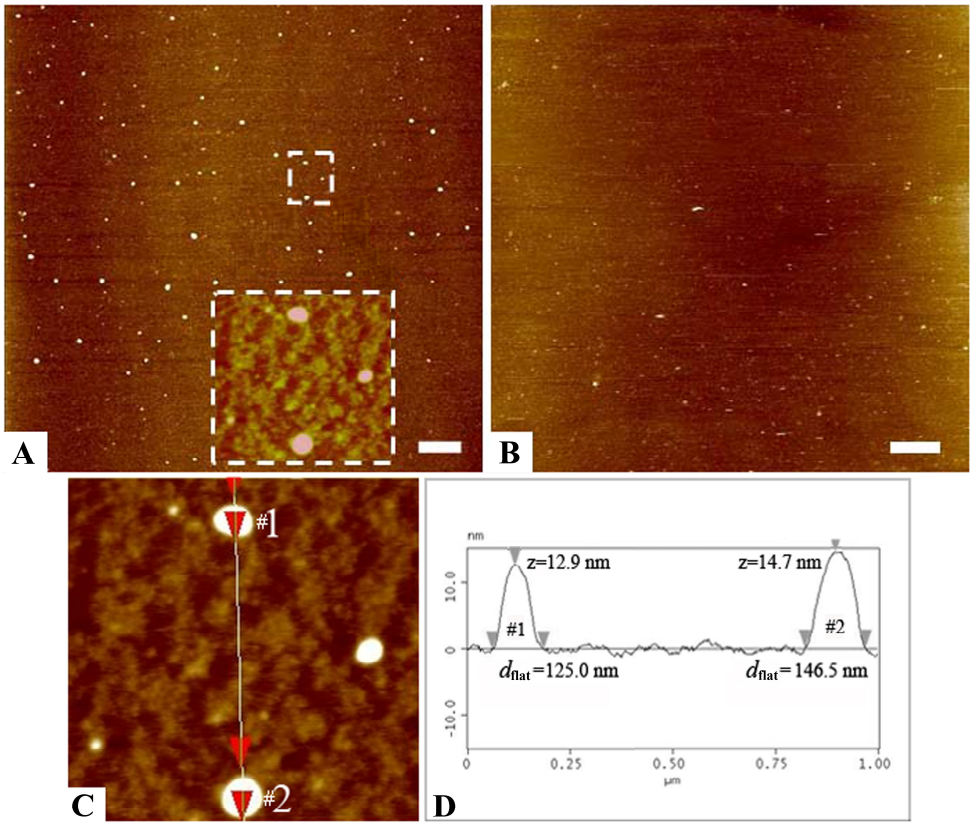


Figure 2. Three-dimensional atomic force microscopy topography of (A) CD41-positive microparticles (MPs) and (B) isotype control (IgG1)-coated mica. The scale bar in these images is 1 µm. The dashed box on the surface (A) was scanned (1 μm^2) and analyzed with NANOSCOPE software by positioning cross-sectional line on two MPs (C; #1 and #2). A histogram of this line presents the MP peak with its diameter (d_{flat}) and height (z) values (D). Note that the scale of the y-axis is smaller than that of the x-axis.

Using NANOSCOPE software version 5.30r2, the diameter and height of MPs in surface topography scans were analyzed. In Figure 2C, a cross-sectional line was positioned on two MPs (#1 and #2). Figure 2D shows the histogram of this line. The values of the edge-to-edge diameter, d_{flat}, of surface-bound MPs were about 10-fold higher than the z-values (for #1 d_{flat}/z = 125.0 nm/12.9 nm; for #2, 146.5 nm/14.7 nm), indicating that bound MPs were flat. Considering the physiological state of unbound MPs, and to facilitate future comparisons with, for example, transmission electron microscopy images, we chose to analyze MPs in terms of their volume. Additionally, a volume measurement is more easily automated and more accurate, because it does not depend on the direction in which the crosssection is made. MP volume is measured by summing the volume of each pixel in the AFM image (using SPMEDIATOR version 6.1), and from this volume the effective diameter, d_{sph}, of the MP is calculated. The effective diameters, d_{sph}, for MPs #1 and #2 were 49.2 and 54.0 nm, respectively. This result shows that d_{sph} of these MPs was approximately two-fold smaller than d_{flat}. In the remainder of this article, all diameters will be given as effective diameter, d_{sph}, unless stated otherwise.

Variation of the incubation time of MPs with the anti-CD41-coated mica (2, 15, 30, and 45 minutes) showed that the total number and size distribution of specifically attached MPs had reached a plateau after 15 minutes (for a particular MP preparation, 323 counts per 100 μm^2).

Figure 3A shows that the MPs attached to the anti-CD41-coated mica had d_{sph} values ranging from 10 to 475 nm (mean: ~ 50 nm). When isolated platelets were stimulated with thrombin (0.5 U/mL), CD41-positive MPs with a similar d_{sph} (mean: 44.1 ± 13.7 nm) were found.

To investigate the relationship between MP concentration and number of CD41-positive MPs detected by AFM, different dilutions of MPs isolated from PPP were incubated with anti-CD41-coated mica and imaged by AFM. A linear relationship was obtained between the number of CD41-positive MPs per 100 μm^2 mica and the MP concentration (100% = undiluted MPs) (Figure 3B). At saturation, the CD41-coated mica can bind about 500 MPs per 100 μm^2. This value was confirmed in several separate experiments. For AFM analysis, samples need to be sufficiently diluted to give a response in the linear part of the dose-response curve.

To determine the reproducibility of the measurements, MPs were isolated from frozen-thawed PPP on three consecutive days, and analyzed by AFM for the presence of CD41-positive MPs. The between-assay variation for MP isolation and

AFM measurement (including mica modification) was 16% (mean 528 x 10^9 CD41-positive MPs/L; standard deviation 83 x 10^9 CD41-positive MPs/L).

To investigate the effect of freezing and thawing on the number and size distribution of CD41-positive MPs measured by AFM, MPs were isolated from PPP of three donors before and after freezing-thawing. For two donors, there was no significant difference in size distribution of the CD41-positive MPs before and after freezing-thawing, although the number of CD41-positive MPs decreased (two-fold and seven-fold, respectively) after freezing-thawing. For one donor, we found a two-fold increase in number and a slight shift in the effective diameter (d_{sph}) of the CD41-positive MPs in MPs isolated after freezing and thawing of the PPP (from 50-250 nm to 10-200 nm).

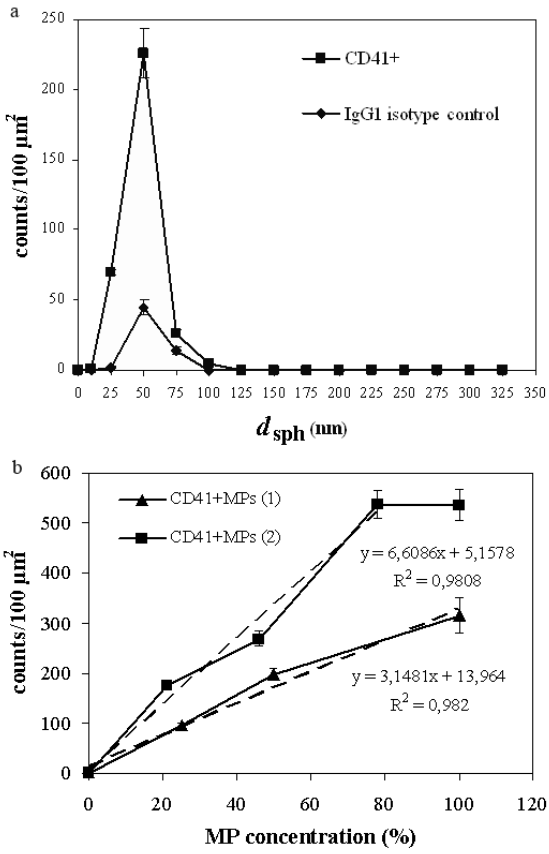


Figure 3. Atomic force microscopy (AFM) detection of CD41-positive microparticles (MPs) isolated from fresh platelet-poor plasma. (A) Size distribution (d_{sph}) and counts of MPs per 100 µm^2 surface area and (B) relationship between the MP concentration in the sample and the number of CD41-positive MPs detected by AFM; results are shown for two different MP preparations; the dotted lines represent regression lines.

Flow cytometry

The CD41-positive MPs were quantified by flow cytometry, using a known concentration of counting beads as external standard in the measurement. The singlet population of these beads could be detected as shown in the forward scatter plot of Figure 4A. By counting the number of beads, the volume used for the measurement could be calculated. The mean volume analyzed by flow cytometry was 80 ± 4 µL.

MPs were characterized by their CD41 expression (Figure 4B, C). The number of CD41-positiveMPs was calculated after correction for the number of MPs staining with the IgG1 isotype (negative control). The reproducibility of MP measurement with flow cytometry was assessed on three consecutive days by one single operator performing the CD41-positive MP measurement in triplicate. For these experiments, MPs were isolated from aliquots of frozen PPP. The variation in the number of CD41-positive MPs was 10% (mean 389 x 10^6 MPs/L; SD 41 x 10^6 MPs/L).

The effect of freezing and thawing on the number of CD41-positive MPs measured by flow cytometry was also assessed. Flow cytometric analysis of MPs isolated from PPP of four donors before and after thawing revealed that, depending on the donor, two-fold to 10-fold more CD41-positive MPs were detected in the MP fraction prepared from frozen-thawed PPP than in the MPs isolated from fresh PPP.

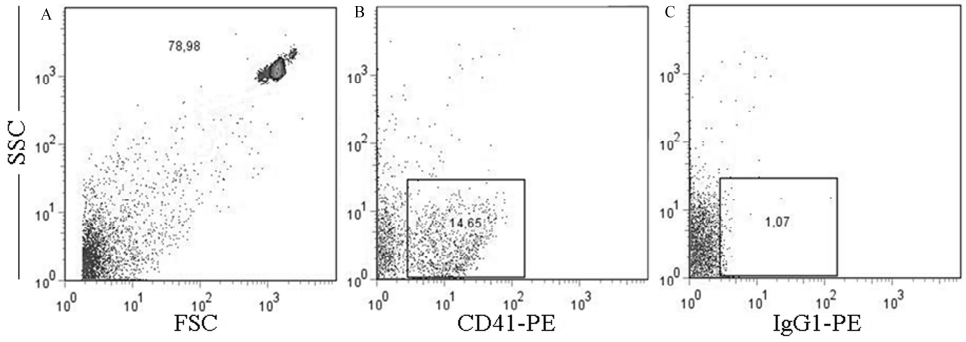


Figure 4. Flow cytometry plots representing the measurement of the absolute count beads (A), the detection of CD41-positive microparticles (B), and IgG1 isotype control (C). PE, phycoerythrin.

AFM vs. flow cytometry

AFM seems to be able to detect nanosized MPs (Figs 2 and 3). To confirm this, isolated MPs were passed through a 0.22-µm filter (Puradisc 30; Whatman Nederland BV., 's-hertogenbosch, the Netherlands). Subsequently, the MPs isolated from the filtrate were used for AFM and flow cytometry measurements. Figure 5 shows that AFM could still detect CD41-positive MPs in the filtrate, with sizes ranging from 10 to 120 nm (mean d_{sph} 37.2 ± 11.6 nm), whereas flow cytometry could not.

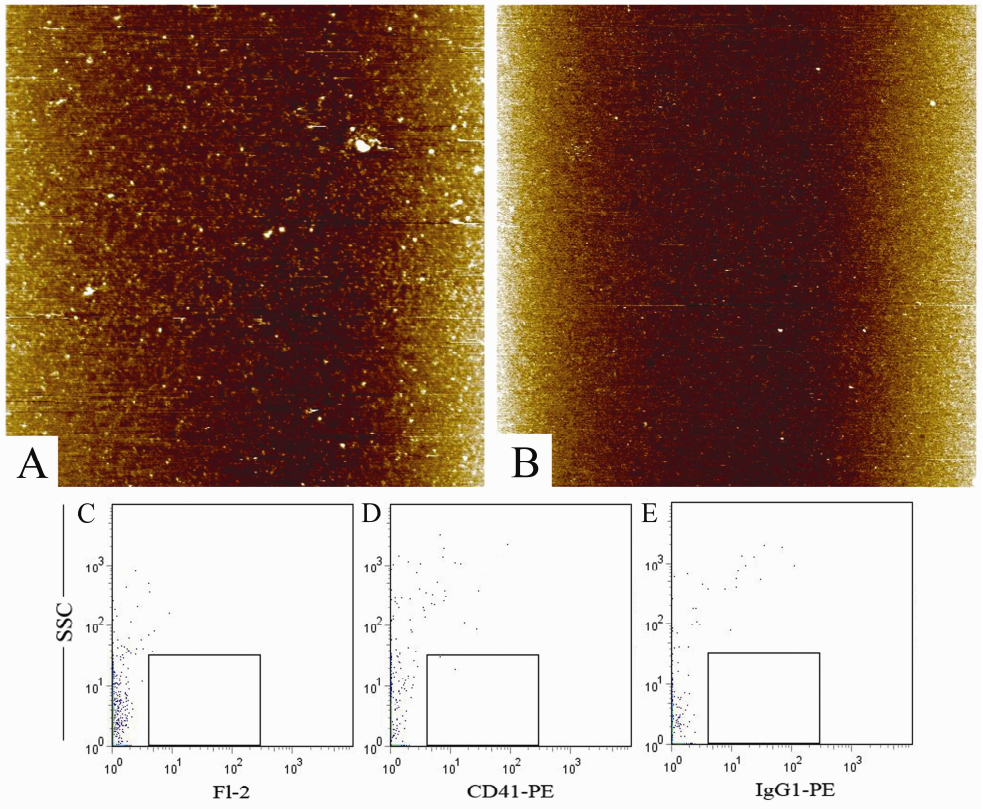


Figure 5. Analysis of isolated microparticles (MPs) after filtration through a 0.22-µm filter by atomic force microscopy (AFM) (A, B) and by flow cytometry (C-E). AFM still detects CD41-positive MPs (A), whereas MPs are hardly found on IgG1-coated mica (B). Flow cytometry fails to detect CD41-positive MPs with sizes below 0.22 µm (D). Controls were Hepes buffer only (C) and MPs labeled with IgG1 isotype control (E). PE, phycoerythrin.

MPs were isolated from fresh PPP of seven donors (MPs 1-7). From one donor, PPP for MP isolation was obtained on three different days (MPs 1a, 1b and 1c). All nine MP preparations were analyzed simultaneously by AFM and flow cytometry for numbers and size distribution of CD41-positive MPs (Table 1).

Depending on the MP preparation, four to 10 images of 100 μm^2 were scanned. About 255 CD41-positive MPs were detected by AFM per 100 μm^2 of anti-CD41-coated mica surface, whereas about 48 MPs per 100 μm^2 attached non-specifically to IgG1 isotype control-coated mica. We found that the number of CD41-positive MPs detected by AFM (3-702 x 10^9 L/PPP) was about 1,000-fold higher than the number of CD41-positive MPs detected by flow cytometry (11-291 x 10^6/L PPP). In all seven donors, the size of the CD41-positive MPs calculated from AFM images ranged from 10 to 475 nm (mean d_{sph} 67.5 ± 26.5 nm). On the IgG1 isotype control-coated mica, particles were found ranging in size from 10 to 200 nm, with the majority of MPs having a d_{sph} of 53.8 ± 13.4 nm. The diameters of particles detected on anti-CD41 antibody-coated mica and on IgG1 isotype control coated mica were not significantly different (P = 0.07).

The interindividual variation in the number of CD41-positive MPs was quite high: 75% for AFM measurements, and 86% for flow cytometry measurements (n = 7).There was only a weak correlation between the numbers of CD41-positive MPs detected with AFM and with flow cytometry (r = 0.17, P > 0.05).

MPs isolated from the blood of three cancer patients were used to measure the number of CD41-positive MPs simultaneously by AFM and flow cytometry (Table 1). MPs were isolated from fresh plasma and analyzed by AFM in three different dilutions, both on CD41-coated mica and on IgG1-coated mica. For all three patients, the number of CD41-positive MPs per 100 μm^2 was linearly related to the concentration of MPs (R2 > 0.95). AFM detected 83-333 x 10^9 CD41-positive MPs/L PPP, whereas flow cytometry detected 98-626 x 10^6 CD41-positive MPs/L PPP (Table 1). The effective diameter of these MPs was 51.4 ± 14.9 nm (range 5-204 nm).

Discussion

In this study, we report a method for the detection of CD41-positive MPs with AFM.We found that the number of CD41-positive MPs detected by AFM was about 1,000-fold higher than the number detected by flow cytometry. Mica modification, and detection of CD41-positive MPs on anti-CD41-coated mica with AFM, resulted in reproducible numbers of CD41-positive MPs (coefficient of variation = 16%).

Table 1. AFM and flow cytometry detection of CD41-positive microparticles (MPs) isolated from fresh PPP

	AFM								Flow cytometry	
	Count/100 µm^2									
	CD41+ MPs			Isotype control (IgG1)			x10^6 CD41+ MPs/L PPP		x10^6 CD41+ MPs/L PPP	
	Total image	Mean	Std	Total image	Mean	Std	Mean	Std	Mean	Std
Donor										
1a	10	92	50	8	23	7	89 654	55 894	63	15
1b	10	100	51	9	12	5	114 029	59 195	82	34
1c	9	582	221	7	45	24	702 201	257 894	161	20
2	6	39	16	1	15	-	3 161	20 326	21	9
3	7	264	81	5	53	7	276 582	95 854	-	-
4	4	352	82	5	63	33	378 043	64 257	11	4
5	9	321	263	9	47	66	358 629	257 217	98	18
6	10	175	113	7	60	18	150 440	123 755	109	30
7	10	371	214	6	112	35	337 899	234 280	291	29
Patient										
1	12	274	21	6	19	3	333 080	23 067	626	153
2	12	73	5	10	10	1	82 512	4 534	98	8
3	10	202	9	10	17	2	241 780	10 001	541	48

AFM quantification is presented as the number of MPs per 100 µm^2 scanned image. For both AFM and flow cytometry measurements, the number of CD41-positive MPs/L PPP was calculated after correction for IgG1 control-bound MPs.

The high interindividual variation in the number of CD41-positive MPs isolated fromfresh PPP (75% for AFM and 86% for flow cytometry) mainly reflects biological variation.

Immobilization of mouse anti-human CD41 antibody and of mouse IgG1 isotype as a control on modified mica was successful. There was a linear relationship between the MP concentration in the sample and the number of CD41-positive MPs detected by AFM up to about 500 CD41-positive MPs per 100 μm^2. Binding of MPs to anti-CD41-coated mica seemed to be specific, as we found many fewer MPs bound to IgG1 isotype control-coated mica (see Table 1). The particles bound to IgG1 isotype control-coated mica had a similar size. We do not know what these objects were. Theoretically, they could be non-specifically bound MPs, (aggregates of) plasma proteins still present in the MP preparation, or even contaminants from the environment. However, the last of these is not likely, because buffer controls were negative (Figure 1C, D).

Guidelines have currently been developed to standardize CD41-positive MP counting by FACS [14]. We have compared the results obtained with our settings on the FACS Calibur with those obtained with an LSRII calibrated following the SSC guidelines. No significant difference in the number of CD41-positive MPs was obtained with the two methods (our setting = 105 x 10^6 CD41-positive MPs/L PPP vs. SSC proposed setting = 109 x 10^6 CD41-positive MPs/L PPP).

Filtration of isolated MPs through a 0.22-µm filter confirmed that AFM detects nanosized CD41-positive MPs (mean d_{sph} 37.2 ± 11.6 nm), whereas flow cytometry does not. This is not due to the flow cytometry settings used, as CD41-positive MPs were detected in the non-filtered MP preparations tested (see Table 1 and Figure 4).

Our results showed that AFM detected 1000-fold higher numbers of CD41-positive MPs than flow cytometry did in all MP preparations. Furthermore, the number of CD41-positive MPs detected by AFM correlated only weakly with those detected by flow cytometry ($r = 0.17$, $P > 0.05$). A similar observation by Zwicker (19) showed that the number of tissue factor-bearing MPs measured by light scatter flow cytometry was 10,000-fold less than what was observed with the use of an impedance-based flow cytometer. Apparently, conventional flow cytometry is not suitable for the detection of nanosized MPs.

The diameter of CD41-positiveMPs isolated from fresh PPP ranged from 10 to 475 nm, with the majority clustering at an effective diameter, d_{sph}, of 67.5 ± 26.5 nm.

The height of MPs bound to mica (z = 17.4 ± 8.6 nm) was approximately 10-fold smaller than their edge-to-edge diameter, d_{flat}, indicating that these MPs were flat, which may be related to the process of binding to the antibody-coated mica surface. Interestingly, Harrison et al. (20) recently reported, in an abstract, similar numbers (~200-260 x 10^9/L) and size distributions (< 50 to> 300 nm) of MPs in plasma, determined with the dynamic light scattering Nanosight LM10 system.

Siedlecki et al. (21) reported that PMPs generated from thrombin-stimulated platelets deposited on glass and measured by AFM had an edge-to-edge diameter of 125 ± 22 nm and a height of 4.1 ± 1.6 nm. We also generated PMPs by stimulating isolated platelets with thrombin. Similar to Siedlecki's results, AFM analysis showed that these contained CD41-positive MPs with an edge-to-edge diameter of 125.3 ± 11.7 nm and a height of 4.3 ± 1.9 nm. The effective diameter of these MPs was 44.1 ± 13.7 nm (range 4-189 nm), corresponding to the effective diameter observed for CD41-positive MPs from fresh PPP.

There is no generally accepted protocol for the isolation of MPs from plasma (12). In this study, fresh PPP was used for isolation of MPs to overcome artefacts of the freeze-thawing procedure (11). We observed that, after freezing and thawing, a decrease in the number of CD41-positive MPs was found by AFM, whereas an increase in the number of MPs was found by flow cytometry. We do not have a satisfactory explanation for this observation, and further investigations will be needed.

Recently, the question has been raised (22) of whether MP preparations might contain exosomes, which are secreted microvesicles formerly present in large multivesicular endosomes. Exosomes have diameters ranging from 30 to 90 nm (23), whereas the effective diameters of the CD41-positive MPs detected by AFM ranged from 10 to 475 nm. Further experiments, which are beyond the scope of the present study, using exosome-specific antibodies such as anti-CD63 and anti-CD81 (23,24), and density-gradient differential ultracentrifugation, are needed to investigate whether a proportion of the MPs isolated from PPP consists of exosomes.

In the present study, we demonstrated that AFM is a suitable method for the sensitive and reproducible detection of CD41-positive MPs, and that their plasma concentration is 1,000-fold higher than measured by conventional flow cytometry. The present AFM method has also its disadvantages, particularly in dealing with large cohorts of plasma samples, as the procedure from blood withdrawal until the AFM measurement and analysis is labour-intensive. Therefore, we are working on modifications that will allow the detection of specific populations of MPs directly in

plasma, to preserve the morphology of MPs and to reduce the time needed for the MP detection.

Acknowledgements

The authors thank M. E. Tesselaar, F. Galli and M. van Es for their excellent technical support. This work was supported by the Dutch Cancer Society (KWF UL 2006-3618).

References

(1) Burnier L, Fontana P, Kwak BR, Angelillo-Scherrer A. Cell-derived microparticles in haemostasis and vascular medicine. Thromb Haemost 2009;101:439-451.
(2) Castellana D, Kunzelmann C, Freyssinet JM. Pathophysiologic significance of procoagulant microvesicles in cancer disease and progression. Hamostaseologie 2009;29:51-57.
(3) Horstman LL, Ahn YS. Platelet microparticles: a wide-angle perspective. Crit Rev Oncol Hematol 1999;30:111-142.
(4) Tesselaar ME, Romijn FP, van der Linden IK, Prins FA, Bertina RM, Osanto S. Microparticle-associated tissue factor activity: a link between cancer and thrombosis? J Thromb Haemost 2007;5:520-527.
(5) Hron G, Kollars M, Weber H, Sagaster V, Quehenberger P, Eichinger S, et al. Tissue factor-positive microparticles: Cellular origin and association with coagulation activation in patients with colorectal cancer. Thromb Haemost 2007;97:119-123.
(6) Bidot L, Jy W, Bidot C, Jr., Jimenez JJ, Fontana V, Horstman LL, et al. Microparticle-mediated thrombin generation assay: increased activity in patients with recurrent thrombosis. J Thromb Haemost 2008;6:913-919.
(7) Habib A, Kunzelmann C, Shamseddeen W, Zobairi F, Freyssinet JM, Taher A. Elevated levels of circulating procoagulant microparticles in patients with beta-thalassemia intermedia. Haematologica 2008;93:941-942.
(8) VanWijk MJ, VanBavel E, Sturk A, Nieuwland R. Microparticles in cardiovascular diseases. Cardiovasc Res 2003;59:277-287.
(9) Zwaal RF, Comfurius P, Bevers EM. Surface exposure of phosphatidylserine in pathological cells. Cell Mol Life Sci 2005;62:971-988.
(10) Hugel B, Martinez MC, Kunzelmann C, Freyssinet JM. Membrane microparticles: two sides of the coin. Physiology (Bethesda) 2005;20:22-227.
(11) Jy W, Horstman LL, Jimenez JJ, Ahn YS, Biro E, Nieuwland R, et al. Measuring circulating cell-derived microparticles. J Thromb Haemost 2004;2:1842-1843.
(12) Enjeti AK, Lincz LF, Seldon M. Detection and measurement of microparticles: an evolving research tool for vascular biology. Semin Thromb Hemost 2007;33:771-779.
(13) Furie B, Furie BC. Cancer-associated thrombosis. Blood Cells Mol Dis 2006;36:177-181.
(14) Robert S, Poncelet P, Lacroix R, Arnaud L, Giraudo L, Hauchard A, et al. Standardization of platelet-derived microparticle counting using calibrated beads and a Cytomics FC500 routine flow cytometer: a first step towards multicenter studies? J Thromb Haemost 2009;7:190-197.
(15) Parot P, Dufrene YF, Hinterdorfer P, Le Grimellec C, Navajas D, Pellequer JL, et al. Past, present and future of atomic force microscopy in life sciences and medicine. J Mol Recognit 2007;20:418-431.
(16) Klein DC, Stroh CM, Jensenius H, van Es M, Kamruzzahan AS, Stamouli A, et al. Covalent immobilization of single proteins on mica for molecular recognition force microscopy. Chemphyschem 2003;4:1367-1371.

(17) Radmacher M, Tillmann RW, Fritz M, Gaub HE. From Molecules to Cells - Imaging Soft Samples with the Atomic Force Microscope. Science 1992;257:1900-1905.

(18) Muller DJ, Amrein M, Engel A. Adsorption of biological molecules to a solid support for scanning probe microscopy. J Struct Biol 1997;119:172-188.

(19) Zwicker JI. Tissue factor-bearing microparticles and cancer. Semin Thromb Hemost 2008;34:195-198.

(20) Harrison P, Dragovic R, Albanyan A, Lawrie AS, Murphy M, Sargent I. Application of dynamic light scattering to the measurement of microparticles. J Thromb Haemost 2009;7(Suppl):OC-TU-056.

(21) Siedlecki CA, Wang IW, Higashi JM, Kottke-Marchant K, Marchant RE. Platelet-derived microparticles on synthetic surfaces observed by atomic force microscopy and fluorescence microscopy. Biomaterials 1999;20:1521-1529.

(21) Horstman LL, Jy W, Minagar A, Bidot CJ, Jimenez JJ, Alexander JS, et al. Cell-derived microparticles and exosomes in neuroinflammatory disorders. Int Rev Neurobiol 2007;79:227-268.

(22) Thery C, Zitvogel L, Amigorena S. Exosomes: composition, biogenesis and function. Nat Rev Immunol 2002;2:569-579.

(23) Heijnen HF, Schiel AE, Fijnheer R, Geuze HJ, Sixma JJ. Activated platelets release two types of membrane vesicles: microvesicles by surface shedding and exosomes derived from exocytosis of multivesicular bodies and alpha-granules. Blood 1999;94:3791-3799.

CHAPTER 4

The detection of tissue factor bearing-microparticles by atomic force microscopy

Yuana Yuana, Nicole de Groot, Rogier M. Bertina,
Tjerk H. Oosterkamp and Susanne Osanto

Partially published in: Nanomedicine and the Cardiovascular System.
Science Publishers 2011.

Abstract

TF associated with cell-derived vesicles (MPs) in blood has been shown to be involved in (cardio) vascular disorders, inflammation, and cancer. However, such studies have been hampered by the lack of methods for the sensitive detection and accurate quantification of MPs. In a previous study, our group demonstrated that atomic force microscopy (AFM) can be used to sensitively detect and accurately quantify a specific subset of MPs.

In the current study, we investigated whether TF-bearing MPs could be captured on mica coated with anti-TF antibody and sensitively be detected by AFM operated in fluid tapping mode. MPs derived from the supernatant of MDA-MB231 cells stimulated with calcium ionophore were used as an experimental model. We showed that FITC-labelled anti-TF monoclonal antibody (MoAb) evenly coated the surface of modified mica. This coated surface captured TF-positive MPs which have diameters (d_{sph}) ranging from 6-296 nm (median: 40.4 nm; mean: 46.4 ± 26.0 nm). These MPs were virtually absent on the mica surface coated with FITC-labelled mouse IgG1 isotype control MoAb. Numbers of TF-positive MPs were 2,000-fold higher than those measured by flow cytometry (8×10^6 per µL supernatant vs. 4×10^3 per µL supernatant).

In conclusion, AFM provides a sensitive detection of TF-positive MPs. We propose that this method may be used for the detection of TF-positive MPs in patient samples.

Introduction

The role of tissue factor (TF) as the major player in initiation of blood coagulation has been known for more than 100 years (1). TF is a 47 kDa transmembrane glycoprotein consisting of 263 amino acids: 219 amino acids on the extracellular domain, 23 amino acids on the transmembrane domain, and 21 amino acids on the cytoplasmic tail.

TF is normally not expressed by cells within the vasculature; rather, it is found predominantly in the adventitial and much less within the medial layers around blood vessels (2). Later, fibroblasts, adipocytes (3) and pericytes (4) were also shown to constitutively express TF. Smooth muscle cells, endothelial cells, and peripheral blood mononuclear cells (e.g. monocytes, neutrophils) do not express TF constitutively, but TF expression can be induced in these cells *in vitro* and *in vivo* by various agonists (5;6). Most of the TF antigen in plasma is encrypted and not biologically active (7;8). In 1999 Giessen et al (9) demonstrated the presence of TF antigen and activity on monocytes, neutrophils, and cell-derived vesicles (also named 'blood-borne TF') in blood and plasma of healthy volunteers. In the mouse model TF-bearing vesicles have been shown to bind to the developing thrombus and play a role in the propagation of the fibrin clot (10;11). These vesicles, later known as microparticles (MPs) based on their submicron diameter, express protein surface antigens from the parent cells from which they are derived (12;13).

In recent years, blood MPs have increasingly received attention as potential biomarkers in the diagnosis and prognosis of disease (12-14). However, such studies have been hampered by the lack of methods for the sensitive detection and accurate quantification of MPs and also by variations in pre-analytical conditions related to plasma and MPs preparation (15;16).

New methods to provide sensitive detection of MPs have been proposed (17). By using an impedance-based flow cytometer, Zwicker et al (18) characterized TF-bearing MPs in plasma of cancer patients. Harrison et al (19) used a nanoparticle tracking analysis to measure MPs size distribution and quantify MPs in isolated MPs fraction and platelet-poor plasma (PPP). Our group (20) has chosen atomic force microscopy (AFM) operated in fluid tapping mode to analyse a defined subset of MPs (platelet MPs) in the MPs isolated from PPP. We demonstrated that AFM detects 1,000-fold more CD41-positive MPs than conventional flow cytometry, a commonly used method for MPs detection, and that the size of the majority of these MPs (mean d_{sph}: 67.5 ± 26.5 nm) is well below the detection limit of conventional flow cytometry.

In the current study, we investigated whether TF-bearing MPs could be captured on mica coated with anti-TF antibody and detected by AFM operated in fluid tapping mode. The number of TF-bearing MPs in plasma of healthy subject is low (18;21). Therefore, as an experimental model we used TF-bearing MPs isolated from the supernatant of cultured breast carcinoma cells (MDA-MB-231), which constitutively express TF, and were stimulated with calcium ionophore.

Assuming a spherical shape of unbound MPs, we found that the calculated diameter (d_{sph}) of TF-positive MPs ranged from 6-296 nm (median: 40.4 nm; mean: 46.4 ± 26.0 nm) in the supernatant of MDA-MB231 cells stimulated with calcium ionophore. These MPs were barely found attached on IgG1 isotype control-coated mica. We propose AFM as a suitable method for the detection and analysis of TF-positive MPs.

Materials and methods

Cell culture

Breast carcinoma cell line, MDA-MB-231, was cultured in DMEM (Invitrogen, Breda, The Netherlands) with 10% fetal bovine serum (Invitrogen), 1% L-glutamine (Lonza, Cologne, Germany) and 1% Penicillin/Streptomycin (Invitrogen) at 37ºC in an incubator with humidified atmosphere under 5% CO_2. Cells at 80% confluence were subcultured twice a week.

Generation and isolation of microparticles

Cells grown at 80% confluence in a T75 flask (Greiner Bio One, Alphen a/d Rijn, The Netherlands) were used for the experiment. To stimulate cells with calcium ionophore (A23187, VWR International, Amsterdam, The Netherlands), the culture medium was removed from the cells and cells were washed twice with Hank's buffered salt solution (HBSS) without $CaCl_2$ (Sigma-Aldrich Chemie, Zwijndrecht, The Netherlands). Next, 10 mL of Dulbecco's modified eagle medium (DMEM) containing 10 µM calcium ionophore was added to the cells. Cells were placed at 37°C in the incubator for 30 minutes.

After stimulation, the culture medium was collected and centrifuged for 20 minutes at 2,000g, at room temperature (RT) without brake to remove dead cells and debris. The supernatant was collected, aliquoted in 1 mL-portions and centrifuged for 30 minutes at 18,890g at RT with minimum brake. The supernatant was discarded except for the 25 µL containing the MPs pellet. The MPs pellets isolated from 3 mL supernatant were pooled, resuspended in 1 mL Hepes buffer [10 mM

Hepes (Merck, Darmstad, Germany), 137 mM NaCl (Merck), 4 mM KCl (Merck), 0.1 mM Pefabloc SC (Fluka, Munich, Germany), pH 7.4], and centrifuged for 30 minutes at 18,890g at RT with minimum brake. The supernatant was discarded except for the 25 µL containing the MPs pellet. These preparations were used immediately or snap-frozen in liquid nitrogen and stored at –80ºC.

Flow cytometry analysis of TF-positive microparticles

Flow cytometry analysis was performed using a FACS Calibur flow cytometer with CELLQUEST PRO software (Becton Dickinson, CA, USA). Five µL of MPs fraction was incubated with 5 µL of fluorescein (FITC)-labelled mouse anti-human TF monoclonal antibody (MoAb) (clone CLB/TF-5, Sanquin, Amsterdam, The Netherlands) and 5 µL of allophycocyanin (APC)-labelled annexin V (Caltag Laboratories,CA, USA) in 35 µL of Hepes buffer containing 2.5 mM $CaCl_2$ (Sigma Aldrich) for 30 minutes, in the dark, at RT. Anti-human TF-FITC MoAb was 20 times diluted, whereas annexin V-APC was 300 times diluted in the final mixture. As negative controls, FITC-labelled mouse IgG1 isotype control MoAb (clone X40, Becton Dickinson) was used at the same concentration as FITC-labelled anti-TF MoAb. As a control of annexin V staining, Hepes buffer without $CaCl_2$ was used.

Before flow cytometry measurement, the labelled MPs were diluted with 300 µL of Hepes-citrate buffer. For counting absolute numbers of MPs per µL supernatant, 200 µL of flow cytometry absolute count standard beads (Bang Laboratories, IN, USA) was mixed with Hepes buffer to a volume of 600 µL and then measured in triplicate. For measurement of counting beads as well as MPs, the flow cytometer was programmed to count events in 1 minute.

Modification of mica for immobilization of mouse anti-human TF antibody

The surface of mica was modified as described by Yuana et al (20). Fifty µL of FITC-labelled mouse anti-human TF MoAb (clone CLB/TF-5, Sanquin) (0.1 mg/mL) was applied onto the modified mica and incubated for 30 minutes at RT. Excess of FITC-labelled anti-human TF MoAb was removed by washing with Hepes buffer. As a negative control, FITC-labelled mouse IgG1 isotype control MoAb (clone X40, Becton Dickinson) was used at the same concentration of 0.1 mg/mL.

AFM analysis of TF-positive microparticles

Frozen MPs isolated from the supernatant of MDA-MB231 cells stimulated with calcium ionophore were quickly thawed at 37ºC, diluted 2 times with Hepes buffer, and used immediately for AFM measurement. Twenty µL of the MPs fraction was

applied to the FITC labelled-anti-human TF and IgG1 isotype control-coated mica surfaces and incubated for 30 minutes. To remove unbound MPs, the mica was washed twice with Hepes buffer. During the incubation step and before imaging, the mica surface was kept in a closed container. AFM imaging, image analysis, and calculation of diameter of MPs were performed as described by Yuana et al (20). For each sample, the mica surface was scanned at different positions to obtain 10 images with a scan size of 100 μm^2.

Results and discussions

Flow cytometry

Using flow cytometry we compared the number of MPs and the expression of TF and annexin V on MPs in fresh and frozen-thawed MPs fractions isolated from the supernatant of MDA-MB231 stimulated with calcium ionophore. MPs detected in fresh and frozen-thawed fractions expressed both TF and annexin V (Table 1). We observed about a 2-fold decrease in the total number of MPs, TF-positive MPs, and annexin V-positive MPs after one freeze-thaw cycle. In contrast to what is observed in plasma, depending on the centrifugation speed used for plasma isolation, some groups observed an increase in the number of platelet MPs and annexin V-positive MPs caused by freezing and thawing the plasma (22-24).

Table 1. Flow cytometry analysis of MPs from fresh and frozen-thawed MP fractions isolated from supernatant of MDA-MB231 cells stimulated with calcium ionophore.

Flow cytometry analysis	**Fresh**		**Frozen-thawed**	
	Per µL supernatant	**%**	**Per µL supernatant**	**%**
Total MPs	1,1725		7,479	
TF-positive MPs	10,293	88	4,076	55
Annexin V-positive MPs	8,794	75	3,416	46
TF and annexin V-positive MPs	5,870	50	3,248	43

In fresh and frozen-thawed MPs fractions, flow cyotmetry measured the total number of MPs, TF and annexin V-positive MPs per µL supernatant of MDA-MB231 cells after stimulation with 10 µM calcium ionophore for 30 minutes and also the percentage of TF- and annexin V-positive MPs. Experiments were performed in duplicate.

AFM

Before antibody was immobilized to the modified mica surface, we first scanned the surfaces of the cleaved mica and the modified mica by AFM. The surface topography of cleaved mica was flat (height (z): ~0.1 nm) and after modification, the mica surface was still flat, with an apparent height of less than 0.5 nm (Figure 1A).

Immobilization of the anti-human TF MoAb on the modified mica surface should be optimal and evenly distributed over the surface. In our previous study (20), we found that for immobilizing the anti-human CD41 MoAb a concentration of 0.01 mg/mL was needed for the optimal capture of CD41-positive MPs on the mica surface (100 μm^2). Therefore, we tested different concentrations of unlabelled mouse anti-human TF MoAb (clone CLB/TF-5, Sanquin), 0.01, 0.02, 0.1, and 0.2 mg/mL, to coat the modified mica surface. It appeared that at 0.01 and 0.02 mg/mL anti-human TF the antibody did not distribute homogenously on the mica surface (100 μm^2). There were also small protein aggregates found and the number of these aggregates increased with increasing concentration of anti-TF (0.1 and 0.2 mg/mL) used. Apparently this particular anti TF was not suitable for the production of homogeneously coated mica surfaces.

Subsequently we compared the unlabelled anti-human TF MoAb with the FITC-labelled anti-human TF MoAb from the same manufacturer. Similar to our previous observation, unlabelled anti-human TF MoAb (0.1 mg/mL) formed aggregates on the mica surface (Figure 1B). The surface topography of aggregates was 20 nm (Figure 1B, z_1), whereas that of a single molecule of anti-TF was 5 nm (Figure 1B, z_2). In contrast, FITC-labelled anti-human TF MoAb (0.1 mg/mL) coated the mica surface evenly without any aggregates and has an apparent height of 4.9 nm (Figure 1C). As a negative control, FITC-labelled mouse IgG1 isotype control MoAb (0.1 mg/mL) was immobilized on the modified mica (Figure 1D, z= 1 nm). Possibly, the FITC molecules attached to the anti-TF IgG create a spacer between anti-TF molecules in the solution which prevents aggregation.

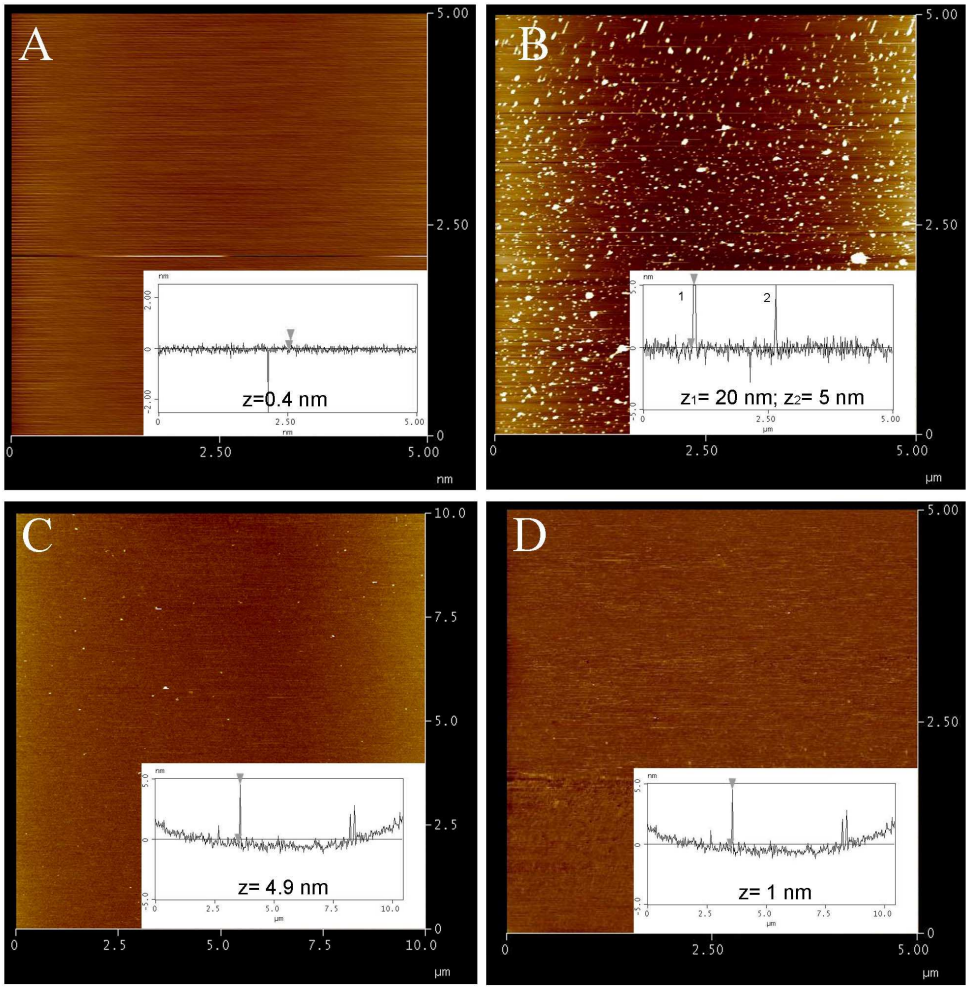


Figure. 1. AFM images showing the three-dimensional surface topography of (A) modified mica, (B) unlabelled anti-TF MoAb-coated mica (0.1 mg/mL), (C) FITC-labelled anti-TF MoAb-coated mica (0.1 mg/mL), and (D) FITC-labelled IgG1 isotype control MoAb-coated mica (0.1 mg/mL). Inserts show the results of the height analysis (z) of the surfaces.

After the mica surface was coated with FITC-labelled anti-human TF MoAb, frozen-thawed MPs were applied. FACS analysis showed that about 50% of the MPs in the frozen-thawed fraction still express TF (Table 1). As expected, three-dimensional AFM topography also showed that there were MPs captured on the mica surface coated with FITC-labelled anti-human TF MoAb (Figure 2A), whereas these were virtually absent on the mica surface coated with FITC-labelled mouse IgG1 isotype control (Figure 2B).

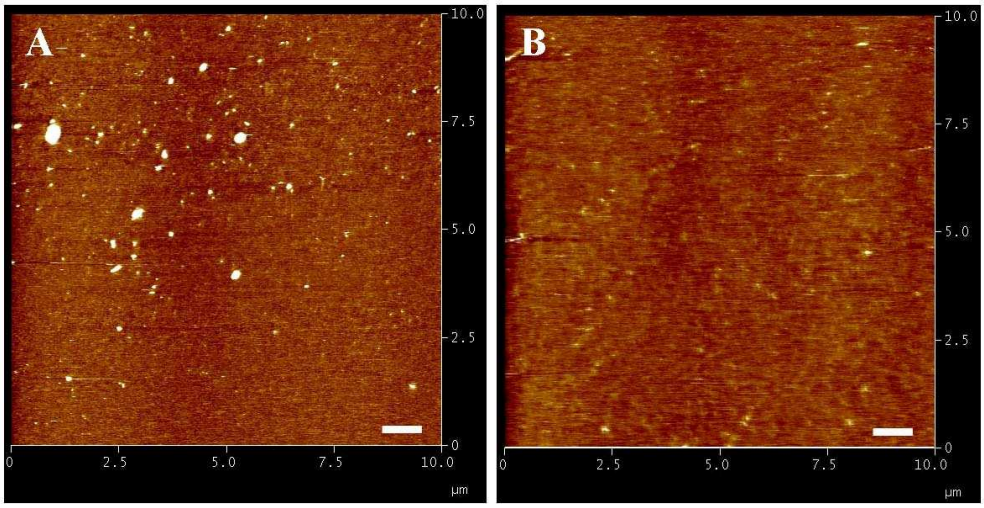


Figure 2. Three-dimensional AFM topography of MPs bound to (A) FITC-labelled anti-TF coated mica and (B) FITC-labelled isotype control (IgG1)-coated mica. The scale bar in these images is 1 µm.

The size of the TF-positive MPs calculated from the AFM images ranged from 6 to 296 nm (median d_{sph}: 40.4 nm; mean d_{sph}: 46.4 ± 26.0 nm) (Figure 3). About 113 TF-positive MPs were detected by AFM per 100 µm^2 of FITC-labelled anti-TF-coated mica surface, whereas about 11 MPs per 100 µm^2 attached non-specifically to FITC-labelled IgG1 isotype control-coated mica (Figure 3). After correction for the number of MPs found on FITC-labelled-IgG1 control-coated mica, the total number of TF-positive MPs detected by AFM is 8 x 10^6 per µL supernatant. This number is 2,000-fold higher than the number of TF-positive MPs from the same MPs preparation detected by flow cytometry (4 x 10^3 per µL supernatant, Table 1). Interestingly, we previously reported that AFM detects 1,000-fold more CD41-positive MPs than flow cytometry (20).

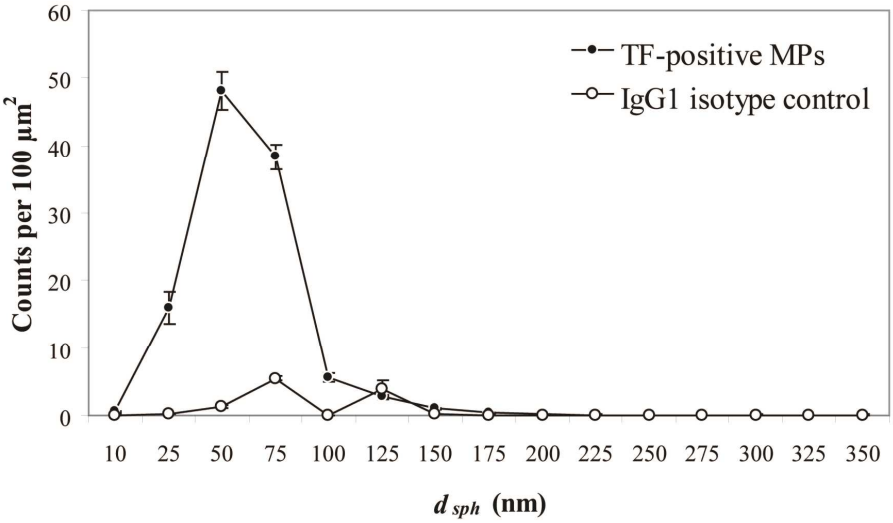


Figure 3. Size distribution (d_{sph}) and counts of TF-positive MPs per 100 µm^2 surface area.

Conclusions

The results of this study show that FITC-labelled mouse anti-human TF MoAb at a concentration of 0.1 mg/mL coated the modified mica surface homogenously. This coated surface could capture TF-positive MPs isolated from the supernatant of MDA-MB231 stimulated with calcium ionophore. AFM operated in fluid tapping mode sensitively detected MPs with sizes ranging from 6 to 296 nm (median d_{sph}: 40.4 nm; mean d_{sph} 46.4 ± 26.0 nm). There were only about 11 MPs captured on the mica surface coated with FITC-labelled mouse IgG1 isotype control MoAb. Numbers of TF-positive MPs were 2,000-fold higher than those measured by flow cytometry (8 x 10^6 per µL supernatant vs. 4 x 10^3 per µL supernatant). In this study, we frozen-thawed MPs isolated from cell culture supernatant for the AFM measurement. However, when a precise quantification of the number of TF-positive MPs in the sample is needed, AFM measurement on freshly prepared samples is preferred.

Acknowledgments

This work was supported by the Dutch Cancer Society (KWF UL 2006-3618). The authors thank Dr. F. Galli for the excellent technical support.

References

(1) Bachli E. History of tissue factor. Br J Haematol 2000;110:248-255.

(2) Drake TA, Morrissey JH, Edgington TS. Selective cellular expression of tissue factor in human tissues. Implications for disorders of hemostasis and thrombosis. Am J Pathol 1989;134:1087-1097.

(3) Wilcox JN, Smith KM, Schwartz SM, Gordon D. Localization of tissue factor in the normal vessel wall and in the atherosclerotic plaque. Proc Natl Acad Sci U S A 1989;86:2839-2843.

(4) Bouchard BA, Shatos MA, Tracy PB. Human brain pericytes differentially regulate expression of procoagulant enzyme complexes comprising the extrinsic pathway of blood coagulation. Arterioscler Thromb Vasc Biol 1997;17:1-9.

(5) Daubie V, Pochet R, Houard S, Philippart P. Tissue factor: a mini-review. J Tissue Eng Regen Med 2007;1:161-169.

(6) Mackman N, Tilley RE, Key NS. Role of the extrinsic pathway of blood coagulation in hemostasis and thrombosis. Arterioscler Thromb Vasc Biol 2007;27:1687-1693.

(7) Bach RR. Tissue factor encryption. Arterioscler Thromb Vasc Biol 2006;26:456-461.

(8) Versteeg HH, Ruf W. Tissue factor coagulant function is enhanced by protein-disulfide isomerase independent of oxidoreductase activity. J Biol Chem 2007;282:25416-25424.

(9) Giesen PL, Rauch U, Bohrmann B, Kling D, Roque M, Fallon JT, et al. Blood-borne tissue factor: another view of thrombosis. Proc Natl Acad Sci U S A 1999;96:2311-2315.

(10) Falati S, Liu Q, Gross P, Merrill-Skoloff G, Chou J, Vandendries E, et al. Accumulation of tissue factor into developing thrombi in vivo is dependent upon microparticle P-selectin glycoprotein ligand 1 and platelet P-selectin. J Exp Med 2003;197:1585-1598.

(11) Chou J, Mackman N, Merrill-Skoloff G, Pedersen B, Furie BC, Furie B. Hematopoietic cell-derived microparticle tissue factor contributes to fibrin formation during thrombus propagation. Blood 2004;104:3190-3197.

(12) Burnier L, Fontana P, Kwak BR, Angelillo-Scherrer A. Cell-derived microparticles in haemostasis and vascular medicine. Thromb Haemost 2009;101:439-451.

(13) Anderson HC, Mulhall D, Garimella R. Role of extracellular membrane vesicles in the pathogenesis of various diseases, including cancer, renal diseases, atherosclerosis, and arthritis. Lab Invest 2010;90:1549-1557.

(14) Piccin A, Murphy WG, Smith OP. Circulating microparticles: pathophysiology and clinical implications. Blood Rev 2007;21:157-171.

(15) Yuana Y, Bertina RM, Osanto S. Pre-analytical and analytical issues in the analysis of blood microparticles. Thromb Haemost 2010;2105.

(16) Enjeti AK, Lincz LF, Seldon M. Detection and measurement of microparticles: an evolving research tool for vascular biology. Semin Thromb Hemost 2007;33:771-779.

(17) Van Der Pol E, Hoekstra AG, Sturk A, Otto C, Van Leeuwen TG, Nieuwland R. Optical and non-optical methods for detection and characterization of microparticles and exosomes. J Thromb Haemost 2010;8:2596-2607.

(18) Zwicker JI, Liebman HA, Neuberg D, Lacroix R, Bauer KA, Furie BC, et al. Tumor-derived tissue factor-bearing microparticles are associated with venous thromboembolic events in malignancy. Clin Cancer Res 2009;15:6830-6840.

(19) Harrison P, Dragovic R, Albanyan A, Lawrie AS, Murphy M, Sargent I. Application of dynamic light scattering to the measurement of microparticles. J Thromb Haemost 7(Suppl):OC-TU-056.

(20) Yuana Y, Oosterkamp TH, Bahatyrova S, Ashcroft B, Garcia RP, Bertina RM, et al. Atomic force microscopy: a novel approach to the detection of nanosized blood microparticles. J Thromb Haemost 2010;8:315-323.

(21) Tesselaar ME, Romijn FP, van der Linden IK, Prins FA, Bertina RM, Osanto S. Microparticle-associated tissue factor activity: a link between cancer and thrombosis? J Thromb Haemost 2007;5:520-527.

(22) Weber H, Kollars M, Kyrle PA, Weltermann A. Comparison of different methods for isolation and storage of microparticles from human blood. J Thromb Haemost 2007;5(suppl 2):P-M-445.

(23) Trummer A, De Rop C, Tiede A, Ganser A, Eisert R. Recovery and composition of microparticles after snap-freezing depends on thawing temperature. Blood Coagulation & Fibrinolysis 2009;20:52-56.

(24) Mobarrez F, Antovic J, Egberg N, Hansson M, Jorneskog G, Hultenby K, et al. A multicolor flow cytometric assay for measurement of platelet-derived microparticles. Thromb Res 2010;125:e110-e116.

CHAPTER 5

Determination of the size distribution of blood microparticles directly in plasma using atomic force microscopy and microfluidics

Brian A. Ashcroft*, Jan de Sonneville*, Yuana Yuana*, Susanne Osanto, Rogier M. Bertina, Maxim E. Kuil and Tjerk H. Oosterkamp

*These authors contributed equally to this work

Submitted for publication

Abstract

Microparticles, also known as microvesicles, found in blood plasma, urine, and most other body fluids, may serve as valuable biomarkers of diseases such as cardiovascular diseases, systemic inflammatory disease, thrombosis, and cancer. Unfortunately, the detection and quantification of microparticles are hampered by the microscopic size of these particles and their relatively low abundance in blood plasma.

The use of a combination of microfluidics and atomic force microscopy to detect microparticles in blood plasma circumvents both problems. In this study, capture of a specific subset of microparticles directly from blood plasma on antibody-coated mica surface is demonstrated. The described method excludes isolation and washing steps to prepare microparticles, improves the detection sensitivity, and yields the size distribution of the captured particles.

The majority of the captured particles have a size ranging from 30 to 90 nm, which is in good agreement with prior results obtained with microparticles immediately isolated from fresh plasma. Furthermore, the qualitative shape of the size distribution of microparticles is shown not to be affected by high-speed centrifugation or the use of the microfluidic circuit, demonstrating the relative stable nature of microparticles *ex vivo*.

Introduction

Blood microparticles (MPs), also known as microvesicles, are small particles shed from the surface of many cells upon stimulation or apoptosis (1). For a long time they were considered as platelet dust (2), but now they have been recognized to participate in important biological processes (3). Examples of such processes are surface-membrane traffic and the horizontal transfer of protein and RNAs among neighboring cells, which are necessary for rapid phenotype adjustments in a variety of conditions (3). In addition, blood MPs have important physiological and pathological roles in blood coagulation, inflammation and tumor progression (4;5).

Flow cytometry (FCM) and capture-based assays are commonly used methods to measure the number of MPs, define their origin based on membrane antigen expression, and asses their procoagulant features (6-8). However, these methods have their drawbacks. FCM employs laser light which excites at 488 nm, while MPs may have sizes far below this wavelength (9). Yuana et al. (10) reported the presence of MPs bearing CD41 antigen in plasma with sizes ranging between 10-475 nm using atomic force microscopy (AFM). They also found that the MP numbers detected by AFM are 1,000-fold higher than those detected by FCM. Although capture-based assays using annexin V or MP-specific antibodies allow high throughput assessment of procoagulant features of MPs (11-13), these assays give no information on the size and total number of MPs in plasma.

Electron microscopy (EM) has been used for detection of MPs (14-16), but this method only provides semi-quantitative information on MPs. Furthermore, sample dehydration and vacuum procedures required in EM might affect the characteristics of MPs. Recently, a promising method, nanoparticle tracking analysis (NTA), has been applied to count MPs in plasma (17). This method uses a CCD camera system that allows simultaneous tracking of multiple particles. In the future NTA may be able to detect, count, and size antibody-labeled MPs efficiently, thus allowing the detection of subsets of MPs.

Not only is the analytical measurement of MPs a challenge, but also there is no golden standard yet to prepare MPs (18). Many studies have isolated MPs from platelet free or platelet poor plasma by applying high speed centrifugation or even ultracentrifugation (19;20). To prevent loss and phenotypic changes of MPs during the isolation procedure, using blood plasma directly for MP measurement would be preferable (21). Furthermore, the time between blood withdrawal and the actual MP test should be as short as possible to avoid activation of cells and coagulation processes which may affect MP numbers and characteristics.

We propose a method to detect MPs directly in blood plasma by using a microfluidic flow cell and performing subsequent analysis using AFM in liquid-tapping mode. Laminar flow patterns within the flow cell ensure complete fluid turnover in a controlled manner. The flow cell allows experimentation with very small sample volumes. In this study, a detachable flow cell was developed to enable direct contact between the fluid in the microfluidic channel and the surface. Diluted plasma was flown through the microfluidic channel with a controlled pressure driven laminar flow and made to be directly in contact with anti-CD41 antibody-coated mica. MPs exposing CD41 antigen were captured on this surface and subsequently imaged by AFM. We employed the AFM method for MP detection previously used in the study of Yuana et al. (10).

Clotting of the plasma and clogging of the microfluidic channel pose a potential problem within such small volumes and with such a sensitive detection method as AFM. These problems have been solved by diluting plasma with either citrate or EDTA-enriched Hepes buffer and coating the microfluidics channels and the tubing of the microfluidics system. We demonstrated that this method increases the sensitivity of detecting specific MPs in a sample 100 to 1,000-fold. In conclusion, the application of a flow cell allows the AFM measurement of a specific subset of MPs directly in blood plasma.

Materials and Methods

Blood collection and plasma preparation

After giving their informed consent, venous blood of three healthy volunteers is collected by using a 21-gauge needle (BD Vacutainer, San Jose, CA) with minimal stasis. Except for the first four ml, the blood is collected either in 1/10 volume of sodium citrate (3.2%, 0.105 M) or in K2 EDTA (3.6 mg) using 4.5 mL BD Vacutainer tubes (Becton Dickinson, San Jose, CA). Within 10-15 minutes after withdrawal, the collected blood is centrifuged at 2,000g for 10 minutes at 20℃, without brake. The supernatant plasma is carefully collected and centrifuged again at 2,000g for 10 minutes, 20℃, without brake, to obtain platelet poor plasma (PPP). PPP was aliquotted in 250 µL portions, snap frozen in liquid N_2, and stored at -80℃ until used. Before used, PPP is quickly frozen-thawed at 37℃. Unless stated otherwise PPP is used in the experiments.

Microparticles isolation

For MP isolation, 750 µL of frozen-thawed citrate PPP is centrifuged at 18,890g

and 20℃ for 30 minutes, with minimum brake. The supernatant is removed carefully, except for 25 µL containing the MP pellet. This pellet is resuspended in 1 mL of Hepes buffer [10 mM Hepes (Merck, Darmstad, Germany), 137 mM NaCl (Merck), 4 mM KCl (Merck), 0.1 mM Pefabloc SC (Fluka, Munich, Germany), pH 7.4], vortexed, and centrifuged as before. The supernatant is removed, leaving a volume of 25 µL containing the MP pellet. Subsequently, this 25 µL is carefully diluted with 725 µL of Hepes buffer to reconstitute to the original plasma volume (750 µL) before use in the experiment.

Flow cell: mold fabrication

A flow cell mold is fabricated from brass. This brass is milled so that ridges with dimensions of 10 mm x 300 µm x 100 µm are created that shape the liquid channels during polymerization. The top surface of the ridges is polished to allow viewing through the channel from bottom to top after molding. At the end of the ridges, small holes are drilled and small pins are inserted with a diameter of 1 mm and a height of about 1 mm.

Flow cell: fabrication

Polydimethylsiloxane (PDMS) flow cells are fabricated using a Sylgard 184 kit (Dow Corning, UK). Silicone primer and catalyst are mixed in a 10:1 ratio by weight and this mixture is placed in a vacuum chamber for 1 hour to remove air bubbles trapped during mixing. Next, the mixture is slowly poured into the mold and then the mold is carefully closed with a glass plate. The mold containing the polymer solution is placed in an oven at 70°C for 1 hour. Afterwards, the glass slide with the PDMS flow cell is released from the mold and covered with a clean glass slide to keep the chip channel area dust-free. The polymerized flow cell is shown in Figure 1A.

Flow cell: setup

The complete microfluidic setup is shown in Figure 1B. To prepare the flow cell setup, a mica surface (1) is placed on a metal support disc (2). The metal support disc is placed onto the bottom plate of the holder device (4), in a small cavity that closely fits the metal disc. The PDMS flow cell (3) is placed onto the top plate with the open microfluidic channels facing down. Two pins, situated in the holder top plate (5) align the flow cell (see the two holes next to the channels in Figure 1A) with respect to the mica surface and the holes for the glass capillaries (7) (TSP Fused Silica Tubing, ID/OD 150/375 micrometer, deactivated with DPTMDS, from

BGB Analytik Vertrieb, Germany). Then the top and bottom plate are pressed onto each other with four screws (6). Using microscopic inspection the screw pressure is carefully adjusted. The glass capillary tubes are beveled to 45 degrees before use, using a mechanical grinder (Michael Deckel S0) with a disc containing diamond dust. After careful rinsing with water, to remove remaining grinding dust, the glass capillary tubes are gently forced into the PDMS flow cell, and guided through alignment holes situated in the holder top plate.

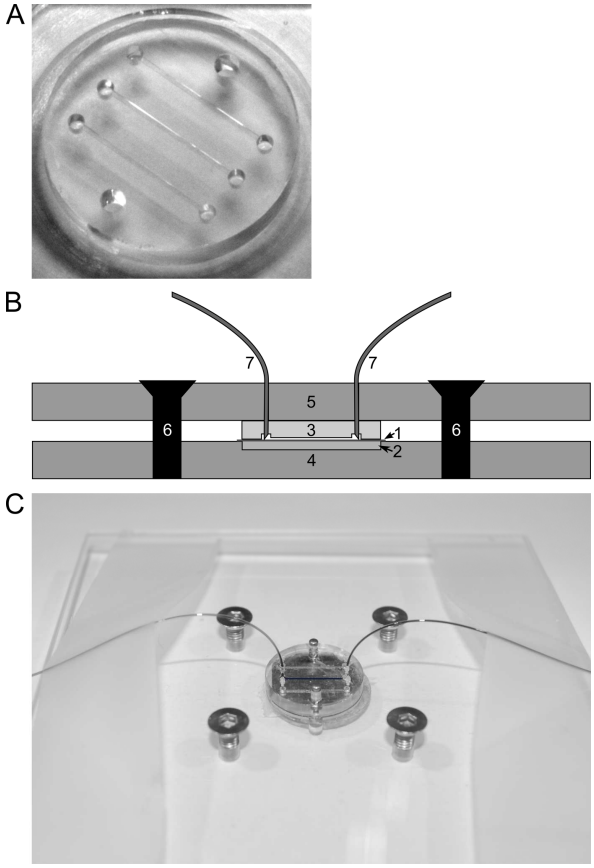


Figure 1. Flow cell setup
(A) Open PDMS flow cell. (B) Microfluidic flow cell setup with schematic side view. The holder system (4,5,6) is used to press the PDMS chip (3) onto the mica surface (1). The glass capillary tubes (7) are guided through holes in the holder top plate (5) to reach the connection chambers in the chip (3). The metal disc (2) is used as a support for the mica surface. In the photo (C), the middle channel is connected and filled with a dark blue solution; the glass capillary tubes are bent towards the side using scotch tape. The blue solution and scotch tape are for illustration purposes and are not used in experiments.

Mica Surface preparation for attachment of anti-human CD41 monoclonal antibody

The surface of mica (Electron Microscopy Sciences, Washington) for MP attachment is prepared as described before (10) with a slight modification. Freshly cleaved mica disks (diameter 12 mm) are overnight immersed in DMSO containing 55% (w/v) ethanolamine at 70℃. Subsequently, the m ica surfaces are rinsed twice with dry DMSO at 70°C and then with HPLC grade ethanol to remove the DMSO. Next, the mica surfaces are put for 10 minutes into 30 mL phosphate buffered potassium (PBK) (10.2 g KCl, 0.97 g $K_2H_2PO_4$ and 5.71 g K_2HPO_4 per L) (pH 7.4) previously saturated with EGTA by adding 100 mg EGTA. The surfaces are then rinsed with Hepes buffer, before 20 µL of 0.05 mg/mL (in Hepes buffer) mouse anti-human CD41 antibody clone P2 (Beckman Coulter, Fullerton, CA) is applied to the surface and incubated for 3 hours. Excess anti-CD41 is removed by washing with Hepes buffer. Anti-CD41 antibody coated-mica surfaces are stored in Hepes buffer until used. As a negative control, mouse IgG1 pure clone X40 (Becton Dickinson, San Jose, CA) is used (0.05 mg/mL in Hepes buffer). The IgG1 isotype control antibody is allowed to incubate for 3 hours on the functionalized mica surfaces. All chemicals are purchased from Sigma Aldrich (Munich, Germany) unless otherwise indicated.

Prior to the attachment of MPs antibody-coated mica surfaces were inspected by using AFM to ensure that the number of false spots and holes in the antibody coating was minimized.

Attachment of microparticles without using microfluidics

PPP (100 µL EDTA plasma) is dropped onto the mica surface coated with IgG1 isotype control and anti-CD41 antibody (“drop method”). To check the saturation of MPs on the anti-CD41-coated surface, PPP is incubated on the surfaces for 2, 30, and 60 minutes. Similar to what was found by Yuana et al (10), 30 minutes incubation seemed to be sufficient. On anti-IgG1-coated surface PPP was incubated for 60 minutes to match the long exposure time on the anti-CD41 surface. The surfaces are carefully rinsed with Hepes buffer and then scanned by AFM to determine the number of MPs captured on CD41- and IgG1 isotype control-coated mica surfaces.

Attachment of microparticles using microfluidic flow cell

The open microfluidic flow cell (PDMS) is attached to a mica surface as described above. A 1 mL-syringe (Becton Dickinson, San Jose, CA, USA) is connected to a

Harvard Apparatus PicoPlus (Harvard apparatus, Holliston, MA, USA) syringe pump and set at a constant flow speed of 0.01 mL/minute. The syringe is connected to the glass capillary tubes using Luer-Lock Adapters and One-Piece Fittings from LabSmith (Livermore, CA, USA). The glass capillary tubes are gently forced into the microfluidic chip using the beveled end.

The channels of the flow cell are rinsed with 50 µl EGTA-enriched Hepes buffer (5 mM EGTA, 10 mM Hepes, 137 mM NaCl, 4 mM KCl, 0.1 mM Pefabloc® SC, pH 7.4) buffer for about 5 minutes. Hundred fifty µL of either EDTA plasma diluted with EDTA-enriched Hepes buffer (20 mM EDTA (Sigma Aldrich), 10mM Hepes, 137 mM NaCl, 4 mM KCl, 0.1 mM Pefabloc® SC, pH 7.4) or isolated MPs diluted with Hepes buffer is allowed to flow through the channel in the flow cell for about 15 minutes total flow time. The channel is then rinsed with 50 µL Hepes buffer (~5 minutes flow time). Before removal from the flow cell, the back of the mica is carefully marked to indicate the location of the channel in the AFM. Subsequently, the flow cell is removed and the coated surface with the attached MPs is rinsed with Hepes buffer and stored in Hepes buffer until imaged by AFM. All steps are performed at room temperature (RT).

AFM imaging

AFM imaging is performed with a Digital Instruments Multi-mode AFM (Veeco, New York, NY, USA) using the E scanner. Olympus cantilevers (Olympus, Tokyo, Japan) with force constant of 2 N/m and a resonant frequency of 70 kHz are used. The liquid cell tip holder (Veeco) is rinsed with ethanol and milli-Q water between each sample to prevent contamination. Each image was scanned at 10 x 10 µm and 10 images are taken at a variety of locations on the surface. For each particle, the sum of pixel heights multiplied by the pixel area is used to estimate a volume and subsequently to calculate its (spherical) diameter.

Results

Generally, glass, polymer or similar materials are used with microfluidics. However, the AFM cantilever must have physical access to the top of the sample and AFM requires an atomically flat background to give the best image of the sample. Mica is preferred surface material because it has distinct atomically flat layers that can be easily separated for cleaning and functionalization. As PDMS binds strongly to mica, the mica surface can be pealed away when the PDMS is removed, ruining the sample. In our study, the mica surface is functionalized with antibodies to produce a hydrophilic mica surface that cannot bind to the PDMS flow cell. Anti human-CD41 antibody was used to coat the functionalized mica to capture platelet

MPs (PMPs) bearing CD41 surface antigen. PMPs constitute 80-95% of blood MPs detected by FCM (22;23). The IgG1 isotype control is used as a control for nonspecific binding of MPs on anti-CD41-coated surface. A schematic overview of the experiment is given in Figure 2. The microfluidic setup used in Figure 2B is constructed from a PDMS flowcell (Figure 1B), attached to the mica surface by a removable holder system (Figure 1B,C) so that the flow cell can be removed from the surface of the sample without damaging either the attached MPs or the mica.

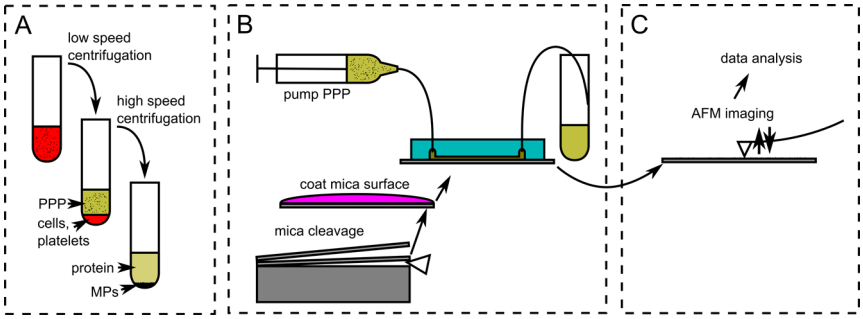


Figure 2. Schematic overview of experiments
Collected blood plasma is centrifuged twice to acquire PPP. In some experiments blood plasma proteins are removed by use of high-speed centrifugation (A). Using an antibody coated mica surface, a fresh PDMS chip and a holder system a microfluidic setup is build, and the PPP is run over a small surface area (B). Finally, mica surface is removed and imaged using AFM, followed by automated image analysis (C).

Application of microfluidic system to count MPs in plasma

With microfluidics many more MPs in the plasma sample will have a chance to interact with the antibody-coated mica surface by flowing an equal volume of plasma over a very small active surface area in the confined volume of the microfluidic channel. To examine this we applied the microfluidic system and compared it with the drop method to count MPs in plasma obtained from two healthy donors. For the microfluidic system two samples were prepared: the first sample consists of MPs isolated from citrate PPP, reconstituted to the original plasma volume, and subsequently diluted 5 times with Hepes buffer; the second sample is EDTA PPP diluted 5 times with EDTA-enriched Hepes buffer. For the drop method undiluted EDTA plasma is used.

In all samples processed by the microfluidic system, the AFM detected MPs attached on anti-CD41-coated mica surface (Table 1). The attachment of these MPs was specific because there were at least two times less particles found attached on the IgG1-coated surface compared to those on the anti-CD41-coated

surface (Table 1). This also confirms that these MPs bear CD41 surface antigen (CD41-positive MPs). Using image quantification software we found in the samples processed by microfluidic system that there is no significant difference in the number of MPs attached on anti-CD41-coated surface (218, 276, 203, and 240 MPs/100 μm^2). Strikingly, there were hardly any MPs captured on anti-CD41 coated-surface by using the drop method, even after one hour incubation of plasma on the surface (3 MPs/100 μm^2 anti-CD41-coated surface and 3 MPs/100 μm^2 IgG1-coated surface, Table 1).

Table 1. Comparison of microfluidic method and drop method to count CD41-positive MPs.

Samples	Number of particles attached on anti-CD41-coated mica		Number of particles attached on IgG1 isotype control-coated mica	
	Mean	SEM	Mean	SEM
Reconstituted isolated-MPs D1	218	51	82	22
Reconstituted isolated-MPs D2	276	50	1.7	0.6
EDTA plasma D1	203	80	70	19
EDTA plasma D2	240	40	1.8	0.04
EDTA plasma drop D1	0.15	0.09	2	0.55
EDTA plasma drop D2	3	1.5	3	1.0

For the microfluidic method MPs isolated from citrate PPP and diluted EDTA PPP of two healthy donors, D1 and D2, were used. Isolated MPs were reconstituted to the original plasma volume and subsequently five-fold diluted in Hepes buffer (Reconstituted isolated-MPs D1/D2). EDTA PPP was diluted five-fold with EDTA-enriched Hepes buffer (EDTA plasma D1/D2). For the drop method undiluted EDTA PPP from the same healthy donors was used (EDTA plasma drop D1/D2).

It has been reported in the literature (24;25) that when EDTA is used as anticoagulant for blood collection, the CD41/CD61 complex on the plasma membrane of platelets may loose their affinity for anti-CD41 and CD61 antibodies. To check this we have used FCM to measure the binding of anti-CD61 and anti-CD41 antibodies to platelet MPs in citrate- and EDTA-anticoagulated blood plasma. We found that the numbers of CD41/CD61-positive MPs in citrate and EDTA plasma are not significantly different (Figure 3).

Despite the fact that macroscopic clotting could be prevented by diluting EDTA PPP with EDTA-enriched Hepes buffer, we noticed in preliminary experiments that there still was some clotting in the small confinements of the microfluidic channel.

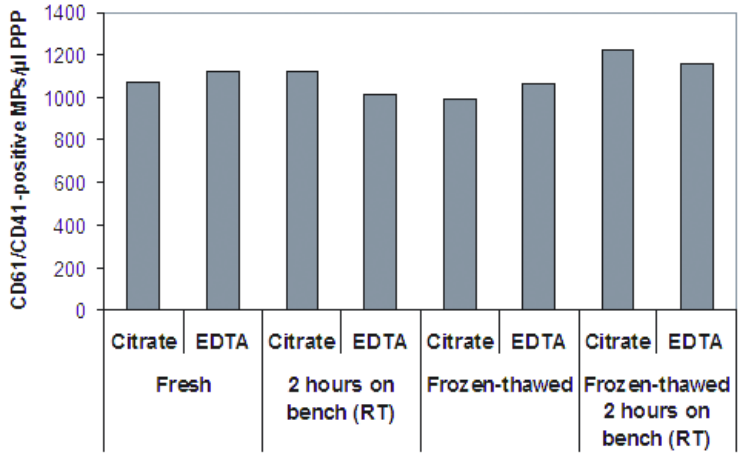


Figure 3. Comparison of CD41/CD61-positive MPs in citrate and EDTA plasma.
EDTA and citrate PPP were isolated from blood of a healthy volunteer. EDTA and citrate PPP are assayed fresh, after storage for 2 hours at room temperature (RT), after frozen-thawed at 37°C, and after frozen-thawed at 37°C and stored for 2 hours at RT. These PPP samples were directly stained by using PE-labeled anti-CD41 and FITC-labeled anti-CD61. The number of CD61/CD41-positive MPs was measured by FCM. All experiments were performed in duplicate.

In some studies it has been shown that unmodified PDMS is not compatible with some of the blood/plasma components and may initiate activation of the clotting system (26;27). Platelets adhere more strongly to the surface of unmodified PDMS than to the modified PDMS (28). Moreover, unmodified PDMS is hydrophobic and this might induce clotting when plasma is introduced in the microfluidic channel (29;30). To prevent this clotting in the microfluidic channels, a solution of EGTA-enriched Hepes buffer was flowed through the channel before application of the plasma. EGTA is also known as a strong chelator of calcium ions, but it is not known to the authors whether the EGTA also can physically be adsorbed on the PDMS, acting to prevent clotting on the surface of the channel, or if EGTA performs its anti-clotting action in some other way.

Analysis of AFM images

The AFM images provide a unique challenge for image processing. As images are generated by scanning line after line, each neighboring line scan can have a different offset, slope or parabolic background (Figure 4A,E). This background must be dealt with for the accurate determination of neighboring scan lines to calculate the heights and volumes of the MPs correctly. The most commonly used techniques involve performing linear regression on the fast scan line and then subtracting the background estimate from each line. This technique is frequently

foiled by small, high features on the surface, such as MPs. To overcome this difficulty, a special technique is developed in our lab. First, a standard linear regression subtraction is performed (Figure 4B,F). Second, Labview IMAQ is used to find all the particles (Figure 4C,G). Third, the regions containing the particles are then removed from the background subtraction input and the linear regression subtraction is performed again to provide a much flatter surface (Figure 4D,H). While this is a computationally expensive task, it provides the high precision background subtraction for the needed accurate determination of the particle volumes.

Particle counting is performed by using the Labview IMAQ library to determine the location of the particles. The Imaq Count Objects 2 VI is first used to filter and obtain a list of possible particles. This software uses a threshold to make a binary image, and then uses the watershed method to count the particles. Particles that touch the boundaries will not be counted. Additionally, all holes within the particles are automatically filled. The lower limit of height, width, and breadth of the particles is set to separate them from the background. For counting, the particle must at least 3 nm high and occupies at least 3 pixels. The particle must be larger than 1 pixel in width or breadth. By setting this limit constant selection rules can be applied throughout a large dataset of AFM images.

As can be deduced from Figure 4 the height is smaller than the width in detected MP profiles, the MPs appear disc shaped after binding to the surface. Using the disc radius and height, the particle volume is estimated and converted into an effective diameter assuming that MP have a spherical shape in solution (10). This procedure ignores the effects of tip flattening. It seems that this does not have a major effect on the final calculated volume of the particles (results not shown), and only a small systematic error exists in the volume calculations from the tip broadening effect. The size distribution of the example image is shown in Figure 4I.

Size distribution graphs are made to further analyze possible differences between MPs captured from diluted isolated MPs and from diluted EDTA plasma, to see if high-speed centrifugation has an effect on the particle size. No significant differences in the number and size distribution of CD41-positive MPs was observed before and after high-speed centrifugation (Table 2, Figure 5). As mentioned before, we do not need to concentrate particles using high-speed centrifugation; however the clotting probability is strongly reduced by removal of blood plasma proteins. Therefore we use purified MPs, reconstituted to the original volume for all further experiments.

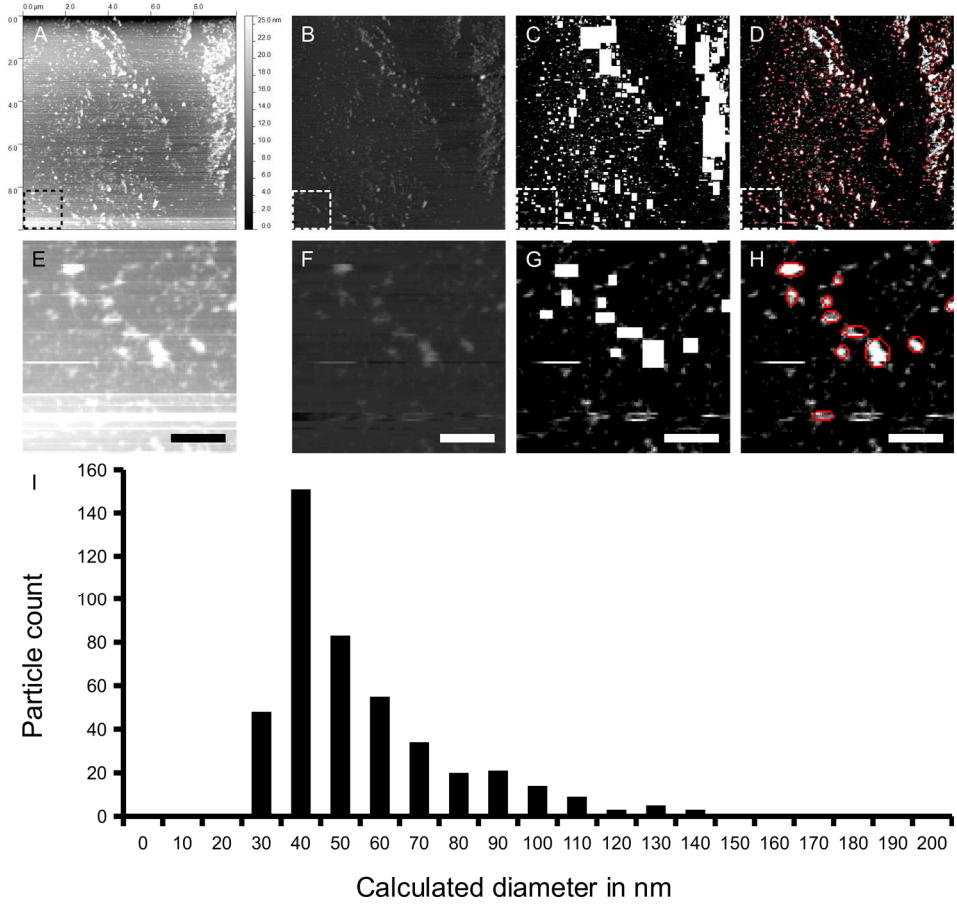


Figure 4. AFM image quantification

Original AFM image, intensity represent height, see scale bar on the right side (A). This image is flattened using the standard linear regression background subtraction (B). White squares show all the particles that are found on the image from image A (C). The background is subtracted, corrected for the shadowed regions, and the particles are correctly sized (D). The bottom row (E,F,G,H) shows an enlarged region of (A,B,C,D) respectively, scale is 500 nm. The measured particles are indicated with red ellipses (D,H). The size distribution graph of particles detected from this image (100 μm^2) is depicted (I).

Table 2. Statistics obtained from comparing distributions of isolated MPs against plasma MPs (see also Figure 5).

	MPs in PPP (plasma MPs)	High-speed centrifuged, washed MPs (isolated MPs)
Number of processed images	8	9
Number of particles	1992	527
Mean*	58	63
Median*	52	50
Standard deviation*	23	43
Range*	223	367
Min*	26	23
Max*	249	390

*Values based on calculated particle diameter in nanometer

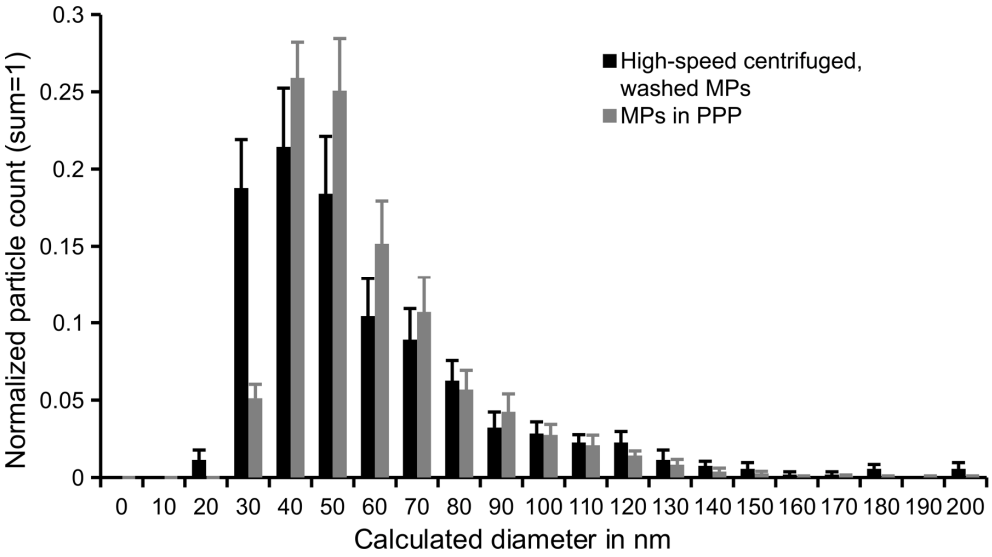


Figure 5. Distributions of the effective diameter of CD41-positive MPs.
Black bars show the size distribution of particles captured from MPs isolated from frozen-thawed citrate PPP. Grey bars show sizes of particles captured from frozen-thawed EDTA PPP diluted five-fold with EDTA-enriched Hepes buffer. All counts are normalized so the sum of the probabilities is 1.

Relationship between MP concentration and number of MPs captured on anti-CD41-coated surface

Prior to measuring the concentration of MPs in a sample, the dynamic range should first be established. Therefore we used MPs isolated from frozen-thawed citrate PPP of a healthy volunteer. Isolated MPs are first reconstituted with Hepes buffer to reach the original plasma volume before isolation (100%) and subsequently diluted 2 to 40-fold. These diluted MP fractions are run through the microfluidics system to measure the number of captured CD41-positive MPs. Figure 6A shows that only at sufficiently low concentrations (<10%) there is a linear relationship between the MP concentration and the number of particles attached on the anti-CD41-coated surface. Probably because of unspecified binding in the microfluidics circuit the line does not cross the origin (0,0). At higher concentrations (>10%) the number of MPs captured to the anti-CD41-coated surface reaches a maximum of ~250 particles/100 μm^2. This number of captured MPs is very similar to those reported in Table 1 for the reconstituted isolated MP fraction and EDTA plasma which are diluted 5 times before processing with the microfluidic system.

The AFM images show that, typically, the particles are not uniformly distributed on the surface (Figure 4A). As a result, the standard error of the mean is quite large (Figure 6A). The linear range is rather small, and it may be difficult to find a suitable working range when samples differ as strongly in particle counts as mentioned before (10). Interestingly, it is found that the size distribution does not differ significantly between different images (Figure 6B), and different dilutions (Figure 6C, Table 3) of the same sample, with the exception of the highest dilution. This sets microfluidic capture combined with AFM imaging as the first method able to measure the size distribution of a specific subset of MPs directly in PPP.

Discussion

We report on a novel method to identify and characterize a specific subset of MPs directly in plasma. To enable the measurement of MPs directly in plasma, we have developed a method that combines a microfluidic system and AFM detection. Microfluidic channels allow blood plasma to flow over a small surface of antibody coated mica, resulting in a high enough surface concentration of specifically bound MPs to detect and quantify using AFM. A much higher number of MPs is captured from (diluted) plasma on antibody-coated mica than without, using this microfluidic method (plasma drop system). Further optimization of the method is required for high-throughput measurements.

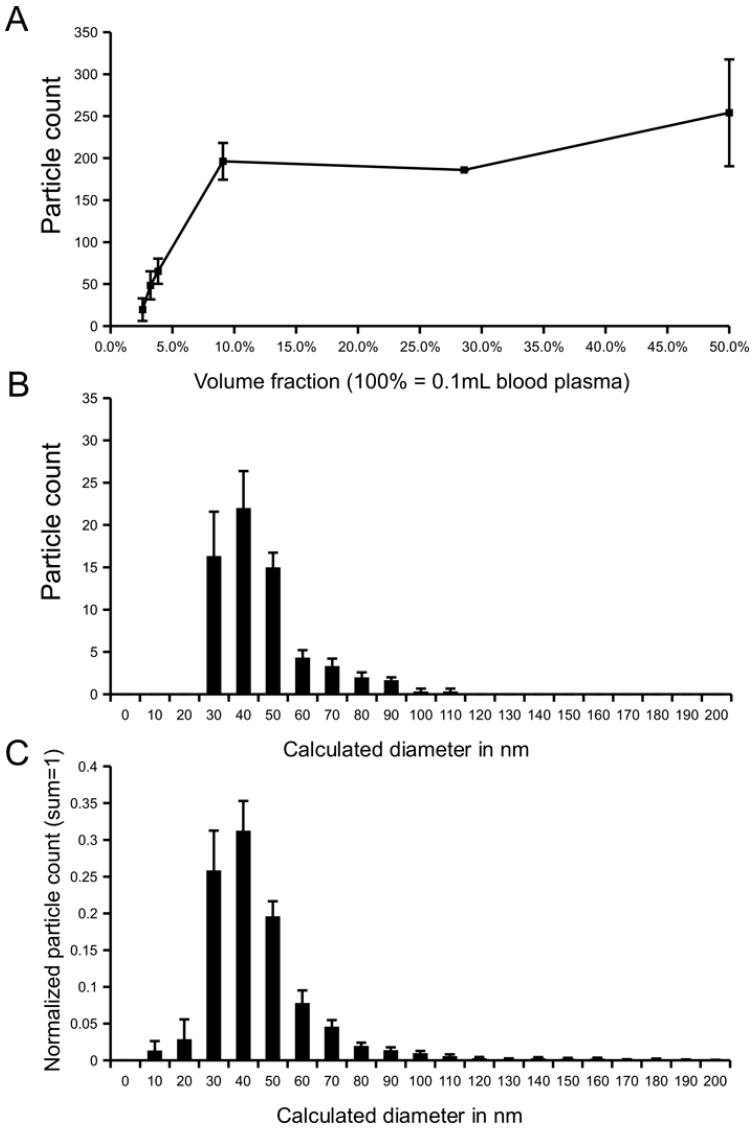


Figure 6. Relationship between the MP concentration in the sample and the number of CD41-positive MPs detected by AFM.

MPs isolated from frozen-thawed citrate PPP are diluted from 50% to 2.5% (100% is undiluted reconstituted-isolated MPs) in Hepes buffer and run through the microfluidics device. These experiments were done on two different days using the same plasma pool of one healthy volunteer and the particles were counted from images of 100 μm^2 (A). The size distribution from a single dilution (3.8%) is based on three images of 100 μm^2 (B). A normalized size distribution of all dilutions averages is weighted equally (C). Scale bars represent the standard error of the mean.

Table 3. Statistics obtained from the dilution experiment of Figure 6A

Percent Reconstituted MPs	2.6%	3.2%	3.8%	9.1%	29%	50%	80%
Dilution	75	60	50	20	5	2	1
Number of processed images	5	7	3	9	1	5	5
Number of particles	98	339	196	1766	186	1270	373
Mean*	30	49	46	54	50	45	51
Median*	29	42	42	46	46	40	41
Standard deviation*	12	27	15	28	20	17	34
Range*	68	192	87	301	152	160	283
Min*	8	26	27	26	26	25	23
Max*	76	218	114	327	177	185	306

*Values based on calculated particle diameter in nanometer

For the first time it is demonstrated that the size distribution of CD41-positive MPs is robust against high-speed centrifugation and dilution. However, to prevent clotting to occur, the use of MPs isolated by means of high-speed centrifugation is advised.

Yuana et al (10) have shown that MPs isolated from fresh citrate PPP have calculated, spherical like diameters (d_{sph}) of ~50 nm (range 10-475 nm). Using microfluidics we found that MPs isolated from frozen-thawed citrate PPP and frozen-thawed EDTA PPP have a similar calculated diameter (d_{sph}) of ~45 nm. Software has been developed to automate the measurement and counting of MPs. This results in much more consistent results and provides faster data analysis. By comparing the results from previous experiments by Yuana et al (10) to the new automated quantification of the same dataset we observed that the size distribution was similar to those reported earlier (data not shown).

There are advantages and disadvantages in using the microfluidic system and AFM to measure MPs. In this study we found that about 10 µL of plasma is enough to count significant number of MPs and determine their size distribution. Furthermore, the microfluidic system allows the measurement of MPs directly in plasma thus reducing time between venepuncture and MP measurement and also preventing MP loss because of washing steps in the isolation procedure. However, the preparation of mica (modification and coating) typically takes two days. In 20% of all cases we also dealt with leakage from microfluidic channels during plasma injection. AFM scanning of the surface is also time-consuming. It takes at least an hour finding a right surface to position the AFM tip and scanning 10 images of 100

μm^2 at different locations on the surface.

Therefore, when this present method will be used as a diagnostic tool, the throughput needs to be increased by developing high speed AFM and automated sample handling. Additionally, if fluorescent labeling can be implemented efficiently, the number of particles captured should allow optical detection of these particles by means of fluorescence imaging. With the AFM technique being used for calibration, it should be possible to fluorescently tag the MPs to provide optical quantification of the number of MPs on the mica surface.

Conclusion

In this study, it is demonstrated that by using a removable microfluidic circuit, CD41-positive MPs can be captured directly from diluted blood plasma, and detected by AFM. Quantification of MPs is automated to allow consistent and fast quantification. Use of the microfluidic system increases the sensitivity of MP detection considerably, leading to a higher surface concentration of attached MPs, reducing the AFM scanning time. Direct use of plasma as opposed to isolated MPs shortens the pre-processing time and enables the detection of MPs in a more natural state. Ten µL EDTA plasma is sufficient to quantify the number and determine the size distribution and shape of CD41-positive MPs using microfluidics and AFM.

In future experiments the characterization of MPs from other origins (endothelial cells, monocytes, tumor cells, etc) by using antigen-specific monoclonal antibodies will be addressed. This will help in monitoring subsets of MPs that may play a specific role in the development of certain diseases.

Acknowledgments

We thank G.J. van Baarle for assisting with the software that counts and measures the size of the particles. We thank Henk Verpoorten (Department of Fine Mechanics) for the construction of the microfluidic chip mold and the holder device. This work was supported by the Dutch Cancer Society (KWF UL 2006-3618) and Cyttron, in the Besluit Subsidies Investeringen Kennisinfrastructuur program (J.S.), which in turn is financially supported by the Nederlandse Organisatie voor Wetenschappelijk Onderzoek.

References

(1) Diamant M, Tushuizen ME, Sturk A, Nieuwland R. Cellular microparticles: new players in the field of vascular disease? Eur J Clin Invest 2004;34:392-401.

(2) Wolf P. The nature and significance of platelet products in human plasma. Br J Haematol 1967;13:269-288.

(3) Cocucci E, Racchetti G, Meldolesi J. Shedding microvesicles: artefacts no more. Trends Cell Biol 2009;19:43-51.

(4) Burnier L, Fontana P, Kwak BR, Angelillo-Scherrer A. Cell-derived microparticles in haemostasis and vascular medicine. Thromb Haemost 2009;101:439-451.

(5) Pap E, Pallinger E, Pasztoi M, Falus A. Highlights of a new type of intercellular communication: microvesicle-based information transfer. Inflamm Res 2009;58:1-8.

(6) Nomura S, Shouzu A, Taomoto K, Togane Y, Goto S, Ozaki Y, et al. Assessment of an ELISA kit for platelet-derived microparticles by joint research at many institutes in Japan. J Atheroscler Thromb 2009;16:878-887.

(7) Lacroix R, Robert S, Poncelet P, Kasthuri RS, Key NS, Dignat-George F. Standardization of platelet-derived microparticle enumeration by flow cytometry using calibrated beads: results of ISTH SSC collaborative workshop. J Thromb Haemost 2010;8:2571-2574.

(8) Aupeix K, Hugel B, Martin T, Bischoff P, Lill H, Pasquali JL, et al. The significance of shed membrane particles during programmed cell death in vitro, and in vivo, in HIV-1 infection. J Clin Invest 1997;99:1546-1554.

(9) Furie B, Furie BC. Cancer-associated thrombosis. Blood Cells Mol Dis 2006;36:177-181.

(10) Yuana Y, Oosterkamp TH, Bahatyrova S, Ashcroft B, Garcia RP, Bertina RM, et al. Atomic force microscopy: a novel approach to the detection of nanosized blood microparticles. J Thromb Haemost 2010;8:315-323.

(11) Freyssinet JM. Cellular microparticles: what are they bad or good for? J Thromb Haemost 2003;1:1655-662.

(12) Habib A, Kunzelmann C, Shamseddeen W, Zobairi F, Freyssinet JM, Taher A. Elevated levels of circulating procoagulant microparticles in patients with beta-thalassemia intermedia. Haematologica 2008;93:941-942.

(13) Jy W, Horstman LL, Jimenez JJ, Ahn YS, Biro E, Nieuwland R, et al. Measuring circulating cell-derived microparticles. J Thromb Haemost 2004;2:1842-1843.

(14) Heijnen HF, Schiel AE, Fijnheer R, Geuze HJ, Sixma JJ. Activated platelets release two types of membrane vesicles: microvesicles by surface shedding and exosomes derived from exocytosis of multivesicular bodies and alpha-granules. Blood 1999;94:3791-3799.

(15) Hughes M, Hayward CP, Warkentin TE, Horsewood P, Chorneyko KA, Kelton JG. Morphological analysis of microparticle generation in heparin-induced thrombocytopenia. Blood 2000;96:188-194.

(16) Aras O, Shet A, Bach RR, Hysjulien JL, Slungaard A, Hebbel RP, et al. Induction of microparticle- and cell-associated intravascular tissue factor in human endotoxemia. Blood 2004;103:4545-4553.

(17) Harrison P, Dragovic R, Albanyan A, Lawrie AS, Murphy M, Sargent I. Application of dynamic light scattering to the measurement of microparticles. J Thromb Haemost 2009;7(Suppl):OC-TU-056.

(18) Yuana Y, Bertina RM, Osanto S. Pre-analytical and analytical issues in the analysis of blood microparticles. Thromb Haemost 2010;105:396-408.

(19) Piccin A, Murphy WG, Smith OP. Circulating microparticles: pathophysiology and clinical implications. Blood Rev 2007;21:157-171.

(20) Enjeti AK, Lincz LF, Seldon M. Detection and measurement of microparticles: an evolving research tool for vascular biology. Semin Thromb Hemost 2007;33:771-779.

(21) Robert S, Poncelet P, Lacroix R, Arnaud L, Giraudo L, Hauchard A, et al. Standardization of

platelet-derived microparticle counting using calibrated beads and a Cytomics FC500 routine flow cytometer: a first step towards multicenter studies? J Thromb Haemost 2009;7:190-197.

(22) Horstman LL, Ahn YS. Platelet microparticles: a wide-angle perspective. Crit Rev Oncol Hematol 1999;30:111-142.

(23) Tesselaar ME, Romijn FP, van der Linden IK, Prins FA, Bertina RM, Osanto S. Microparticle-associated tissue factor activity: a link between cancer and thrombosis? J Thromb Haemost 2007;5:520-527.

(24) Gachet C, Hanau D, Spehner D, Brisson C, Garaud JC, Schmitt DA, et al. Alpha IIb beta 3 integrin dissociation induced by EDTA results in morphological changes of the platelet surface-connected canalicular system with differential location of the two separate subunits. J Cell Biol 1993;120:1021-1030.

(25) Rao GH, Peller JD, White JG. Influence of ionized calcium on thrombin-induced down regulation of GPIb/IX receptors on human platelets. Thromb Res 1997;85:23-31.

(26) Belanger MC, Marois Y. Hemocompatibility, biocompatibility, inflammatory and in vivo studies of primary reference materials low-density polyethylene and polydimethylsiloxane: a review. J Biomed Mater Res 2001;58:467-477.

(27) Whitlock PW, Clarson SJ, Retzinger GS. Fibrinogen adsorbs from aqueous media to microscopic droplets of poly(dimethylsiloxane) and remains coagulable. J Biomed Mater Res 1999;45:55-61.

(28) Khorasani MT, Mirzadeh H. Laser surface modification of silicone rubber to reduce platelet adhesion in vitro. J Biomater Sci Polym Ed 2004;15:59-72.

(29) Thorslund S, Sanchez J, Larsson R, Nikolajeff F, Bergquist J. Bioactive heparin immobilized onto microfluidic channels in poly(dimethylsiloxane) results in hydrophilic surface properties. Colloids Surf B Biointerfaces 2005;46:240-247.

(30) Thorslund S, Sanchez J, Larsson R, Nikolajeff F, Bergquist J. Functionality and stability of heparin immobilized onto poly(dimethylsiloxane). Colloids Surf B Biointerfaces 2005;45:76-81.

CHAPTER 6

Cryo-electron microscopy of submicron particles in plasma

Yuana Yuana*, Roman I. Koning*, Maxim E. Kuil, Patrick C.N. Rensen, Abraham J. Koster, Rogier M. Bertina and Susanne Osanto

*These authors contributed equally to this work

Submitted for publication

Abstract

There is increasing interest in measuring submicron particles (microparticles, exosomes) in plasma as disease biomarkers. Often these particles need to be isolated from plasma before the actual measurements can be performed. There is little information on the structure of these particles in plasma and how these structures may be influenced by isolation procedures.

We used cryo-electron microscopy (cryo-EM) to visualize and determine the size distributions of submicron particles in plasma. Freshly prepared plasma was directly applied on the electron microscope specimen support (grid) and vitrified by rapid cryo immobilization to enable observation of biological structures in their native state (in plasma).

In citrate platelet-rich plasma platelets were slightly activated as shown by budding of vesicles from the membrane, although clearly less than in samples of thrombin-activated platelets. Platelets in EDTA platelet-rich plasma were less activated than in citrate platelet-rich plasma. In EDTA and citrate plasma (platelet-rich, platelet-poor, and platelet-free plasma) most particles have no apparent lipid bilayer and an electron dense appearance. Most likely these represent lipoprotein particles. A fraction of the total number of particles observed had a discernable lipid bilayer and could be identified as lipid vesicles. Both types of particles have about the same size distribution (median: 30 nm; range: 25-260 nm). Most likely the lipid vesicles represent microparticles and exosomes. In thrombin-activated platelets similar lipid vesicles were observed. Isolated microparticles were shown to contain predominantly lipid vesicles.

In conclusion, cryo-EM proved to be a useful method to perform structural studies and determine the morphology and size distributions of submicron particles in plasma. A combination of cryo-EM and (e.g. antibody-gold or fluorescent) labelling of the different types of submicron particles in plasma will enable a further characterization of the variations in size and morphology.

Introduction

Microparticles (MPs) are submicron particles that are formed by budding of cell membranes upon activation or apoptosis and are released into body fluids, such as blood, urine and synovial fluid. MPs are present in the blood of healthy subjects. Elevated concentrations of plasma MPs have been associated with the manifestation and development of disease (1-4).

To date, there is only limited information on the morphology, composition and size distribution of plasma MPs because of the limitations of the analytical methods used and the largely unknown influence of pre-analytical variables such as blood collection, plasma and MP preparation and storage (5). Recently, the application of novel analytical tools like atomic force microscopy (AFM) and dynamic light scattering indicated that the large majority of plasma MPs have a size much smaller than previously reported using flow cytometry (6-8). Conventional transmission electron microscopy (TEM) has been used to study the morphology of MPs (9-13). However, for the investigation of the morphology of MP in their native state (in plasma), conventional TEM has significant shortcomings since the sample preparation steps and imaging techniques in conventional TEM require dehydration, chemical fixation, and/or staining of specimens.

Cryo-electron microscopy (cryo-EM) on vitrified aqueous suspensions and cells has been shown to enable the observation of biological structures in their native state (14;15). Vitrification is a cryo fixation method to preserve biological specimens to atomic resolution while water is transformed into a glass-like state without the formation of ice crystals. Cryo-EM does not use staining or chemical fixation procedures and samples are directly applied onto an EM grid and vitrified.

Despite increasing interest in the measurement of plasma MPs as biomarker for certain diseases, most pre-analytical parameters are not well standardized (5). Blood collection, plasma and MP preparation and storage all may affect the outcome of the MP measurements. Plasma is usually prepared from blood collected in 1/10 volume of sodium citrate (0.105 or 0.129 mol/L). The choice of this anticoagulant is based on international guidelines which are widely followed in routine haematology testing (16), but might be less optimal for MP measurements. Furthermore, the whole procedure from blood collection until plasma preparation should be rapid, but gentle to avoid *in vitro* activation of blood cells and in particular platelets. To prepare platelet-poor/free plasma, blood has to be subjected to (multiple) centrifugation steps. The centrifugal force applied is crucial for the removal of blood cells and platelets, but at the same time this force should not trigger inadvertent formation of MPs. Preferably, MPs are directly measured in

fresh plasma to maintain the characteristics and morphology of MPs in their native state (17;18).

In the current study cryo-EM imaging has been used to determine the size and morphology of submicron particles and to estimate their numbers in fresh plasma samples. Since platelet activation during sample processing may lead to inadvertent formation of platelet microparticles (PMPs) and release of alpha and dense granules, and since it has been reported that most plasma MPs are derived from platelets (19-21), we studied platelets and submicron particles in citrate- and EDTA-anticoagulated plasma, and in isolated platelet and MP preparations. We observed that platelets in citrate platelet-rich plasma are more activated than in EDTA platelet-rich plasma, although not as much as in samples of thrombin-activated platelets. In citrate platelet-poor plasma various types of submicron particles and cellular debris like microtubules and actin filaments were found, whereas in EDTA platelet-poor plasma there was less variation in the types of particles.

Most of the submicron particles found in plasma of healthy volunteers are spherical electron dense particles with a size ranging from at least 25 nm to a few hundred nanometers resembling lipoprotein particles. In the same plasma samples only a few lipid vesicles were found. Based on their morphology and structure such lipid vesicles could be microparticles and exosomes. Similar lipid vesicles could be found in samples of thrombin-activated isolated platelets.

Materials and Methods

Blood collection and plasma isolation

Venous blood was collected after fasting for more than 12 hours from three healthy volunteers (one female and two males, 34, 38 and 57 years old), who gave informed consent to donate blood. Blood was drawn using a 21-G needle. The first five mL of blood were discarded. The next 4.5 mL were collected into a five-mL sodium citrate (0.105 mol/L) vacutainer tube, after which the next ten mL were collected into K_2EDTA (1.8 mg EDTA/mL blood) vacutainer tubes. The needles and blood collection tubes were purchased from BD Biosciences, USA. Plasma was prepared within 30 minutes (min) after blood collection.

Three types of plasma were prepared: platelet-rich plasma (PRP), platelet-poor plasma (PPP), and platelet-free plasma (PFP). Blood was centrifuged at 160g, 20°C for 13 min without brake to obtain PRP. For PPP preparation, blood was centrifuged twice at 2,000g, 20°C for 10 min without brake. PFP was prepared by

centrifuging the blood first at 1,500g, 20°C for 15 min and then at 13,000g, 20°C for 2 min, without brake (18). During aspiration of supernatant plasma, about 700 µL plasma was left above the white blood cell layer to avoid contamination of the plasma with white cells and platelets. All plasma samples were vitrified within two hours after blood collection for cryo-EM analysis. The scheme of plasma preparation is depicted in Figure 1.

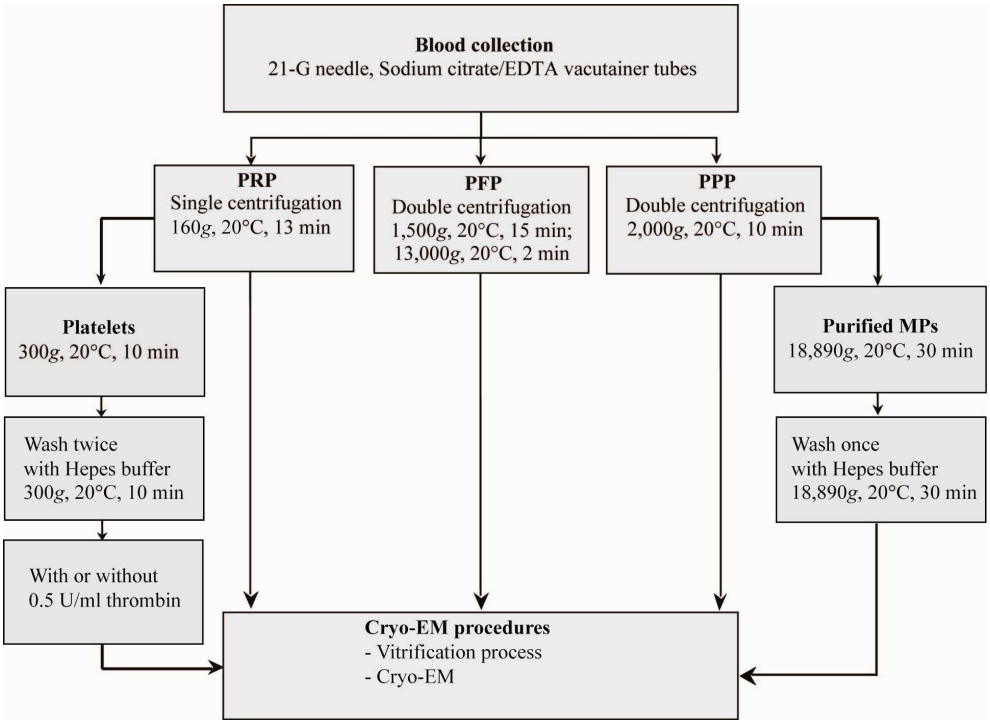


Figure 1. Scheme of the procedures used for blood collection and isolation of plasma, platelets, and MPs for cryo-EM analysis.

MP isolation

MPs were isolated from 750 µL of fresh citrated or EDTA PPP by centrifugation at 18,890g, 20°C for 30 min. The supernatant (725 µL) was removed without disturbing the pellet. Next, this pellet was resuspended in 1 mL Hepes buffer (10 mM Hepes, 137 mM NaCl, 4 mM KCl (all from Merck, Germany), 0.1 mM Pefabloc SC (Fluka, Germany), pH 7.4) and centrifuged again at 18,890g, 20°C for 30 min. Finally, the supernatant was removed leaving an undisturbed pellet in 25 µL of solution. The pellet (isolated MPs) was carefully resuspended and processed for cryo-EM (Figure 1, scheme of MP isolation until cryo-EM).

Thrombin activation of washed platelets

Citrated venous blood of the healthy female volunteer was centrifuged at 160g for 13 min at 20°C, without brake. One mL of PRP was collected and centrifuged at 300g for 10 min at 20°C, without brake. The supernatant was discarded leaving an undisturbed platelet pellet in 25 µL of solution. The platelet suspension was reconstituted to 1 mL by adding Hepes buffer and again centrifuged at 300g for 10 min at 20°C, without brake. After removing the supernatant, the platelet suspension was reconstituted with 1 mL Hepes buffer. This platelet suspension was supplemented with thrombin (Kordia, Leiden, The Netherlands) at a final concentration of 0.5 U/mL, incubated for 10 min, and directly applied on the grid and vitrified for cryo-EM analysis (Figure 1, scheme of platelet isolation and stimulation).

Lipoprotein isolation

Very low density lipoproteins (VLDL; $d < 1.006$ g/mL), low density lipoproteins (LDL; $1.019 < d < 1.063$ g/mL), high density lipoproteins ($1.063 < d < 1.21$ g/mL) and lipoprotein-deficient plasma (LPDP; $d > 1.21$ g/mL) were isolated from 3.5 mL EDTA PFP by density-gradient ultracentrifugation according to Redgrave et al. (22).

Cryo-electron microscopy

Samples were applied on a 300 mesh EM grid with lacey carbon and were vitrified using a Vitrobot Mark IV (FEI Company, The Netherlands) at room temperature and 100% humidity. Excess sample was removed by blotting once between 1 and 2 seconds with filter paper. The blotted grids were plunged into liquid ethane that was kept in equilibrium with solid ethane. After vitrification the grid was stored under liquid nitrogen until further use. Grids were mounted in a Gatan 626 cryo-holder for cryo-EM imaging.

Two dimensional data collection was performed on a Tecnai 12 electron microscope (FEI Company, The Netherlands) operated at 120 keV. Images were recorded on a 4k x 4k Eagle camera (FEI Company, The Netherlands). Images were recorded at 13,000x magnification at 8 micron under focus. For large scale automatic data collection we used custom written software that was able to collect 100 images in 15 min. In each experiment 1,000 non-overlapping images (in total ~3,000 micron^2) were recorded.

Cryo-EM was performed on a Tecnai 20 FEG (FEI Company, The Netherlands) operated at 200 keV. Images were recorded on a 2k x 2k camera mounted behind a GIF energy filter operated at a slit width of 20 eV. Cryo-electron tomograms were recorded from ±60° at a defocus of -50 micron and a magnification of 3,600x corresponding with a pixel size of 3.55 nm.

Results

Isolated MPs versus plasma MPs

Citrate-anticoagulated blood is most frequently used to prepare plasma for MP measurements (directly in plasma or after isolation of MP). Our first investigations of the morphology of MPs with cryo-EM were performed with citrate PPP. This citrate PPP was either directly used for the measurement or first subjected to high-speed centrifugation for the isolation of MPs (see Figure 1). In the isolated MP fraction, various types of particles were found (Figure 2). Most of the particles had a round shape (Figure 2A and B) and were either electron lucent empty structures with a clear lipid bilayer (further referred to as “lipid vesicles”) (Figure 2A, D, G and I) or electron dense structures with diverse morphology (Figure 2B, C, E and F). Surprisingly also actin (Figure 2H) and small microtubules (data not shown) were observed. Similar results were obtained for MPs isolated from EDTA plasma, although the number of particles seemed to be slightly lower than in samples isolated from citrate plasma.

In citrate and EDTA PPP particles were more uniform in type and less variable in shape. Most particles were vesicular structures with a round shape resembling particles found in the isolated MP fraction (see Figure 2A and 2B), with diameters between 25 and 300 nm. Smaller particles, below 25 nm were also present but more difficult to detect unambiguously because of limited contrast due to the technique of cryo-EM and the relative large amount of proteins present in plasma. The size distribution of the isolated MPs was in the same range as observed for particles in plasma (Table 1B).

Thrombin-activated platelets

Cryo-EM images of thrombin-activated platelets showed that the outer membrane of activated platelets is often not observable anymore. Instead, multiple membrane vesicles are observed at the peripheral zone of the platelets, in what seems vesiculation of the platelet membrane (Figure 3A and D). Importantly, platelet granules, mitochondria and membrane vesicles were observed in the near vicinity of the platelet (Figure 3D). When platelets were not activated with thrombin, their

plasma membrane was smooth and its content remained inside the plasma membrane, while no vesicles were observed in the surrounding of these platelets.

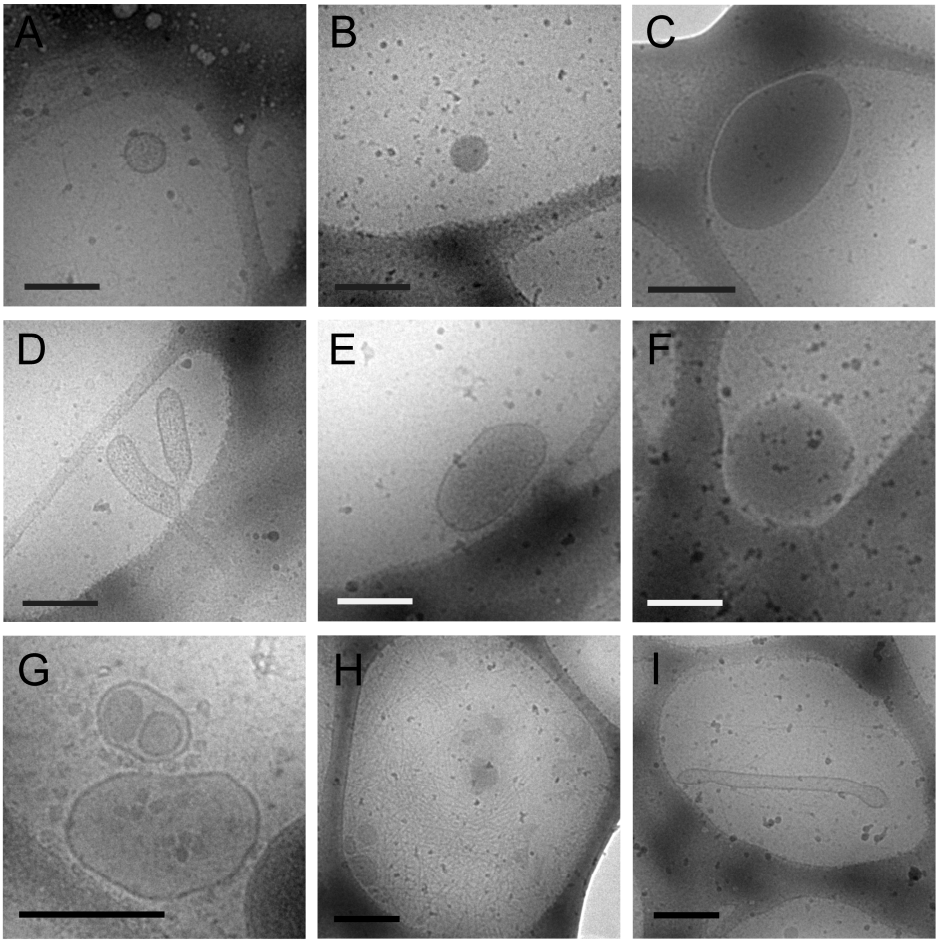


Figure 2. Cryo-EM images of MPs isolated from fresh citrated PPP. In the isolated MP fraction (MPs were 25x concentrated compared with citrated platelet-poor plasma) many different particles were observed by cryo-EM imaging: (A) most frequently observed were round empty particles with a clear lipid bilayer, (B) filled spherical structures without an apparent lipid membrane resembling VLDL, (C) Large dark vesicles, (D) small light vesicles with rough surfaces, (E) dark vesicles, (F) dark structures with no apparent border, (G) multilamellar vesicles, (H) actin filaments, (I) elongated lipid structures. Bars are 200 nm.

Platelets in citrate and EDTA plasma

We investigated whether the anticoagulants sodium citrate and EDTA influence the morphology of platelets in PRP. Figure 3B, C, E and F show the morphology of platelets as observed in citrate and EDTA PRP, respectively. Platelets seemed to be slightly activated in citrate plasma, but to a lesser extent than in samples of thrombin-activated platelets. Platelets in citrate PRP (Figure 3B and E) showed membrane processes, the presence of small vesicles, and membrane-associated lipid structures but their outer membrane was still observable, unlike in thrombin activated platelets. Platelets in EDTA PRP (Figure 3C and F), showed less pronounced activity of the plasma membrane and were largely devoid of budding vesicles or lipid structures. The morphology of platelets in EDTA PRP was similar to that of non-activated isolated platelets.

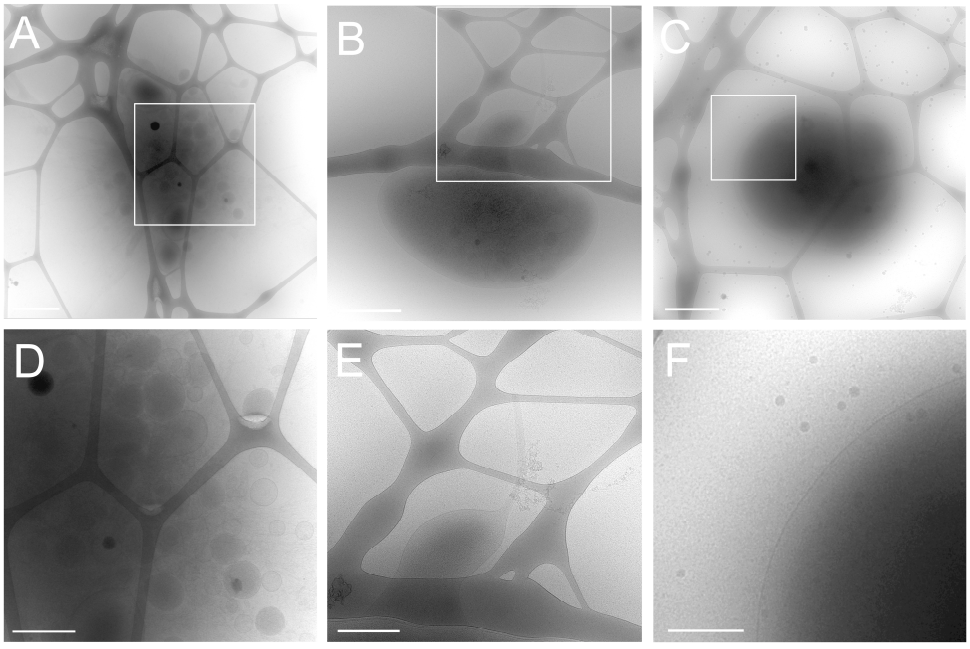


Figure 3. Cryo-EM images of (activated) platelets. Cryo-EM imaging shows the morphology of thrombin activated-platelet (A and D); platelet contents, being vesicles, actin and microtubules are released and the plasma membrane has opened up and is often not present anymore. In citrated PRP (B and E) the platelet plasma membrane is clearly visible and around many platelets budding of small vesicles and lipid structures filled with actin is being observed. In EDTA PRP (C and F) platelets tend to be less flattened while the plasma membrane is clearly visible and usually devoid of budding vesicles or lipid structures. Scale bars in A to C are 1 micron and in D to F 500 nm.

The morphology of submicron particles

Submicron particles in thrombin-activated platelets

Many different vesicles with various sizes and shapes (Figure 4A-D) and also actin (Figure 4E and F) and microtubules filaments (Figure 4F and G) were observed in samples of thrombin-activated platelets. The vesicles included particles with an elongated tubular shape (Figure 4A and B) which in some instances were connected to a platelet. When platelets were not activated, their plasma membrane was smooth and their contents retained inside the plasma membrane. No vesicles were observed in the surrounding of resting platelets (data not shown).

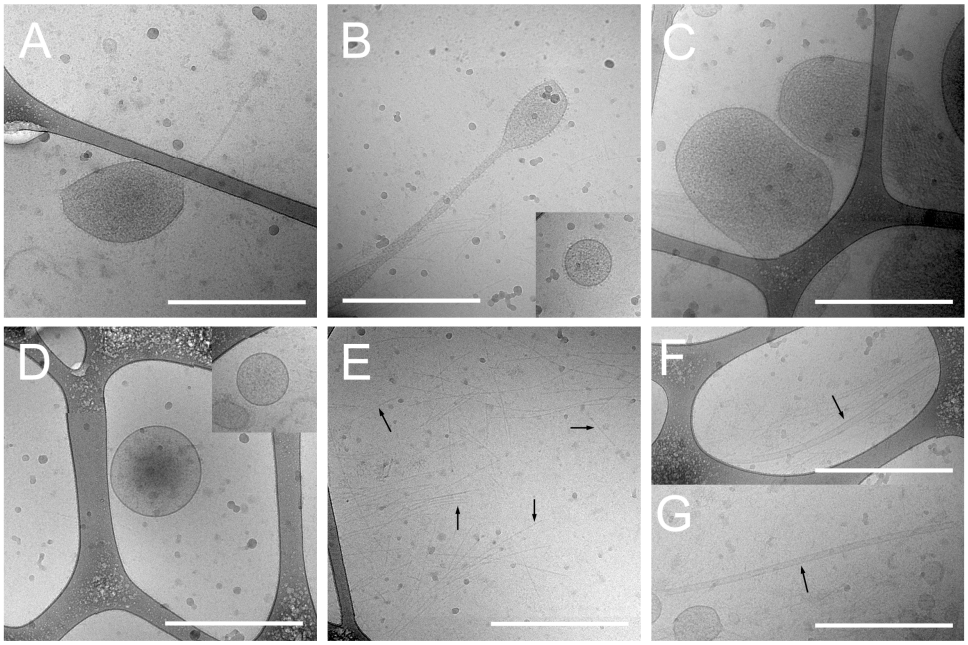


Figure 4. Cryo-EM images of structures/particles present in samples of thrombin-activated platelets. In samples of thrombin-activated platelets many different vesicles can be observed. (A and C) Dense vesicles with a rough surface and probably filled with actin (B and inset) are present around the platelets. Also spherical and less dense vesicles (D and inset), actin (E and F) and microtubules (F and G) are observed. Scale bars are 500 nm.

To obtain a three-dimensional image of the structure of activated platelets and the multitude of vesicles released by these platelets, we performed cryo-EM on activated platelets. The vesicles that are present in platelets, like mitochondria, alpha-granules and dense granules, could be easily observed in the tomograms (Figure 5B and C). These structures were morphologically similar to those reported in earlier morphological studies of platelets (23). Of interest, such vesicles seemed to originate from the outer membrane of the platelet (Figure 5B, D, E and G). Vesicles were also released from the platelet (Figure 5B, C and F), while actin and microtubules (Figure 5B and H) can be observed inside and outside the platelet.

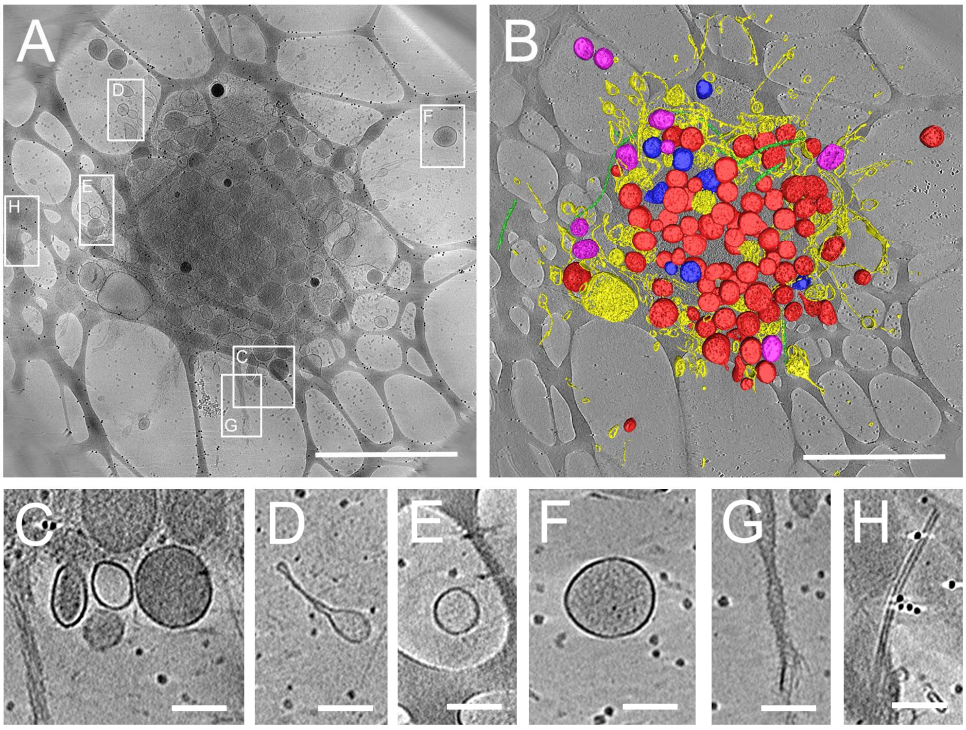


Figure 5. Cryo-EM of activated platelets in EDTA plasma. Cryo-EM shows several types of vesicular structures and cellular debris that can be found in the vicinity of activated platelets. In (A) a 175 nm thick tomographic slice of an activated platelet showing the debris that is released. Boxed show the positions of the enlarged images C to H. A surface rendered representation (B) shows dense granules (red), vesicles and lipid membrane structures (yellow), A-granules (blue), mitochondria (purple) and microtubules (green). Glycosomes and actin filaments are not included in the surface rendering. Small black dots in the background are fiducial gold used for tilt series alignment. The network like structure in the background is the lacey carbon film that is used as support film. Enlargements of several places surrounding the activated platelet show release of dense vesicles (C and F), round vesicles (C, E and F) and elongated lipid membrane structures (D), mixed actin/rough membranous structures (G), and microtubules (H). Scale bars in A and B are 2 micron, in C to H scale bars are 200 nm.

Submicron particles in citrate and EDTA plasma

The morphology of submicron particles in citrate and EDTA plasma was rather similar. In EDTA plasma (PRP, PPP, and PFP), there seemed to be less particles than in citrate plasma. Particles found in plasma have different shapes: some have a lipid membrane and are typically translucent with little material inside (lipid vesicles, Figure 6A-C) but most are typically round, electron dense without a clear visible lipid bilayer (Figure 6D-F).

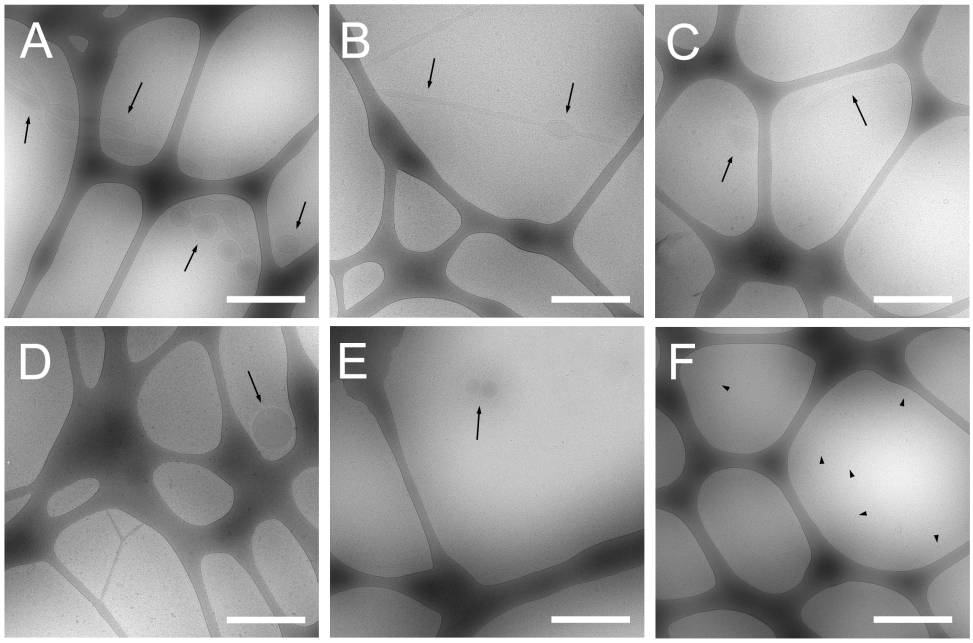


Figure 6. Cryo-EM images of structures/vesicles present in samples of EDTA plasma. The morphology of particles as observed by cryo-EM imaging in EDTA PRP (C and D) , PPP (E) and PFP (A,B and F) typically shows very few vesicles and only of two types. (A-C) Lipid structures (see arrows) are elongated and can be microns long. They also have a lipid membrane and are typically light of nature with little material inside. (C–F) Also lipoprotein-like particles can be observed (see arrows and arrow heads), which are typically round, electron dense, do not have a clear visible lipid bilayer and vary in size between 40 and 80 nm; these particles form the large majority in EDTA plasma. Scale bars are 500 nm.

Previously we noticed that platelets appeared to be slightly activated in citrate PRP. In the medium surrounding these activated platelets we observed many particles (Figure 7), usually clusters of vesicles from opened platelets (Figure 7A and B). Also large single vesicles were observed (Figure 7C-F). Such large vesicles were not observed in EDTA PRP.

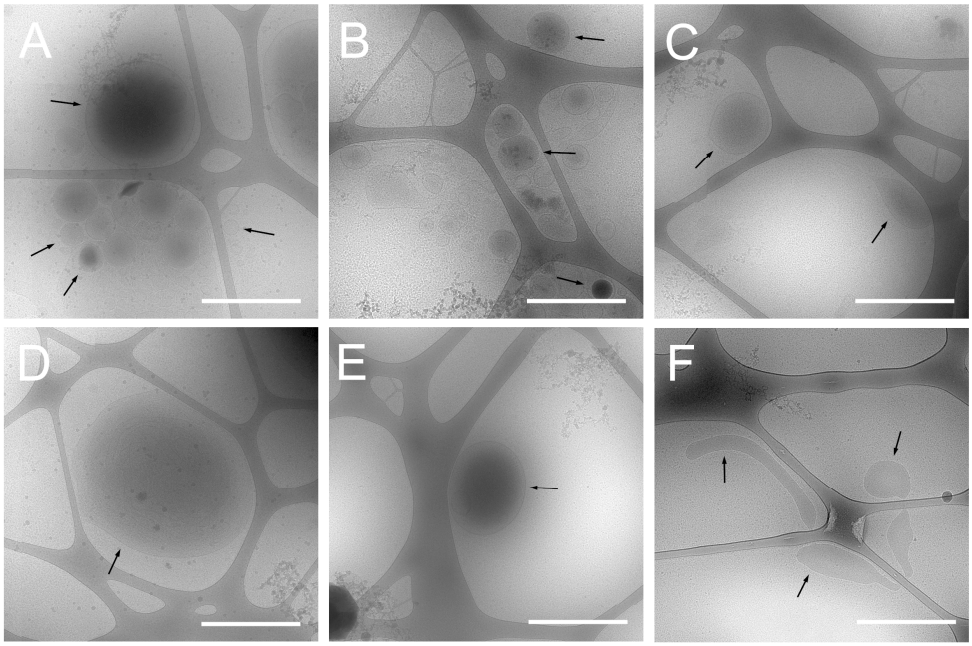


Figure 7. Cryo-EM images of structures/particles present in samples of citrate PRP. The morphology of vesicles in citrated PRP as observed by cryo-EM imaging typically shows different kinds of structures. (A and B) Vesicles are in clusters and mitochondria are also present in these clusters which points towards opening and release of contents of the platelets. Arrows indicate vesicles (C-F) Vesicles have different shapes and can be 500 nm or even larger (A and D). Scale bars are 500 nm.

Lipoproteins

From their appearance it seemed that some electron dense particles observed in plasma (see Figures 2B, 6E and F) did not have an apparent lipid membrane. Given this absence of a clear lipid membrane, their high abundance, the electron dense appearance and the size distribution (from ~25 nm to a few hundred nanometers), these particles could be lipoproteins (VLDL, LDL, and HDL). To test this hypothesis, lipoproteins were isolated from EDTA PFP by density-gradient ultracentrifugation and cryo-EM was performed on the isolated fractions (Figure 8). Cryo-EM imaging of these lipoprotein fractions and also earlier published cryo-EM data of lipoproteins (24-27), confirmed that the electron dense particles without an apparent lipid membrane found in the plasma samples resembled lipoproteins in size and morphology. No particles were observed in the lipoprotein depleted

fraction. Interestingly, especially in the VLDL fraction we observed large dark spots without an apparent border (white arrow in Figure 8A) which were sometimes also observed in plasma fractions (Figure 2F).

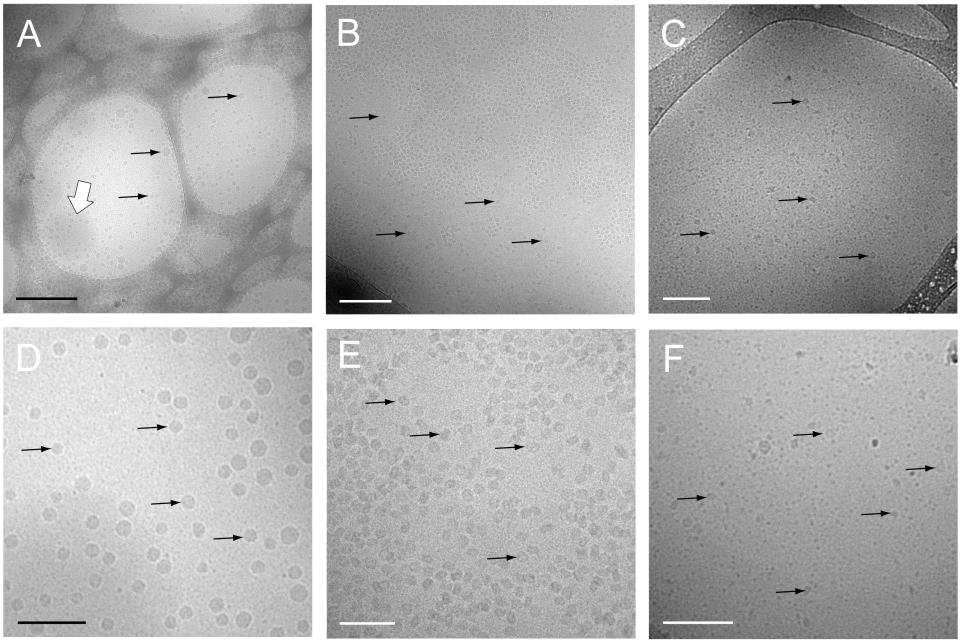


Figure 8. Cryo-EM of freshly isolated lipoprotein fractions. Overviews (A-C) and higher magnification (D-F) images of VLDL (A and D), LDL (B and E) and HDL (C and F) fractions clearly show the different lipoprotein particles (denoted by black arrows). Scale bars are 500 nm (A), 200 nm (B and D) and 100 nm (C, E and F). The white arrow in (A) points to a fuzzy round structure of unknown origin that was observed in several samples, but most common in purified VLDL.

Quantitative analysis

Number of platelets and submicron particles in EDTA plasma

We counted all particles in 1,000 non-overlapping random images of 10 meshes in the cryo-EM samples of EDTA PRP, PPP and PFP of two healthy volunteers. Particles with an apparent lipid membrane were also counted separately. The results of these counts are summarized in Table 1A.

We could detect platelets in EDTA PRP of the two volunteers (14 and 41 platelets per 1,000 images, respectively), but not in EDTA PPP and PFP (Table 1A).

In agreement with our previous observations most particles in the PFP, PPP and PRP have a round shape and an electron dense appearance without a visible

membrane (Figure 6C-F), while a minority of the observed particles are lipid vesicles (Figure 6A and B). The number of electron dense particles was 2 to 3 orders higher than the number of lipid vesicles and depended on the type of plasma and the individual. There seem to be relatively more lipid vesicles in PRP, where there were also more platelets, than in the PPP and PFP.

Size distribution of MPs in EDTA plasma

We analyzed the size of all particles with a size equal or above 25 nm. These particles have diameters ranging from 25 to 260 nm (Table 1B). Particles in PRP, PPP, and PFP have a median size of about 30 nm. Apparently the size of particles is not largely influenced by the procedure used to prepare the plasma, although particles in PRP seem to cover a wider range of sizes.

Table 1. Particle counts in EDTA plasma of two healthy volunteers.

A.

Volunteer	EDTA plasma	Counts per ~3,000 micron^2		
		All particles	Lipid vesicles	Platelets
1	PRP	620	35	14
	PPP	7,580	2	0
	PFP	1,320	10	0
2	PRP	2,210	13	41
	PPP	3,610	3	0
	PFP	6,590	5	0

B.

Volunteer	EDTA plasma	Median (nm)	Range (nm)
1	PRP	28	25-148
	PPP	28	25-75
	PFP	28	25-64
2	PRP	31	25-260
	PPP	32	25-68
	PFP	35	25-92

Particles were counted in cryo-EM images of three types of plasma (PRP, PPP, and PFP) of two healthy volunteers. Also the size of these particles was determined. (A) The table gives the results of counting particles with a size equal or above 25 nm in 1000 images of 10 meshes. (B) The median and range of all particle sizes in these three types of plasma were calculated.

Discussion

To our knowledge, in this study we used for the first time cryo-EM to visualize and characterize the morphology of submicron particles in fresh plasma as well as in isolated MP fractions. It was not possible to discriminate particles with a diameter

smaller than 25 nm due to the limited contrast of cryo-EM and the presence of many proteins in plasma.

In isolated MP fractions we observed submicron particles with sizes ranging from 25 to ~300nm. These particles had a lipid membrane and various shapes, sizes and morphologies. Most have vesicular structures with a round shape. Using conventional EM, Aras et al. (9) observed that MPs isolated from plasma had diameter sizes ranging from 100-500 nm. However, these MPs might be flattened during the preparation of the sample. In cryo-EM some flattening does only occur when particles are larger than the ice thickness. The observation of microtubules in the isolated MPs samples indicates the presence of platelet fragments in these preparations. Most likely this is due to the effect of high-speed centrifugation on residual platelets in the plasma.

In plasma, only a few types of particles were observed. Most particles found in plasma resembled lipoproteins, whereas only a minor part was lipid vesicles (Table 1). The nature of these lipid vesicles cannot be established without the use of specific labelling techniques. The lipid vesicles have a similar morphology as some of the vesicles observed close to activated platelets and to the lipid vesicles present in isolated MP preparations. A portion of the observed lipid vesicles could well be MPs, the small particles shed from the surface of many cells upon stimulation or apoptosis. Another portion might be exosomes, small membrane vesicles of endocytic origin that can be released by many different cells (28-30). At present there is no reliable estimate of the ratio in which MPs and exosomes occur in plasma.

The presence of actin, microtubules and other cellular debris in MPs isolated from citrate and EDTA PPP indicates that PPP still contains cells that are damaged during the high-speed centrifugation used for MP isolation. It is not known to what extent these cellular fragments may influence measurements in these MP preparations.

The morphology of platelets was studied in citrate and EDTA-anticoagulated PRP. We found that platelets tend to be slightly activated in citrate PRP. Platelets show membrane budding and the presence of surrounding vesicles while this occurs much less in EDTA PRP. Therefore, blood collection in EDTA might be preferred for the study of plasma MPs because it will help to reduce *in vitro* activation of platelets and platelet MP formation.

Cryo-EM is a technique suited for the characterization of individual submicron particles, but less a technique for the quantification of the number of submicron

particles in large volume suspensions. The quantification with cryo-EM highly depends on the exact conditions of specimen preparation, and is susceptible for local variations in concentrations of particles on the EM support due to variations in hydrophobicity. Finally, quantification requires that a large number of images containing a large number of submicron particles at high resolution will need to be recorded, which is in most cases not possible using cryo-EM. Nevertheless, in this study a significant number of images were recorded that provides insights in the size distribution and morphology of submicron particles in plasma.

In the EDTA PRP of two volunteers we counted 14 and 41 platelets per 1,000 images, respectively. Assuming a vitreous water thickness of 150 nm, 1,000 images would correspond to a volume of 450 micron^3 or 0.45 pL. This would suggest that the platelet concentration in the PRP sample is 30-90 platelets/pL, about 100-fold higher than expected for PRP prepared from blood of a healthy donor (about 600,000 platelets/µL or 0.6 platelet/pL). Similarly, the concentration of lipid vesicles in PPP is about 5 particles/ pL, about 10-fold higher than for instance the number of PMPs detected by AFM in PPP of healthy donors (6). We can not explain these discrepancies. For instance, we cannot exactly determine the precise volume of sample that was attached to the EM grid. In addition, the measured concentrations of particles might be influenced preferential binding of platelets and vesicles to the EM grid.

The diameters of particles found in the EDTA plasma samples of the two healthy volunteers ranged from 25-260 nm with a median of about 30 nm. Most of these particles resembled lipoprotein particles, while the minority of the observed particles is formed by lipid vesicles. Lipoprotein particles (e.g. VLDL, LDL) have reported sizes of 25 nm to 90 nm, which might explain why the median size of particles in plasma observed by cryo-EM (30 nm) is lower than that of the PMPs detected by AFM (67 nm) (6).

Overall our data indicate that MPs constitute only a minority of all submicron particles in fresh PPP. This observation strongly indicates limitations on the variety of techniques that can be used for MP measurements directly in plasma. For future developments of methods to quantify plasma MPs it will be essential to find ways to label MPs and/or exosomes directly in plasma.

Acknowledgments

This work was supported by the Dutch Cancer Society (KWF UL 2006-3618) and by a Netherlands SmartMix grant and the NIMIC partner organizations (www.nimic-project.com) through NIMIC, a public-private program.

References

(1) Zwicker JI, Liebman HA, Neuberg D, Lacroix R, Bauer KA, Furie BC, et al. Tumor-derived tissue factor-bearing microparticles are associated with venous thromboembolic events in malignancy. Clin Cancer Res 2009;15:6830-6840.

(2) Ghosh AK, Secreto CR, Knox TR, Ding W, Mukhopadhyay D, Kay NE. Circulating microvesicles in B-cell chronic lymphocytic leukemia can stimulate marrow stromal cells: implications for disease progression. Blood 2010;115:1755-1764.

(3) Tesselaar ME, Romijn FP, van dL, I, Bertina RM, Osanto S. Microparticle-associated tissue factor activity in cancer patients with and without thrombosis. J Thromb Haemost 2009;7:1421-1423.

(4) Shantsila E, Kamphuisen PW, Lip GY. Circulating microparticles in cardiovascular disease: implications for atherogenesis and atherothrombosis. J Thromb Haemost 2010;8:2358-2368.

(5) Yuana Y, Bertina RM, Osanto S. Pre-analytical and analytical issues in the analysis of blood microparticles. Thromb Haemost 2010;105:396-408.

(6) Yuana Y, Oosterkamp TH, Bahatyrova S, Ashcroft B, Garcia RP, Bertina RM, et al. Atomic force microscopy: a novel approach to the detection of nanosized blood microparticles. J Thromb Haemost 2010;8:315-323.

(7) Harrison P, Dragovic R, Albanyan A, Lawrie AS, Murphy M, Sargent I. Application of dynamic light scattering to the measurement of microparticles. J Thromb Haemost 7[Supplement 2]. 2009;7(Suppl):OC-TU-056.

(8) Van Der Pol E, Hoekstra AG, Sturk A, Otto C, Van Leeuwen TG, Nieuwland R. Optical and non-optical methods for detection and characterization of microparticles and exosomes. J Thromb Haemost 2010;8:2596-2607.

(9) Aras O, Shet A, Bach RR, Hysjulien JL, Slungaard A, Hebbel RP, et al. Induction of microparticle- and cell-associated intravascular tissue factor in human endotoxemia. Blood 2004;103:4545-4553.

(10) Heijnen HF, Schiel AE, Fijnheer R, Geuze HJ, Sixma JJ. Activated platelets release two types of membrane vesicles: microvesicles by surface shedding and exosomes derived from exocytosis of multivesicular bodies and alpha-granules. Blood 1999;94:3791-3799.

(11) Bernimoulin M, Waters EK, Foy M, Steele BM, Sullivan M, Falet H, et al. Differential stimulation of monocytic cells results in distinct populations of microparticles. J Thromb Haemost 2009;7:1019-1028.

(12) Mobarrez F, Antovic J, Egberg N, Hansson M, Jorneskog G, Hultenby K, et al. A multicolor flow cytometric assay for measurement of platelet-derived microparticles. Thromb Res 2010;125:e110-e116.

(13) Jayachandran M, Litwiller RD, Owen WG, Heit JA, Behrenbeck T, Mulvagh SL, et al. Characterization of blood borne microparticles as markers of premature coronary calcification in newly menopausal women. Am J Physiol Heart Circ Physiol 2008;295:H931-H938.

(14) Adrian M, Dubochet J, Lepault J, McDowall AW. Cryo-electron microscopy of viruses. Nature 1984;308:32-36.

(15) Koning RI, Koster AJ. Cryo-electron tomography in biology and medicine. Ann Anat 2009;191:427-445.

(16) CLSI. Collection, Transport, and Processing of Blood Specimens for Testing Plasma-Based Coagulation Assays and Molecular Hemostasis Assays; Approved Guideline-Fifth Edition. CLSI document H21-A5. 2008. Wayne, PA: Clinical and Laboratory Standards Institute.

(17) Jy W, Horstman LL, Jimenez JJ, Ahn YS, Biro E, Nieuwland R, et al. Measuring circulating cell-derived microparticles. J Thromb Haemost 2004;2:1842-1843.

(18) Lacroix R, Robert S, Poncelet P, Kasthuri RS, Key NS, Dignat-George F. Standardization of platelet-derived microparticle enumeration by flow cytometry using calibrated beads: results of ISTH SSC collaborative workshop. J Thromb Haemost 2010;8:2571-2574.

(19) Burnier L, Fontana P, Kwak BR, Angelillo-Scherrer A. Cell-derived microparticles in haemostasis and vascular medicine. Thromb Haemost 2009;101:439-451.

(20) Tesselaar ME, Romijn FP, van der Linden IK, Prins FA, Bertina RM, Osanto S. Microparticle-associated tissue factor activity: a link between cancer and thrombosis? J Thromb Haemost 2007;5:520-527.

(21) Nieuwland R, Berckmans RJ, Rotteveel-Eijkman RC, Maquelin KN, Roozendaal KJ, Jansen PG, et al. Cell-derived microparticles generated in patients during cardiopulmonary bypass are highly procoagulant. Circulation 1997;96:3534-3541.

(22) Redgrave TG, Roberts DC, West CE. Separation of plasma lipoproteins by density-gradient ultracentrifugation. Anal Biochem 1975;65:42-49.

(23) van Nispen tot PH, de HF, Geerts W, Posthuma G, van DS, Heijnen HF. The platelet interior revisited: electron tomography reveals tubular alpha-granule subtypes. Blood 2010;116:1147-1156.

(24) van AR, Chen GC, Pullinger CR, Kane JP, LaBelle M, Krauss RM, et al. Cryo-electron microscopy of low density lipoprotein and reconstituted discoidal high density lipoprotein: imaging of the apolipoprotein moiety. J Lipid Res 1997;38:659-669.

(25) van AR, La BM, Navratilova E, Krauss RM. Structural heterogeneity of apoB-containing serum lipoproteins visualized using cryo-electron microscopy. J Lipid Res 1999;40:1827-1836.

(26) Orlova EV, Sherman MB, Chiu W, Mowri H, Smith LC, Gotto AM, Jr. Three-dimensional structure of low density lipoproteins by electron cryomicroscopy. Proc Natl Acad Sci U S A 1999;96:8420-8425.

(27) van AR. Preferred orientations of LDL in vitreous ice indicate a discoid shape of the lipoprotein particle. Arch Biochem Biophys 2004;432:122-127.

(28) Laulagnier K, Motta C, Hamdi S, Roy S, Fauvelle F, Pageaux JF, et al. Mast cell- and dendritic cell-derived exosomes display a specific lipid composition and an unusual membrane organization. Biochem J 2004;380:161-171.

(29) de GA, Geminard C, Fevrier B, Raposo G, Vidal M. Lipid raft-associated protein sorting in exosomes. Blood 2003;102:4336-4344.

(30) Duijvesz D, Luider T, Bangma CH, Jenster G. Exosomes as biomarker treasure chests for prostate cancer. Eur Urol 2011;59:823-831.

CHAPTER 7

Use of immuno-magnetic beads for direct capture of nanosized blood microparticles from plasma

Yuana Yuana, Susanne Osanto and Rogier M. Bertina

Submitted for publication

Abstract

The mechanism of cancer-associated thrombosis is still unclear. Recent data indicate that blood microparticles (MPs) carrying active tissue factor (TF) may play a role in cancer-associated thrombosis. Methods such as flow cytometry and impedance based-flow cytometry allow the analysis of MP subsets but give no information on which MPs carry active TF. Conversely, the MP-TF activity itself provides no information, on the cellular origin of the MPs carrying the active TF.

For this reason, we developed an immuno-magnetic beads method to capture subsets of MPs directly from plasma. The method was optimized for the capture of platelet-derived MPs (PMPs) from plasma. Only 100 µL platelet poor plasma (PPP) was needed in combination with 135 µL (27 µg) of biotinylated anti-human CD41 monoclonal antibody (MoAb) and 200 µL of streptavidin beads to achieve complete separation of PMPs from plasma. As a control biotinylated mouse IgG1 isotype control MoAb was used instead of the anti-CD41 MoAb.

Using biotinylated anti-CD14 MoAb, CD14-positive MPs were captured from normal plasma spiked with MPs isolated from the supernatant of LPS-stimulated monocytes (MoMPs). TF activity was found both in the positive (selected) and negative (depleted) fractions indicating that both CD14-positive and -negative MoMPs have active TF.

We propose that this method can be used in the future to investigate the source of MPs carrying active TF in plasma of patients with cancer and other diseases.

Introduction

There appears to be a two-way association between cancer and thrombosis. Cancer is associated with a 4-7 fold increased risk for venous thrombosis (VTE) (1;2), while on the other hand about 10% of patients with an episode of idiopathic VTE will develop cancer within 2 years after the event (3;4). Cancer patients who developed thrombosis also have a poor survival compared to those who did not develop thrombosis (5). Some studies indicate that in cancer patients blood microparticles (MPs) play a role both in the development of VTE and in the progression of disease. MPs, also named microvesicles, are nanosized vesicles which are released from virtually all cells of the body upon activation or apoptosis (6;7) and still express proteins derived from their parental cells (8;9). Some MPs also may carry active tissue factor (TF), a 47 kDa transmembrane glycoprotein, which is the main activator of blood coagulation (10-12). Tesselaar et al (11) reported that cancer patients with disseminated breast and pancreatic cancer, who presented with acute VTE, had higher levels of MP-associated TF activity (MP-TF activity) than healthy subjects, cancer patients without VTE and subjects with idiopathic VTE. Interestingly, in some of these patients a small fraction of their blood MP expressed MUC-1 antigen which raises the question whether a subset of MPs with TF activity is derived from tumour cells themselves. Increased MP procoagulant activity is not only found in cancer patients, but also in patients with cardiovascular and inflammatory diseases (7;13;14)

Blood MPs used to be known as ‘platelet dust’ which was obtained after ultracentrifugation of platelet free plasma (15). Most MPs have sizes below 1 µm and the detection of MPs with sizes less than 0.5 µm is not sensitive when using a commonly applied method such as flow cytometry or bright field microscopy (16;17). Recently, our group reported the use of atomic force microscopy (AFM) operated in fluid-tapping mode to detect platelet-derived MPs (PMPs) and showed that AFM enables sensitive detection of MPs with diameter ranging from 10-475 nm (mean: 67.5 ± 26.5 nm), far below the lower limit of what can be detected by conventional flow cytometry (18).

However, up till now there is no method available to identify the origin of the subsets of plasma MPs carrying active TF. Current methods using flow cytometry (8) and impedance based-flow cytometry (19) only allow the identification of subsets of MPs carrying TF antigen in plasma but provide no information with regard to which MPs carry active TF. In this context it is important to mention that most of the TF antigen in plasma is encrypted and not biologically active (20;21).

For the measurement of MP-TF activity MPs need to be separated from the plasma proteins (11;12;22;23), after which the TF activity of the isolated MPs is measured as the FVII-dependent factor Xa (FXa) generation. However, there is no easy way to measure TF activity in selected subsets of MPs.

For this reason, we developed an immuno-magnetic beads method to directly capture a subset of plasma MPs. The method was optimized for the separation of PMPs, which form about 80% of the total blood MP population (7;9;11), and further tested for capturing monocyte-derived MPs (MoMPs). Biotinylated anti-human CD41 and CD14 monoclonal antibodies were coupled to streptavidin-magnetic beads to separate CD41- and CD14-positive MPs from plasma. Subsequently, the separated fractions were used to isolate and analyze MPs for specific antigens and TF activity.

In this study we demonstrate that the use of immuno-magnetic beads can specifically and efficiently separate a subset of MPs from plasma. We propose to apply this method for further use in the identification of the MP subset(s) carrying active TF in patients.

Materials and Methods

Reagents

The µMACS™ streptavidin kit and CD14 MACS MicroBeads were purchased from Miltenyi Biotec Inc (CA, USA). Biotinylated anti-human CD41 monoclonal antibody (MoAb) clone P2 and biotinylated mouse IgG1 isotype control MoAb were from Beckman Coulter (Marseille, France). Biotinylated anti-human CD14 MoAb clone M5E2 and biotinylated mouse IgG2a, κ isotype control MoAb were from Biolegend (CA, USA). For PMP staining, anti-human CD41- phycoerythin (PE) MoAb clone P2 and anti-human CD61- fluorescein isothiocyanates (FITC) MoAb clone SZ21 from Beckman Coulter were used. MoMPs were stained by anti-human CD14-PE MoAb clone M5E2 from BD Pharmingen (CA, USA) and anti-human tissue factor (TF)-FITC MoAb clone CLB/TF-5 from Sanquin (Amsterdam, The Netherlands). For controls, mouse IgG1 isotype control-PE and -FITC MoAbs clone X40 from Becton Dickinson (CA, USA) and mouse IgG2a, κ isotype control-PE MoAb clone G155-178 from BD Pharmingen were used. Recombinant human annexin V-allophycocyanin (APC) from Caltag Laboratories (CA, USA) was used to stain MPs bearing phosphatidylserine. Megamix beads were purchased from Biocytex (Marseille, France) to calibrate the FACS Calibur flow cytometer. For counting the absolute number of MPs in samples, flow cytometry absolute count standard beads from Bang Laboratories (IN, USA) were used. These beads have a mean diameter

of 7.58 µm per bead and a known concentration. Hepes buffer consists of 10 mM 4-(2-hydroxyethyl)-1-piperazineethanesulfonic acid (Hepes) (Merck, Darmstad, Germany), 137 mM NaCl (Merck), 4 mM KCl (Merck) and 0.1 mM Pefabloc SC (Fluka, Munich, Germany). Hepes-citrate buffer was prepared by adding 10.8 mM sodium citrate (Merck) to the Hepes buffer without Pefabloc. All buffers were set to pH 7.4. For the isolation of human monocytes, phosphate buffered saline (PBS) pH 7.2 was used (LUMC Pharmacy, Leiden, The Netherlands). For some experiments PBS was supplemented with 0.5% bovine serum albumine (BSA) (Sigma-Aldrich, MO, USA) and 2 mM ethylenediaminetetraacetic acid (EDTA) (Sigma-Aldrich) (pH 7.2) (PBS-BE). Ficoll-amidotrizoate was from LUMC Pharmacy. Lipopolysaccharide (LPS) from Sigma-Aldrich was used to stimulate human monocytes. For monocyte culture, RPMI (Invitrogen, Breda, The Netherlands) was supplemented with 1% L-Glutamine (L-Glu) from Lonza (Cologne, Germany) and 1% Penicillin/Streptomycin (Pen/Strep) from Invitrogen.

Blood collection and plasma preparation

After giving informed consent venous blood was collected from three healthy volunteers by using a 21-gauge needle (BD Vacutainer; Becton Dickinson) with minimal stasis. After discarding the first 4 mL of blood, blood was collected in 1/10 volume of sodium citrate (3.2%, 0.105 M) using a 4.5-mL BD Vacutainer tube (Becton Dickinson). Within 10-15 minutes (min) of withdrawal, blood was centrifuged at 2,000g for 10 min at 20°C, without brake. Plasma was carefully collected and centrifuged again at 2,000g for 10 min at 20°C, without brake, to obtain platelet-poor plasma (PPP). PPP was aliquoted in 250-µL portions, snap frozen in liquid N_2, and stored at -80°C. Before use, plasma was thawed quickly with a gentle swirl at 37°C.

Eighteen mL of venous blood was collected in 4.5 ml K2 EDTA tubes (3.6 mg EDTA) (BD Vacutainer, Becton Dickinson). This blood was 3-fold diluted with PBS before use for monocyte isolation.

Human monocyte isolation and stimulation

Fifteen mL of Ficoll-amidotrizoate was pipetted to a Leucosep tube (Greiner Bio-One GmbH; Frickenhausen, Germany) and centrifuged in a swinging bucket rotor for 30 seconds (sec) at 1,000g, room temperature (RT), with brake. Diluted (3-fold) EDTA anticoagulated blood (15-30 mL) was carefully pipetted onto the filled Leucosep tube and centrifuged for 15 min at 800g, RT, without brake. The upper layer of plasma including the interphase (enriched in lymphocytes/mononuclear

cells) was harvested and placed into another centrifugation tube. PBS was added to a total volume of 50 mL and subsequently the cell suspension was centrifuged for 10 min at 300g, RT, with brake. The supernatant was removed and the cell pellet was resuspended in PBS and centrifuged for 10 min at 300g, RT, with brake. This washing step was repeated once. Finally, the cell pellet was resuspended in 5 mL PBS-BE. Cells were stained with Trypan blue (Sigma-Aldrich) to exclude dead cells counted by using a Bürker haemacytometer (Superior, Marienfeld, Germany).

CD14-positive cells were isolated using CD14 MicroBeads (Miltenyi Biotech) following the protocol of the manufacturer. Briefly, 80 µL of anti-human CD14 MACS MicroBeads (diameter: ~50 nm) were mixed with 320 µL of cell suspension ($4x10^7$ cells) and incubated for 15 min in the refrigerator (2-8°C). In the meantime, the MS column was placed on the miniMACS separator (both from Miltenyi Biotech). The column was rinsed with 500 µL of PBS-BE buffer. Then, the cell suspension was applied to the column and the flow through was collected. This flow through was applied again to the column and then discarded. The column was removed from the separator and placed on a collection tube. One mL of PBS-BE was pipetted into the column and immediately a plunger was applied to flush out the magnetically labelled cells.

For monocyte culture, cells were centrifuged for 10 min at 300g, RT, with brake. The cell pellet was resuspendend, counted, and distributed into a 6-wells plate at a concentration of $2x10^6$ cells per well in RPMI medium containing 1% L-Glu and 1% Pen/Strep, and 10 µg/mL LPS. After incubation for 0, 6, 18, and 24 hours (h), the cell supernatant was collected and centrifuged for 20 min at 2000g at RT, with brake to remove cell debris. The supernatant was aliquotted in 500-µL portions, snap frozen in liquid N_2, and stored at -80°C.

Immuno-magnetic beads capture

Hundred µL of PPP was mixed with 135 µL (27 µg) of biotinylated anti-human CD41-/CD14 MoAb and gently rotated for 30 min at RT, shielded from light. As negative controls, PPP was mixed with 135 µL (27 µg) of biotinylated mouse IgG1/IgG2a, κ isotype control MoAb. Next, 200 µL of streptavidin beads were added to the mixture and rotated for 5 min at RT, shielded from light. In the meantime, the µ Column was placed on the µMACS magnet separator (both from Miltenyi Biotech) and rinsed with 100 µL of the equilibration buffer included in the µMACS™ streptavidin kit. Afterwards, the µ Column was rinsed twice with 250 µL Hepes-citrate buffer. The mixture of PPP with antibody and beads was added to the µ Column and the flow through was collected. This flow through was added again into the µ Column to ensure that all the captured MPs were bound to the

magnet and then the flow through was collected (negative fraction). The µ Column was rinsed twice with 500 µL Hepes-citrate buffer. To collect the bound MPs, the µ Column was detached from the magnet after which quickly 75 µL Hepes-citrate buffer was added to the µ Column. The first eluate was collected. The µ Column was rinsed again with 75 µL Hepes-citrate buffer and a syringe plunger (5 mL) was applied to the µ Column to increase elution efficiency. Finally, the second eluate was collected and combined with the first eluate (positive fraction).

MP isolation

To isolate MoMPs, frozen supernatant of LPS stimulated-monocytes was thawed quickly with a gentle swirl at 37°C. The supernatant (500 µL) was centrifuged for 30 min at 18,890g, 20°C, with minimum brake, to isolate MPs and the supernatant was carefully removed, leaving a volume of 50 µL containing the MP pellet. To wash the MPs, 450 µL of Hepes buffer was added, and this mixture was then centrifuged again for 30 min at 18,890g, 20°C, with minimum brake. The supernatant was removed and the residual 50 µL was diluted to 200 µL with Hepes buffer. This MP fraction was directly used for the measurements.

MPs were isolated from plasma as previously described (22;24). Frozen PPP samples (250 µL) were thawed quickly with a gentle swirl at 37°C. Then, they were centrifuged three times at 18,890g for 30 min at 20℃ with minimum brake, to pellet the MPs. MPs were extensively washed between the centrifugation steps with Hepes-citrate buffer to reduce the concentration of plasma proteins to less than 0.5%. To isolate MPs from positive and negative fractions obtained from immuno-magnetic beads capture, the procedure (centrifugation and washing steps) was the same as the procedure to isolate MPs from plasma. At the third centrifugation step, the supernatant was carefully removed, leaving 25 µL of MP suspension. The MP suspensions obtained from plasma and positive/negative fractions were diluted to 100 µL before used for measurement.

Flow cytometry analysis

Flow cytometry analysis was performed using a FACS Calibur flow cytometer with CELLQUEST PRO software (Becton Dickinson). Before measurement the FACS Calibur was calibrated by using Megamix beads (25). Staining plasma MPs for CD41/CD61 after beads separation was done by adding 10 µL of anti-human CD41-PE MoAb and 10 µL of anti-human CD61-FITC MoAb into 15 µL of the MP fraction, and then diluting up to a volume of 50 µL with Hepes-citrate buffer. This mixture is incubated for 30 min at RT in the dark. As negative controls, mouse IgG1

isotype control-PE MoAb and mouse IgG1 isotype control-FITC MoAb were used at the same concentration as the antibodies.

When staining plasma MPs after beads isolation for CD14, 10 µL of anti-human CD14-PE MoAb was added into 15 µL of the MP fraction and diluted with Hepes-citrate buffer up to a volume of 50 µL. This mixture was incubated for 30 min at RT in the dark. As negative controls, mouse IgG2a, κ isotype control-PE MoAb was used at the same concentration as the antibody.

For staining MoMPs isolated from supernatant, 10 µL MPs was mixed with 5 µL anti-human CD14-PE MoAb, 5 µL anti-human TF-FITC MoAb, 5 µL annexin V-APC, and 25 µL Hepes buffer containing 2.5 mM $CaCl_2$. Anti-human CD14-PE MoAb and anti-human TF-FITC MoAb were 20 times diluted, whereas annexin V-APC was 300 times diluted in the final mixture. This mixture was incubated for 30 min, in the dark, at RT. As negative controls, mouse IgG2a, κ isotype control-PE MoAb and mouse IgG1-FITC MoAb were used at the same concentration as the antibodies. As a control of annexin V staining, Hepes buffer without $CaCl_2$ was used.

Before flow cytometry, 500 µL of Hepes-citrate buffer was added to the mixture containing labelled MPs. For counting absolute numbers of MPs per µL plasma or MoMPs per 500 µL supernatant, 200 µL of flow cytometry absolute count standard beads was mixed with Hepes buffer to a volume of 600 µL and then measured in triplicate. For measurement of counting beads as well as MPs, the flow cytometer was programmed to count events in 1 min.

MP-TF activity assay

Freshly isolated MPs were directly used for the measurement of MP-TF activity as previously described (22). In this assay the factor VII (FVII)-dependent factor Xa (FXa) generation was measured. MP-TF activity is expressed as fM FXa/min. The FXa generation was measured in the presence and absence of excess (33 µg/mL) polyclonal sheep anti-human TF IgG (Affinity Biologicals INC, Canada) and (1 nM) human FVII (Kordia, Leiden, The Netherlands). Human factor X (50 nM) (Kordia) was added to start FXa formation. The MP-TF activity (TF-activity in isolated MPs) was FVII and TF dependent confirming the specificity of the assay.

Results

The beads separation method was based on the capture of a specific subset of MPs from plasma by using biotinylated antibody and streptavidin magnetic beads.

We first tested the procedure to capture PMPs. The biotinylated anti-human CD41 MoAb was incubated with the plasma before the streptavidin magnetic beads were added. After application of this mixture to the column, positive and negative fractions were collected (Figure 1). Subsequently, the separated fractions were used to isolate and analyze MPs for specific antigens and TF activity.

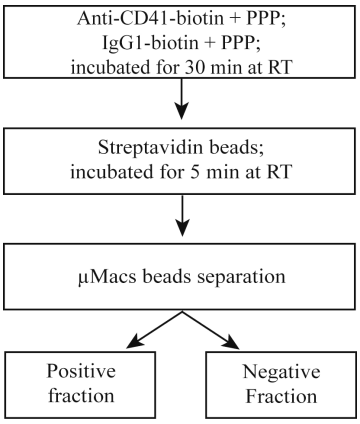


Figure 1. Scheme for the immuno-magnetic beads capture procedure using biotinylated anti-human CD41 MoAb and biotinylated mouse IgG1 isotype control MoAb. After beads separation using biotinylated anti-human CD41 MoAb, MPs in positive and negative fractions were collected.

Optimizing of the concentrations of anti-CD41 antibody and streptavidin magnetic beads

For PMP capture from plasma by antibody-coated magnetic beads both the concentration of antibodies and of streptavidin magnetic beads need to be optimized. To check whether the antibody saturated the surface antigen CD41 of PMPs, PPP (100 µL) was first reacted with different concentrations of biotinylated anti-human CD41 MoAb. Subsequently MPs were labelled by fluorescent antibodies, anti-human CD41-PE MoAb and anti-human CD61-FITC MoAb or the fluorescently labelled isotype controls, and analysed by flow cytometry. These experiments showed that 135 µL (27 µg) biotinylated anti-human CD41 MoAb specifically binds and saturates the surface antigen CD41 of PMPs in 100 µL plasma. Figure 2A and B show flow cytometry analysis of plasma MPs without biotinylated anti-human CD41 MoAb. The PMPs express both CD41 and CD61 (Figure 1A). When biotinylated anti-human CD41 MoAb (27 µg/135 µL) was added, plasma PMPs show only CD61 and no CD41 expression (Figure 2C). Figure 2E shows that when using biotinylated mouse IgG1 isotype control MoAb instead of

biotinylated anti-human CD41 MoAb, the surface antigens CD41 and CD61 could still be detected on PMPs by anti-CD41 and anti-CD61 antibodies.

Streptavidin magnetic beads should be added in excess to bind all biotinylated antibodies present in the plasma. We found that 200 µL streptavidin magnetic beads were needed and that the streptavidin magnetic beads did not interfere with the binding of anti-CD41 and anti-CD61 antibodies to PMPs (Figure 2G). Fluorescently labelled IgG1 were used as controls at the same concentrations as the staining antibodies (Figure 2 B, D, F, and H).

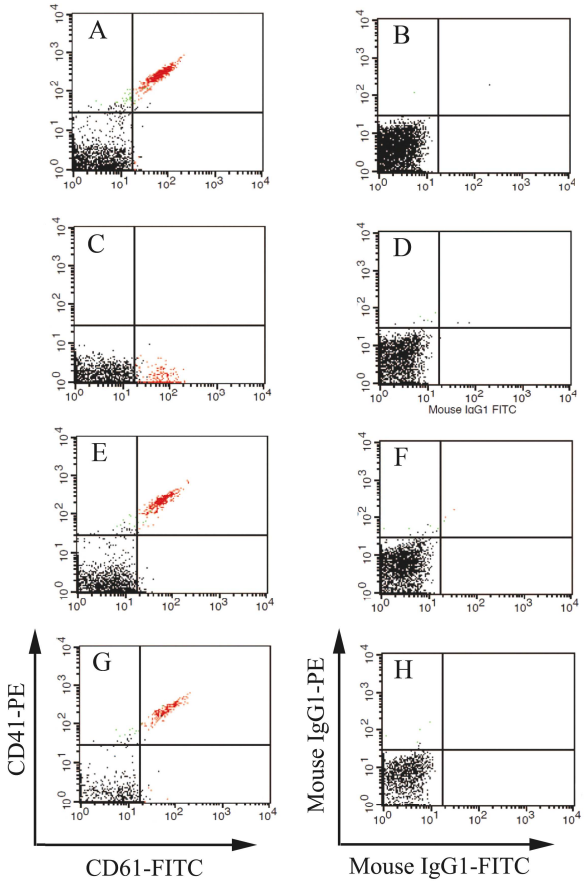


Figure 2. Optimizing the concentration of antibodies, streptavidin magnetic beads, and plasma for the immuno-magnetic beads method. Stainings of samples were performed by using anti-human CD41-PE and anti-human CD61-FITC MoAbs (A, C, E, G). As controls, mouse IgG1-PE and mouse IgG1-FITC MoAbs were used at the same concentrations (B, D, F, H). After staining, PPP (A, B) and PPP incubated with biotinylated anti-human CD41 MoAb (C, D), biotinylated mouse IgG1 isotype control MoAb (E, F), or streptavidin beads (G, H) were measured by flow cytometry. Experiments were done in duplicate.

In conclusion, 135 µL (27 µg) biotinylated anti-human CD41 MoAb and 200 µL streptavidin magnetic beads can be used for optimal capturing of CD41-positive MPs from 100 µL PPP. As PMPs bearing CD41/CD61 are the most abundant MPs in plasma, these optimized conditions can also be applied to capture other subsets of MPs from plasma.

Use of immuno-magnetic beads to capture PMPs from plasma.

After beads separation for PMPs bearing CD41, positive and negative fractions were collected (Figure 1) and stained by using fluorescently labelled anti-human CD41 and anti-human CD61 MoAbs or their isotype controls as described in the methods section. Flow cytometry analysis (Figure 3A) showed that there is no fluorescence signal of the anti-human CD41 MoAb, but only of the anti-human CD61 MoAb on MPs in the positive fraction. This indicated that the surface antigen CD41 of PMPs in this positive fraction still was saturated by the biotinylated anti-human CD41 MoAb. In the negative fraction no CD41- and CD61-positive MPs were detected (Figure 3C). Figure 3B and D show fluorescently labelled isotype controls staining of these fractions.

To check for non-specific binding of biotinylated anti-human CD41 MoAb, biotinylated mouse IgG1 isotype control MoAb was used (Figure 3E-H). In the positive fraction no CD41- and CD61-positive MPs were detected (Figure 3E). These were only present in the negative fraction (Figure 3G) indicating that CD41-positive MPs are specifically captured from plasma by using this procedure. Figure 3F and H show fluorescently labelled isotype controls staining of these fractions.

Flow cytometry quantification of CD41 and CD61-positive MPs

Frozen-thawed PPP from three healthy volunteers was used to perform the immuno-magnetic beads capture of PMP by using biotinylated anti-human CD41 MoAb. Figure 4 shows that no CD41-positive MPs were detected in the negative fractions. In these fractions about 1, 0, and 6% of CD61-positive MPs were found in volunteer 1, 2, and 3 respectively. This indicated that almost all PMPs (CD41-positive MPs) were captured. As the anti-CD41 coated-beads saturated the surface antigen CD41 of MPs, there were no CD41-positive MPs detected in the positive fraction. However, there were also few CD61-positive MPs present in this positive fraction. Possibly the magnetic beads which still present on the surface of MPs in the positive fraction interfere with the fluorescence staining with anti-CD61 antibody causing inaccurate quantification of CD61-positive MPs by flow cytometry.

When biotinylated mouse IgG1 isotype control MoAb was used instead of biotinylated anti-human CD41 MoAb, we found that about 5% and 80% of CD41/CD61-positive MPs were recovered in the positive and negative fractions of the biotinylated IgG1-beads separation.

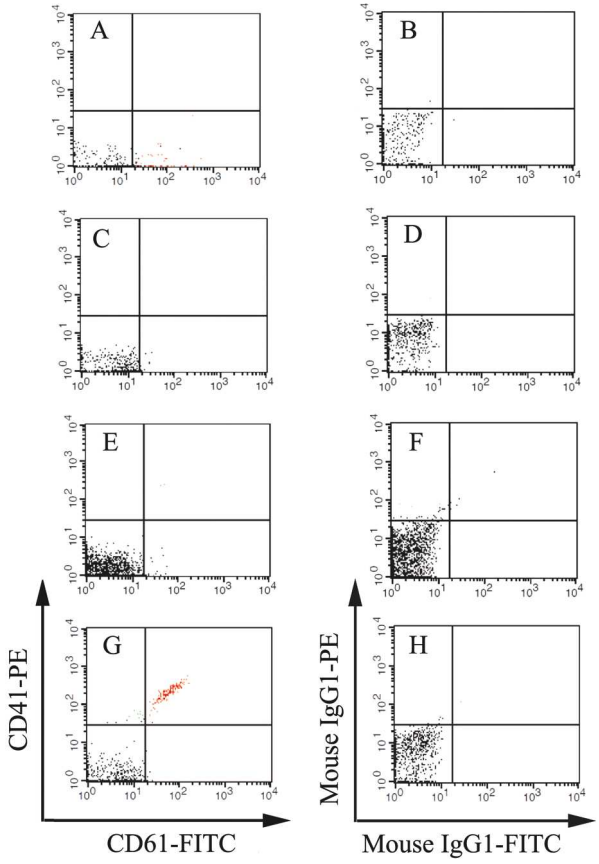


Figure 3. Flow cytometry analysis of positive and negative fractions after beads separation for PMPs bearing CD41. After beads separation using biotinylated anti-human CD41 MoAb, MPs in positive (A, B) and negative fractions (C, D) were collected, stained by anti-human CD41-PE and anti-human CD61-FITC MoAbs (A, C) or isotype controls (B, D), and measured by flow cytometry. Staining was also done for MPs in the positive (E, F) and negative (G, H) fractions collected from beads separation using biotinylated mouse IgG1 isotype control MoAb by using anti-human CD41-PE and anti-human CD61-FITC MoAbs (E, G) or isotype controls (F, H). All measurements were performed in duplicate.

Flow cytometry and MP-TF activity measurements of in vitro generated MoMPs

Monocytes were isolated from human blood and stimulated with LPS for 0, 6, 18, and 24 h to produce MoMPs. MoMPs were isolated from the supernatant, stained

with fluorescently labelled annexin V, anti-human CD14 and anti-human TF MoAbs and analysed by flow cytometry. Figure 5A shows that MoMPs expressed annexin V, CD14 antigen, and TF antigen. However, not all MoMPs were CD14 positive as measured by flow cytometry. After 6, 18 and 24 h stimulation with LPS, there were more TF- and annexin V-positive MoMPs than without LPS stimulation.

MP-TF activity measurements were performed to investigate whether MoMPs derived from LPS-stimulated monocytes carry active TF. The results are summarized in Figure 5B and show that MoMPs isolated from the supernatant of monocytes stimulated with LPS for 6, 18, and 24 h carried active TF and this TF activity could be completely inhibited by an anti-human TF antibody.

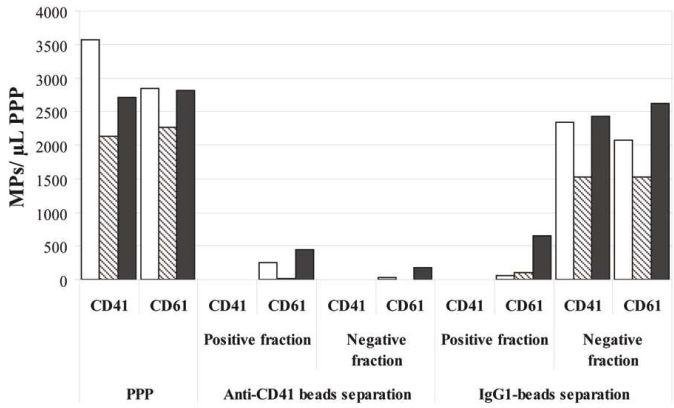


Figure 4. Flow cytometry quantification of CD41/CD61-positive MPs in the positive and negative fractions obtained from immuno-magnetic beads separation using biotinylated anti-human CD41 or mouse IgG1 isotype control MoAb. PPP used in these experiments was prepared from blood of 3 healthy volunteers (white bar: volunteer 1, black bar: volunteer 2, hatched bar: volunteer 3). Measurements were performed in duplicate.

Use of immuno-magnetic beads to capture MoMPs from plasma spiked with in vitro generated MoMP

We added MoMPs carrying active TF (isolated from the supernatant of monocytes stimulated with LPS for 0, 6, 18, or 24 h) to frozen-thawed PPP of a healthy volunteer in a 1:1 ratio (v/v); no visible clot was formed after 30 and 60 minutes at RT. The procedure of immuno-magnetic beads to capture MoMPs was the same as the procedure used to capture PMPs from plasma. Plasma spiked with MoMPs (100 µL) were incubated with biotinylated anti-human CD14 MoAb and streptavidin magnetic beads were added before the mixture was subjected to the column.

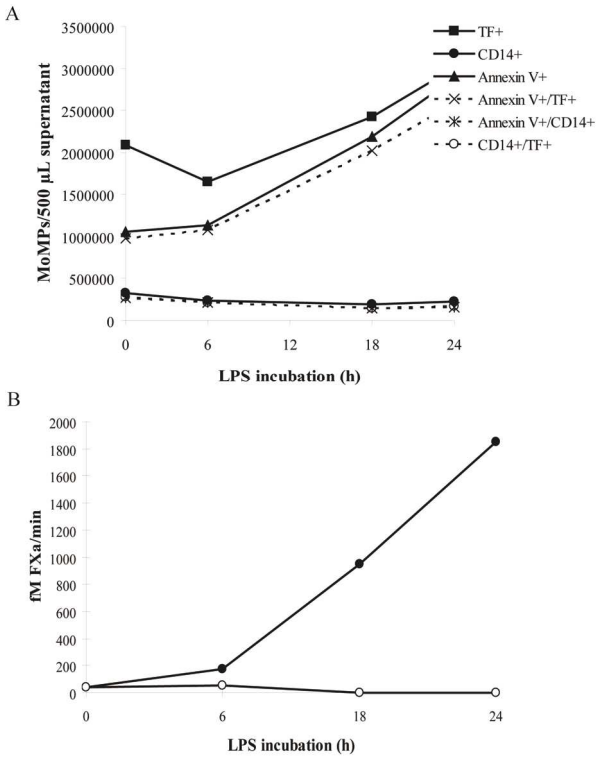


Figure 5. Flow cytometry analysis and MP-TF activity measurements of MoMPs. MoMPs isolated from the supernatant of monocytes stimulated with LPS for 0, 6, 18, and 24 h were stained by using annexin V APC, anti-TF FITC, and anti-CD14 PE antibodies and quantified by flow cytometry (A). The same batch of MoMPs was used for the measurement of TF activity (B) in the presence (○) or absence (●) of an anti-TF antibody.

The concentration of biotinylated anti-human CD14 MoAb used was the same as that of biotinylated anti-human CD41 MoAb in the PMP separations. The positive and negative fractions were collected and subjected to MP-TF activity analysis. For baseline measurements, PPP, MoMPs, and PPP spiked with MoMPs before beads separation were used.

The results of the MP-TF activity measurements are shown in Figure 6 and Table 1. In Figure 6 it is shown that MPs isolated from PPP have no active TF, while as expected MoMPs isolated from supernatant of monocytes stimulated with LPS for 6, 18, and 24 h have active TF, which is completely inhibited by an anti-TF antibody. TF activity was also present in the MPs isolated from PPP spiked with MoMPs; however, the TF activity was 2-fold lower than expected on the basis of the TF activity of the isolated MoMPs added, which might be due to loss of MPs during the isolation of MPs from PPP. After the column separation we found TF activity both in the positive and negative fractions of PPP spiked with MoMPs

isolated from the supernatant of monocytes stimulated with LPS for 0, 6, 18, and 24h. This indicated that both CD14-positive and negative MoMPs have active TF. When the MP-TF activities (fM FXa/min) of PPP spiked with MoMPs before and after beads separation were compared, we found that after beads separation the combined MP-TF activities of the positive and negative fractions were about 1.2-fold lower than those before beads separation (Table 1).

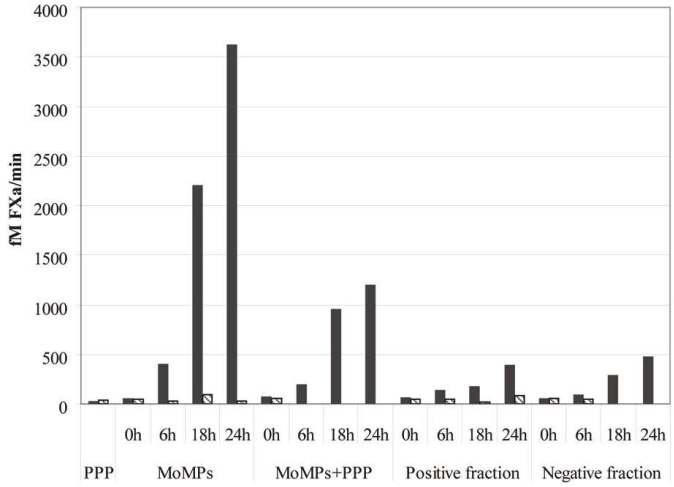


Figure 6. MP-TF activity of PPP spiked with MoMPs before and after beads separation. PPP spiked with MoMPs were incubated with biotinylated anti-human CD14 MoAb and streptavidin magnetic beads. This mixture was subjected to a column for magnetic beads separation. Positive and negative fractions from this beads separation were collected and measured by MP-TF activity assay in the presence (hatched bar) or absence (black bar) of an anti-TF antibody. PPP without MoMPs, MoMPs alone, and PPP spiked with MoMPs before beads separation were used as baseline measurements.

Table 1. TF activity levels (expressed as fM FXa/min) of PPP spiked with MoMPs before and after beads separation are compared.

Samples	**fM FXa/min**
Before beads separation	
MoMPs (0h) + PPP	78.70
MoMPs (6h) + PPP	197.91
MoMPs (18h) + PPP	953.43
MoMPs (24h) + PPP	1202.43
After beads separation	
Positive + negative fractions (0h)	123.67
Positive + negative fractions (6h)	236.78
Positive + negative fractions (18h)	462.34
Positive + negative fractions (24h)	869.42

Discussion

In this study we present a method to use a combination of a biotinylated antibody and streptavidin magnetic beads to capture a specific subset of MPs from plasma. A positive fraction (containing selected subset of MPs) bound to the beads was separated from the negative fraction (containing the depleted plasma) and these fractions can be analysed for specific markers like for instance TF activity.

This immuno-magnetic beads method was optimized to capture PMPs. We used biotinylated anti-human CD41 MoAb at a concentration that saturated the surface antigen CD41 of MPs. The streptavidin beads were added in excess to bind all biotinylated antibodies present in the plasma. To obtain a specific interaction between the antibody and the surface antigen of MPs, it is important to first incubate plasma with the biotinylated antibody before the streptavidin magnetic beads are added. The biotin-streptavidin interaction was chosen for this procedure because the non-covalent interaction between biotin and streptavidin is the strongest interaction known with a dissociation constant, K(d), in the order of $4x10^{-14}$ M (26). The bond also forms very rapidly and is stable over a wide range of pH and temperature (27).

The capture of the CD41-positive MP subset from plasma was successful as flow cytometry analysis demonstrated that these MPs were barely found in the negative (depleted) fraction obtained after column separation (Figure 3). The recovery of the CD41-positive MPs in the positive fraction could not accurately be quantified by flow cytometry. The magnetic beads (diameter: ~50 nm) which were still attached to CD41-positive MPs after the column separation apparently hindered the detection of MPs by using fluorescently labelled anti-human CD61 MoAb and flow cytometry. To capture CD41-positive PMPs, PPP of healthy volunteers were used. As these plasma contained very low MP-TF activity (~20 fM Xa/min), it was not possible to obtain accurate results for the MP-TF activity measurements in the positive and negative fractions.

We also tested the immuno-magnetic beads method to capture CD14-positive MPs from plasma and analysed the positive and negative fractions for MP-TF activity. However, the concentration of MoMPs in plasma of healthy individuals is low (about 2% of the total blood MP population) (8;11). Thus, MoMPs isolated from LPS-stimulated monocytes were used as a model of monocyte derived active TF bearing MPs and spiked to plasma of a healthy volunteer. We found TF activity both in the positive (CD14-positive) and negative (CD14-negative) fractions of plasma spiked with these MoMPs. This is in agreement with our finding that not all

active TF carrying MoMPs isolated from the supernatant of LPS stimulated monocytes were CD14 positive.

In conclusion, the immuno-magnetic beads method can be used for capture specific subsets of MPs directly from plasma. For future application, other specific biotinylated antibodies can be used to capture different subsets of MP from plasma. Ultimately this approach will help us to identify the cellular sources of MP bearing active TF in plasma of patients with cancer or other diseases.

Acknowledgments

The authors thank P. Garcia Rodriguez for her technical support in MP-TF activity measurement. This work was supported by the Dutch Cancer Society (KWF UL 2006-3618).

References

(1) Sorensen HT, Mellemkjaer L, Steffensen FH, Olsen JH, Nielsen GL. The risk of a diagnosis of cancer after primary deep venous thrombosis or pulmonary embolism. N Engl J Med 1998;338:1169-1173.

(2) Blom JW, Doggen CJ, Osanto S, Rosendaal FR. Malignancies, prothrombotic mutations, and the risk of venous thrombosis. JAMA 2005;293:715-722.

(3) Prandoni P, Lensing AW, Buller HR, Cogo A, Prins MH, Cattelan AM, et al. Deep-vein thrombosis and the incidence of subsequent symptomatic cancer. N Engl J Med 1992;327:1128-1133.

(4) Murchison JT, Wylie L, Stockton DL. Excess risk of cancer in patients with primary venous thromboembolism: a national, population-based cohort study. Br J Cancer 2004;91:92-95.

(5) Sorensen HT, Mellemkjaer L, Olsen JH, Baron JA. Prognosis of cancers associated with venous thromboembolism. N Engl J Med 2000;343:1846-1850.

(6) Piccin A, Murphy WG, Smith OP. Circulating microparticles: pathophysiology and clinical implications. Blood Rev 2007;21:157-171.

(7) Burnier L, Fontana P, Kwak BR, Angelillo-Scherrer A. Cell-derived microparticles in haemostasis and vascular medicine. Thromb Haemost 2009;101:439-451.

(8) Hron G, Kollars M, Weber H, Sagaster V, Quehenberger P, Eichinger S, et al. Tissue factor-positive microparticles: Cellular origin and association with coagulation activation in patients with colorectal cancer. Thromb Haemost 2007;97:119-123.

(9) Nieuwland R, Berckmans RJ, Rotteveel-Eijkman RC, Maquelin KN, Roozendaal KJ, Jansen PG, et al. Cell-derived microparticles generated in patients during cardiopulmonary bypass are highly procoagulant. Circulation 1997;96:3534-3541.

(10) Tesselaar ME, Romijn FP, van dL, I, Bertina RM, Osanto S. Microparticle-associated tissue factor activity in cancer patients with and without thrombosis. J Thromb Haemost 2009;7:1421-1423.

(11) Tesselaar ME, Romijn FP, van der Linden IK, Prins FA, Bertina RM, Osanto S. Microparticle-associated tissue factor activity: a link between cancer and thrombosis? J Thromb Haemost 2007;5:520-527.

(12) Manly DA, Wang J, Glover SL, Kasthuri R, Liebman HA, Key NS, et al. Increased microparticle tissue factor activity in cancer patients with Venous Thromboembolism. Thromb Res 2010;125:511-512.
(13) Breitenstein A, Tanner FC, Luscher TF. Tissue factor and cardiovascular disease. Circ J 2010;74:3-12.
(14) Azevedo LC, Pedro MA, Laurindo FR. Circulating microparticles as therapeutic targets in cardiovascular diseases. Recent Patents Cardiovasc Drug Discov 2007;2:41-51.
(15) Wolf P. The nature and significance of platelet products in human plasma. Br J Haematol 1967;13:269-288.
(16) Furie B, Furie BC. Cancer-associated thrombosis. Blood Cells Mol Dis 2006;36:177-181.
(17) Van Der Pol E, Hoekstra AG, Sturk A, Otto C, Van Leeuwen TG, Nieuwland R. Optical and non-optical methods for detection and characterization of microparticles and exosomes. J Thromb Haemost 2010;8:2596-2607.
(18) Yuana Y, Oosterkamp TH, Bahatyrova S, Ashcroft B, Garcia RP, Bertina RM, et al. Atomic force microscopy: a novel approach to the detection of nanosized blood microparticles. J Thromb Haemost 2010;8:315-323.
(19) Zwicker JI, Liebman HA, Neuberg D, Lacroix R, Bauer KA, Furie BC, et al. Tumor-derived tissue factor-bearing microparticles are associated with venous thromboembolic events in malignancy. Clin Cancer Res 2009;15:6830-6840.
(20) Bach RR. Tissue factor encryption. Arterioscler Thromb Vasc Biol 2006;26:456-461.
(21) Versteeg HH, Ruf W. Tissue factor coagulant function is enhanced by protein-disulfide isomerase independent of oxidoreductase activity. J Biol Chem 2007;282:25416-25424.
(22) Garcia RP, Eikenboom HC, Tesselaar ME, Huisman MV, Nijkeuter M, Osanto S, et al. Plasma levels of microparticle-associated tissue factor activity in patients with clinically suspected pulmonary embolism. Thromb Res 2010;126:345-349.
(23) Tilley RE, Holscher T, Belani R, Nieva J, Mackman N. Tissue factor activity is increased in a combined platelet and microparticle sample from cancer patients. Thromb Res 2008;122:604-609.
(24) Auwerda JJ, Yuana Y, Osanto S, de Maat MP, Sonneveld P, Bertina RM, et al. Microparticle-associated tissue factor activity and venous thrombosis in multiple myeloma. Thromb Haemost 2011;105:14-20.
(25) Lacroix R, Robert S, Poncelet P, Kasthuri RS, Key NS, Dignat-George F. Standardization of platelet-derived microparticle enumeration by flow cytometry using calibrated beads: results of ISTH SSC collaborative workshop. J Thromb Haemost 2010;8:2571-2574.
(26) Green NM. Avidin and streptavidin. Methods Enzymol 1990;184:51-67.
(27) Holmberg A, Blomstergren A, Nord O, Lukacs M, Lundeberg J, Uhlen M. The biotin-streptavidin interaction can be reversibly broken using water at elevated temperatures. Electrophoresis 2005;26:501-510.

CHAPTER 8

Microparticle-associated tissue factor activity and venous thrombosis in Multiple Myeloma

Johannes J.A. Auwerda, Yuana Yuana, Susanne Osanto, Moniek P.M. de Maat, Pieter Sonneveld, Rogier M. Bertina and Frank W.G. Leebeek

Thrombosis Haemostasis 2011; 105(1):14-20

Abstract

Multiple myeloma (MM) is associated with an increased risk of venous thromboembolic (VTE) complications. Aim of this study was to measure microparticle-associated tissue factor (MP-TF) activity in patients with newly diagnosed MM before and after chemotherapy and to investigate whether MP-TF activity is associated with VTE. MP-TF activity was assessed in 122 newly diagnosed MM patients who were eligible for combination chemotherapy. MP-TF activity levels (17.6 fM Xa/min [8.6-33.2] (median [IQR]) were higher in untreated MM patients compared to normal healthy volunteers (4.1 fM Xa/min [2.3-6.6], p <0.001). MP-TF activity prior to the start of treatment was not different between patients who developed a VTE during follow-up (n=15) and those who did not (n=107). In 75 patients in whom plasma was obtained before and after chemotherapy, MP-TF activity decreased significantly (from 17.4 [10.2-32.8] to 12.0 [7.0-18.5] fM Xa/min, P=0.006). MP-TF activity remained, however, elevated in patients who developed VTE (15.1 [10.3-25.2]), in contrast to patients not developing VTE (11.4 [7.0-25.2], P<0.001). In conclusion, MP-TF activity is increased in patients with MM. Whether MP-TF activity has a pathogenetic role in VTE in MM patients remains to be established in future studies.

Introduction

An increased risk of venous thrombo-embolism (VTE) is observed in multiple myeloma (MM), especially when these patients are treated with combination treatment including high dose dexamethasone, doxorubicin or multi-agent chemotherapy in combination with thalidomide or lenalidomide (1-2). The exact mechanism of the increased risk of VTE is not yet fully understood, but a number of mechanisms have been proposed to contribute to the development of the hypercoagulable state in these patients. These include increased levels of factor VIII or von Willebrand factor and hypofibrinolysis (3-6). Furthermore, an association between acquired APC resistance and the occurrence of VTE in MM has also been reported (5, 7).

Tissue factor is the principal initiator of the coagulation cascade and can be demonstrated on circulating microparticles that are released from cells following activation or during apoptosis (8-9). In addition tissue factor is expressed on the surface of cells in many tumour types and the expression appears to correlate with grade of malignancy and with tumour progression (10-12) TF expression of various tumour types has been associated with the risk of development of VTE complications (13). Tesselaar et al. observed an association of microparticle associated-tissue factor (MP-TF) activity and VTE using a functional assay to measure TF activity in the MP fraction of plasma (MP-TF activity) in patients with disseminated mucinous adenocarcinoma (14). More recent studies have shown similar results for other types of cancer (15-17). Zwicker et al showed that elevated levels of TF-MP were associated with an increased cumulative incidence of VTE (16, 18). Also Khorana et al. found an association between TF antigen levels, TF MP procoagulant activity and development of VTE (19). Some of these studies indicate that at least part of the TF+ MP is derived from tumour cells, but also platelet-derived and monocyte-derived MPs are increased (16, 20-21). Despite the fact that several patient groups with different types of cancer have been studied, no data are available on MP-TF activity in MM patients, who have a very high risk of developing VTE.

Therefore the aim of the current study was to investigate MP-TF activity in MM patients and to assess a possible association with the development of VTE.

METHODS

Patients

A total of 122 patients with newly diagnosed MM according to the Mayo Clinic criteria who were eligible for chemotherapy followed by autologous stem cell transplantation were included in the study (22). The patients were admitted to the department of Haematology of the Erasmus MC Rotterdam, an academic tertiary referral hospital in the Netherlands. These patients were recruited from the HOVON-50 MM (METC no 01/080) and HOVON-65 MM/GMMG-HD4 (EUDRACT no 2004-000944-26) studies. Only patients who were eligible for intensive chemotherapy with high dose melphalan and autologous stem cell support were included. The Central Medical Ethical Committee of the Erasmus MC approved the study and written informed consent was obtained from all patients before performing the investigation. Patients were randomized to received either 3 courses of VAD (doxorubicin [9 mg/m^2 i.v., day 1-4], dexamethasone [40mg orally, day 1-4, 9-12, 17-20] and vincristine [0.4 mg i.v., day 1-4]), or TAD (thalidomide 200 mg orally daily, doxorubicin [9 mg/m^2 i.v., day 1-4], dexamethasone [40 mg orally, day 1-4, 9-12, 17-20] or PAD (bortezomib [1.3 mg/m^2 i.v., days 1,4,8,11], doxorubicin [9 mg/m^2 i.v., day 1], dexamethasone [40 mg orally day 1-4, 9-12, 17-20]). During thalidomide treatment, patients received a prophylactic dose of LMWH (nadroparin 2850 IE anti-Xa (body weight < 90kg) or 5700 IE anti-Xa (body weight ≥ 90kg) subcutaneously. At entry in the study the patients were staged according to the criteria of Salmon and Durie, as well as to the recently introduced prognostic International Staging System (ISS) (23-24). Plasma levels of MP-TF activity were also determined in twenty healthy volunteers (median age 48 years [range 31-69], 45% males).

In case patients had complaints suggestive of pulmonary embolism, standardized diagnostic strategies were used, including computed tomography of the chest and compression ultrasonography in case of complaints suggestive for deep venous thrombosis of the leg or arm in order to confirm or exclude the VTE. When a VTE was confirmed oral anticoagulant (coumarin) was initiated in therapeutic dose (INR 2.5-3.5).

Materials & methods

Venous blood was collected using a vacutainer system in citrate (0.105 M, Becton-Dickinson, Plymouth, UK). The first five mL of blood were discarded. Platelet-free plasma (PFP) was prepared by double centrifugation (4℃ at 2,000g for 10 minutes [min] followed by 10 min at 4℃ at 21,475g) and sto red in small aliquots at –70℃

until use. The blood samples were collected at time of diagnosis (time point 1) and after three courses of multi-agent chemotherapy (time point 2). Plasma was immediately snap frozen in liquid nitrogen and stored at –70°C until use. The same procedure was used for the preparation of plasma of patients and of healthy volunteers. Plasma was obtained at entry of the study of 122 patients, and plasma was collected at the second time point (after induction chemotherapy) in 75 of the 122 patients. Of the 122 patients 15 developed a VTE during follow-up, of whom plasma samples were available of 11 patients at the second time point.

Dioleoylphosphatidlyserine (DOPS) and Dioleoylphosphatidylcholine (DOPC) were purchased from Avanti Polar Lipids (Alabaster, AL). Hirudin was from Sigma (Germany). The human Factor VII (FVII) and Factor X (FX) were obtained from Kordia Life Sciences (Leiden, NL). Sheep anti-human Tissue Factor IgG1 (TF) was from Affinity Biologicals (Ancaster, Canada). Chromogenic substrate S-2765 was from Instrumentation Laboratory Company (Milano, Italy). Innovin was obtained from Dade Behring (Eschborn, Germany).

Microparticle isolation

The isolation of MP was performed as previously described (25). In order to reduce the contamination with plasma proteins MPs were washed extensively (<0.5% in the final MP preparation). In brief, two vials (each 250 µL) of frozen plasma were thawed at 37°C and then vortexed thoroughly. The vials were centrifuged at 18,890g, 20°C for 30 min. The supernatants were removed carefully except for 25 µL containing the MP pellet. Subsequently, each pellet was washed with 475 µL PBS containing 0.32% citrate (pH 7.45) and centrifuged (18,890g, 20°C, 30 min). This wash and centrifugation step was repeated once with 225 µL PBS-citrate. The supernatants were removed carefully except for the 25 µL containing the MP pellet. Finally, the two MP pellets were resuspended, pooled, and directly assayed for TF activity. The number of platelets in platelet-free plasma (PFP) is 1.72×10^6/L plasma, which is 16-fold lower than in platelet-poor plasma (PPP) prepared by a single centrifugation of 1,550g for 20 min. The MP fraction isolated form frozen/thawed PFP contains 10-fold less MPs when compared to MP fraction isolated from frozen/thawed PPP (1.3×10^8/L and 1.4×10^9/L, respectively). This conclusion is based on the results of flow cytometry measurements (scatter) on MPs isolated from PFP and PPP (Figure 1).

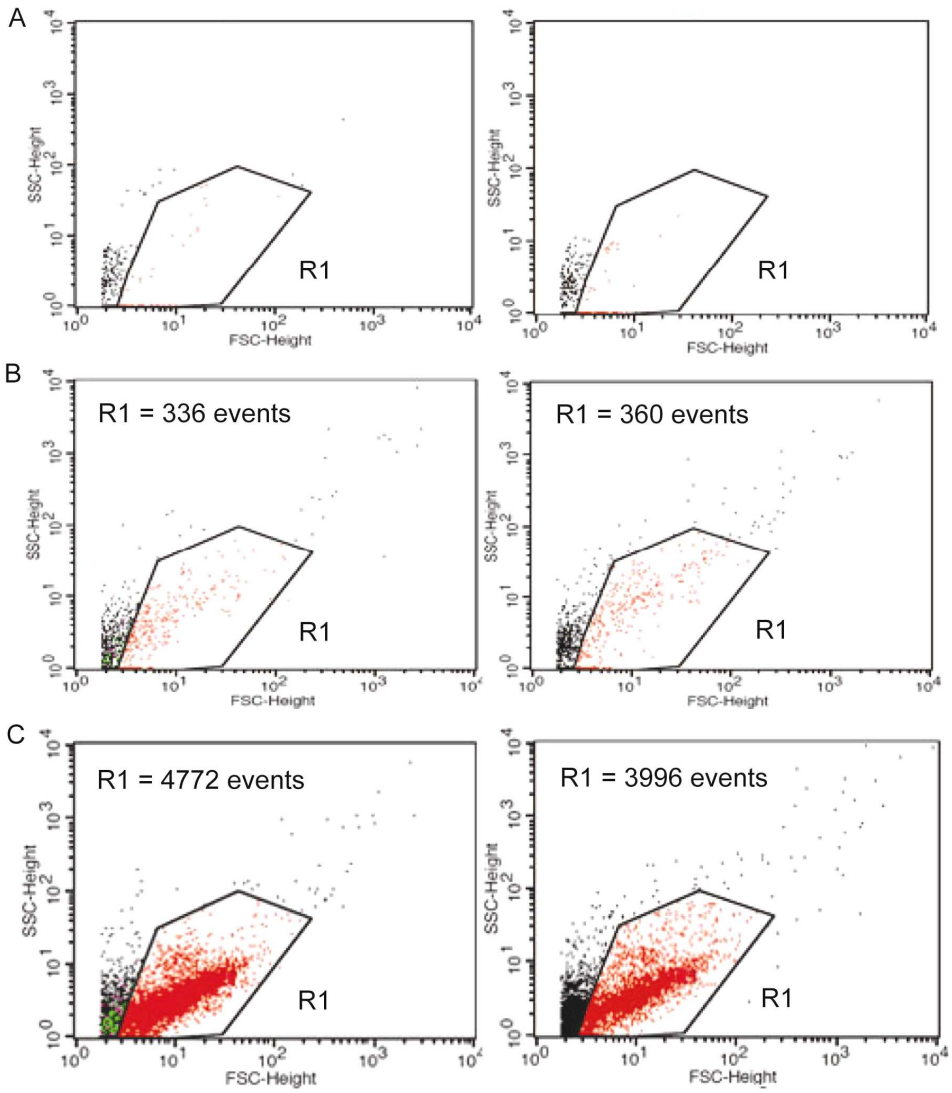


Figure 1: FACS analysis of MPs isolated from PFP (B) and PPP (C). The MP gate (R1) was defined using Hepes buffer (pH 7.45) containing 137 mM NaCl, 4 mM KCl (A.). MPs were isolated from 250 µL plasma and resuspended in 100 µL Hepes buffer; 5 µL of this suspension was diluted to 350 µL for FACS analysis; the Figures show duplicates of the scatter events in 74 µL of the measured suspension.

Tissue factor activity assay

MP-associated TF activity was measured at room temperature by determining the FVII-dependent factor Xa (FXa) generation in the presence of excess negatively charged phospholipids. MP-TF activity is expressed as fM FXa/min. This relates to the activity of the TF-VIIa complex when all TF has been saturated with FVIIa. In all samples, FXa generation was measured both in the presence and absence of FVII and in the presence and absence of sheep anti-human TF IgG_1 to confirm the FVII- and TF-dependence of the FXa generation. Twenty five µM DOPS: DOPC (10:90) were incubated for 15 min in 10 mM Hepes buffer (pH 7.45) containing 137 mM NaCl, 4 mM KCl, 5 mg/mL Ovalbumine, 6 mM $CaCl_2$, and 50 nM Hirudin. In 100 µL of this solution, 20 µL of MP-suspension was added and incubated for 15 min before 40 µL of 1.1 nM FVII (or buffer) was added. After 10 min, 25 µL S2765 was added and the reaction was started by adding 40 µL of 250 nM FX. The rate of p-Nitroaniline (pNA) formation as a product of the reaction was measured at 405 nm (expressed in mAbs) for 90 min, plotted as a function of time (t) and, after correction for the absorbance in the absence of FVII, as a function of t^2. The slope of the latter curve is a measure for the rate of FXa generation and expressed as $mAbs/min^2$ or as fM FXa/min. The MP-associated TF activity was calculated from the difference in the rate of Xa generation in the absence and presence of 11.1 µg/mL anti-TF antibody and reported as fM Xa/min in the assay. Dilutions of a recombinant full length TF (Innovin, 750 pg/mL and 150 pg/mL) were used as positive controls and to monitor interassay variation of the TF activity assay. Plasma of a patient with elevated MP-TF activity was used for the measurement of the interassay variation of the complete procedure, including the isolation of MP from plasma and the measurement of TF activity. Both CVs were <10% (N=9). This variation includes the MP isolation from plasma and the MP-TF activity measurement. The lower detection limit of the assay is about 2 fM Xa/min

Statistical analysis

Since the levels of MP-TF activity are not normally distributed, also not after transformation, the basic descriptive statistics are presented as median and interquartile range for continuous variables and as count (percentages) for categorical variables. Differences between two groups were tested with the Mann-Whitney test. Comparisons over time were evaluated with a paired analysis using the Wilcoxon signed rank test. The association between VTE risk and MP-TF activity was assessed by logistic regression analysis. All statistical analyses were performed using SPSS for windows, version 14 (SPSS Inc, Chicago, USA).

RESULTS

Patient characteristics

A total of 122 patients with MM were included in this prospective study, of whom 39 (32%) had stage I, 66 (54%) stage II and 16 (13%) had stage III disease according to the ISS criteria (23). The median age was 55 years (range 29-71) and 58% were males. Seventy patients received VAD, thirty-six TAD and fifteen PAD induction chemotherapy. The baseline patient characteristics are summarized in Table 1. Of the 122 included patients a post-treatment blood sample was obtained of 75 patients. The baseline characteristics were not different between these 75 patients and the 47 of whom only a pre-treatment plasma sample was obtained, with the exception of a slightly lower hemoglobin level at diagnosis (7.1 [6.4-7.9] vs 6.5 [5.7-7.2], p=0.01 (Table 2).

Table 1. MM patient characteristics

Table I. Multiple Myeloma patient characteristics

		Total group	No VTE	VTE
Number of patients		122	107	15
Age yrs (median, range)		55 (29-71)	56 (29-71)	52 (38-65)
Male gender		58 %	59 %	53 %
β2 microglobulin (mg/l)*		3.08 (2.02-4.63)	3.18 (2.12-4.79)	2.40 (1.37-3.25)
Platelets ($x10^9$/l)*		242 (182-287)	236 (178-283)	268 (179-291)
Albumin (g/l)*		37 (32-42)	37 (32-42)	39 (33-44)
Calcium (mmol/l)*		2.33 (2.21-2.42)	2.33 (2.20-2.41)	2.334 (2.24-2.50)
Hemoglobin (mmol/l)*		6.9 (5.9-7.7)	6.8 (6.0-7.7)	7.8 (6.1-8.3)
Monoclonal protein	kappa	82 (66%)	71 (67%)	11 (73%)
(IgG and IgA)	lambda	40 (34%)	36 (33%)	4 (27%)
ISS stage	I	39 (33%)	30 (28%)	9 (60%)
	II	67 (54%)	62 (58%)	5 (33%)
	III	16 (13%)	15 (14%)	1 (7%)
Treatment	VAD	71 (58%)	64 (59%)	7 (47%)
	TAD	36 (30%)	30 (28%)	6 (40%)
	PAD	15 (12%)	13 (12%)	2 (13%)
Durie & Salmon	II a & b	23 (19%)	16 (15%)	7 (47%)
	III a & b	99 (81%)	91 (85%)	8 (53%)

VAD; vincristine, adriamycin and dexamethasone, TAD; thalidomide, adriamycin and dexamethasone, PAD; bortezomib, adriamycin and dexamethasone. *Median and 25-75% range.

MP-TF activity at baseline and after induction chemotherapy

The results of the MP-associated tissue factor activity levels are summarized in Table 3. The median MP-TF activity of the total group of patients with MM was 17.6 fM Xa/min (IQR 8.6-33.2), which was significantly higher than that in healthy volunteers (4.1 fM Xa/min (IQR 2.3-6.6); P<0.001, range 0-11.8) (Figure 2).

Table 2. Baseline characteristics of MM patients

Multiple Myeloma patient baseline characteristics

		Total group	Patients with only pretreatment plasma sample available	Patients with pre-and post treatment sample available	P value
Number of patients		122	47	75	
Age yrs (median, range)		55 (29-71)	57 (50-62)	58 (50-61)	0.46
Male gender		58 %	51%	62%	0.24
β2 microglobulin (mg/l)*		3.08 (2.02-4.63)	2.90 (2.06-4.44)	3.08 (1.80-4.67)	0.73
Platelets (x 10^9/l)*		242 (182-287)	236 (187-279)	245 (178-287)	0.61
Albumin (g/l)*		37 (32-42)	37 (32-40)	38 (32-42)	0.39
Calcium (mmol/l)*		2.33 (2.21-2.42)	2.30 (2.21-2.40)	2.36 (2.21-2.46)	0.22
Hemoglobin (mmol/l)*		6.9 (5.9-7.7)	6.5 (5.7-7.2)	7.1 (6.4-7.9)	0.01
Monoclonal protein (IgG and IgA)	kappa	82 (66%)	26 (58%)	56 (74%)	0.07
	lambda	40 (34%)	19 (42%)	20 (26%)	
ISS stage	I	39 (33%)	14 (30%)	25(34%)	0.71
	II	67 (54%)	27 (59%)	39 (51%)	
	III	16 (13%)	5 (11%)	11 (14%)	
Treatment	VAD	71 (58%)	30 (65%)	41 (54%)	0.47
	TAD	36 (30%)	11 (24%)	25 (33%)	
	PAD	15 (12%)	5 (11%)	10 (13%)	
Durie & Salmon	II a & b	23 (19%)	5 (9%)	18 (24%)	0.09
	III a & b	99 (81%)	40 (91%)	58 (76%)	

VAD; vincristine, adriamycin and dexamethasone, TAD; thalidomide, adriamycin and dexamethasone, PAD; bortezomib, adriamycin and dexamethasone. *Median and 25-75% range

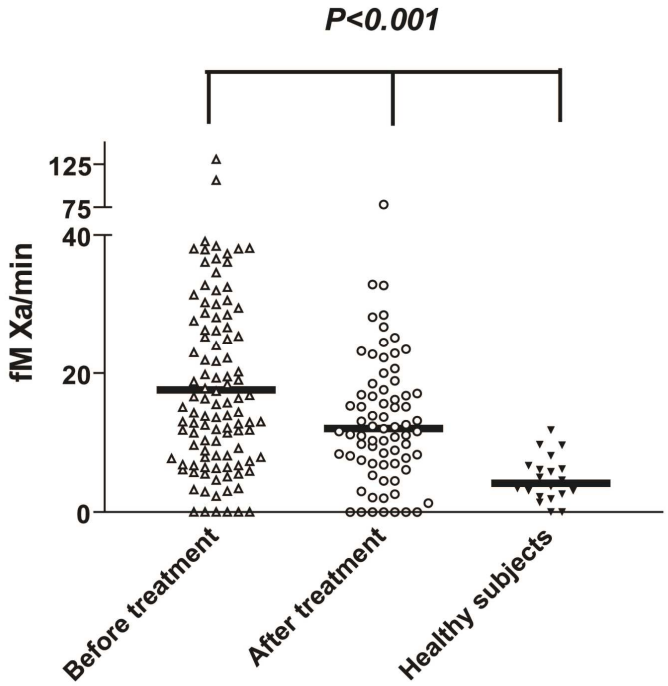


Figure 2: MP-Tissue factor activity in fM Xa/min in MM patients, before (n=122) and after induction chemotherapy (n=75) and in healthy subjects (n=20). The horizontal line indicates the median level. P-value denotes the difference between both before and after treatment versus healthy subjects. The p-values of paired analysis between before and after treatment are given in Table 3.

We observed significantly lower MP-TF activity levels in MM patients with light chain lambda (12.1 fM Xa/min [IQR 5.7-18.4] than in MM patients with light chain kappa (24.0 fM Xa/min [11.8-37.9]; $p<0.05$). None of the clinical patient characteristics (sex, beta-2 microglobulin, albumin, calcium, hemoglobin, platelets or disease stage) correlated with the MP-TF activity levels. MP-TF levels were not associated with age (r^2 =0.102). There was no significant difference in TF-MP activity at baseline between the 47 patients of whom no second blood sample was obtained (17.8 fM Xa/min [6.7-36.1]) and the 75 patients of whom also blood was drawn after chemotherapy (17.4 fM Xa/min [10.2-32.8], p=0.45).

Table 3. MP-TF activity in fM Xa/min

MP-TF activity in fM Xa/min						
	Total group at baseline		MM patients with pre- and post treatment plasma sample			p-value
	Number of patient	Before treatment	Number of patients	Before treatment	After treatment	
Total group	122	17.6 (8.6-33.2)	75	17.4 (10.2-32.8)	12.0 (7.0-18.5)	0.006
ISS stage						
1	39	14.4 (5.7-28.5)	25	14.4(6.6-27.4)	13.2 (6.5-19.2)	0.47
2	67	19.4 (11.9-32.6)	39	19.8 (11.8-36.1)	11.0 (7.0-18.9)	0.02
3	16	15.9 (6.7-40.3)	11	16.3(6.8-38.0)	12.6 (9.4-16.2)	0.11
		P=0.37			P=0.96	

ISS; International Staging System, VTE; venous thrombo-embolism. Data of MP-TF activity are given in median (25-75%).
P-value is on the effect of treatment using a paired analysis, thus only including patients that were measured at both time points, before and after chemotherapy.

Paired analysis in 75 patients of whom plasma was obtained at two time points, before and after chemotherapy, of MP-TF activity revealed a significant reduction of MP-TF activity following induction treatment (from 17.4 fM Xa/min [10.2-32.8] to 12.0 fM Xa/min [7.0-18.5], P=0.006, Table 3). This reduction was observed in all ISS stages of disease. Subgroup analysis for the different induction treatments revealed that VAD, TAD and PAD induced similar decrease of MP-TF activity levels (data not shown). When comparing MP-TF activity at the moment of response evaluation after the induction chemotherapy, no relationship between the change in MP-TF activity and the remission status (CR versus PR versus SD/PD) could be observed (data not shown). In addition the MP-TF activity levels were independent from the absolute or relative M-protein levels before and after induction therapy.

MP-TF activity and venous thrombosis

Fifteen of the 122 patients (12%) developed a VTE complication during the induction treatment (n=13) or high dose melphalan treatment and autologous stem cell transplantation (n=2). The baseline characteristics were similar for patients who did and did not develop VTE (Table 1). The incidence of VTE was 10% in the VAD treated patients, 16.7% in patients treated with thalidomide (TAD) and 13% in

patients who received Bortezomib (PAD). The MP-TF activity prior to the start of treatment was not different between patients who developed VTE (16.8 [11.4-36.1]; n= 15), and those who did not (17.8 [8.1-32.5]; n=107). In the 75 patients of whom plasma was obtained before and after chemotherapy we found that in the patients who did not develop VTE (n=64) during the course of treatment, the MP-TF activity levels decreased significantly (from 18.3 [IQR 9.8-32.6]) to 11.4 [IQR 7.0-25.2]; P<0.001). In contrast, in patients who did develop VTE (n=11) the MP-TF activity levels remained unchanged after induction chemotherapy (from 16.8 [IQR 11.4-34.6]) to 15.1 [IQR 10.3-25.2]; P=0.71, Figure 3). We calculated the risk of VTE in MM patients based on MP-TF activity levels below (n=40) and above (n=82) the upper limit in the healthy volunteers (11.8 fM Xa/min). The calculated risk for VTE in individuals with high MP-TF levels was 1.4 (0.4-4.7) [OR (95% CI)], for TF levels measured before start of induction and 3.0 (0.7-12.4) for MP-TF levels measured after induction therapy.

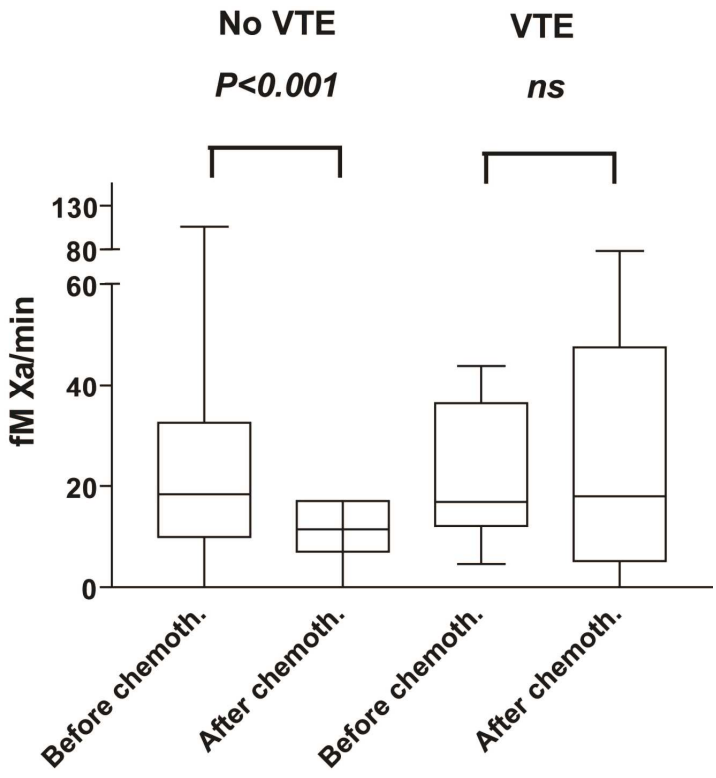


Figure 3: MP-Tissue factor activity in fM/Xa/min before and after induction chemotherapy in 75 MM patients, of whom plasma was available for two time points who did (VTE, n=11) and who did not (no VTE, n=64) develop VTE.

DISCUSSION

In this study we have shown that MP-TF activity levels are increased in patients with MM. The MP-TF activity levels in these patients decrease after induction chemotherapy. In patients experiencing VTE during or following treatment of MM, MP-TF activity levels did not decrease in contrast to the non-VTE patients in whom MP-TF activity decreased significantly compared to baseline.

Tissue factor is commonly regarded as the main determinant of a hypercoagulable state in patients with cancer (26). We measured tissue factor activity on circulating microparticles, small membrane vesicles derived from different cell types, including monocytes, platelets and tumour cells (14). In patients with untreated MM we observed increased MP-TF activity levels compared to healthy controls. From previous studies it is well known that several tumour types express high levels of tissue factor on their surface (13, 27). In addition, Kakkar et al. have shown that plasma tissue factor levels are increased in patients with malignancy (28). Also in patients with haematological disease, including acute myeloid leukaemia and malignant lymphoma, high plasma tissue factor antigen levels have been observed (29). Tissue factor messenger RNA levels in leukocytes from patients with hematopoietic tumours are increased compared to healthy controls (30). More recently plasma levels of tissue factor antigen were not found to be elevated in a small number of MM patients and also tissue factor mRNA levels measured in peripheral blood mononuclear cells were not elevated in these patients (31). In a recent study Shimizu described tissue factor production by clonal plasma cells in a patient with MM. In these plasma cells the cytoplasm stained positive for TF, which disappeared after chemotherapy (32). Since membrane-bound tissue factor exists both in an encrypted, inactive form as in an active form, tissue factor plasma antigen levels may not be representative of tissue factor activity in plasma, and therefore measurement of plasma tissue factor activity levels is preferred. We measured increased MP-TF levels in myeloma patients compared to healthy individuals. The levels of MP-TF activity in our study are lower in patients and control subjects than those reported previously by Tesselaar et al. (14). Centrifugation speed during plasma preparation has an effect on the number MPs in the final preparation. In the present study we used platelet-free plasma for the MP isolation (10 min at 2,000g followed by 10 min at 21,475g), while Tesselaar et al. used platelet-poor plasma (single centrifugation, at 1,550g for 20 min). This double centrifugation resulted in an about tenfold reduction of MP numbers in the isolated MP preparation as measured by FACS analysis (see methods section and Figure 1).

At present we do not know the cellular source of the MPs carrying active TF. Previously it has been shown that TF bearing MPs may be derived form cancer cells, platelets and leucocytes (14, 21, 33). Information on the cellular source of the MPs that carry TF activity would be extremely helpful to determine the pathogenetic role of these MPs in the development of thrombosis.

The stage of disease according to Salmon-Durie or the prognostic ISS stages were not correlated with the levels of MP-TF activity, suggesting that the tumour load is not associated with MP-TF activity levels. Remarkably, patients with a lambda type M-component exhibited significantly lower MP-TF activity compared to the kappa type M-component. The clinical significance of this observation is not yet clear since there are no data in the literature, which indicate a different incidence of thrombo-embolic complications.

Thrombo-embolic complications were observed in 15 patients (12%) and occurred with a similar frequency during all three chemotherapeutic regimens. It should be noted that patients, who were treated with chemotherapy in combination with the anti-angiogenic drug thalidomide, also received thromboprophylaxis with LMWH. Despite this thromboprophylaxis, 17% of patients treated with TAD experienced a thrombo-embolic complication. Interestingly, in patients who developed VTE, MP-TF activity levels remained elevated after induction treatment, while in patients who did not develop VTE the levels decreased significantly.

The high levels of MP-TF activity measured after induction treatment may suggest a pathogenetic role of MP-TF in the development of VTE in patients with MM. However the persistent high MP-TF levels may also be a result of thrombus formation. Because we measured MP-TF activity only twice it is difficult to establish that the highest levels of MP TF activity were observed at a time associated with thrombosis. It is known from previous studies that VTE in MM patients is most frequently observed during the first months of treatment (3, 34-35). This coincides with the highest MP-TF activity levels in plasma, as found in our study. It is also possible that MP-TF activity levels remained high as a consequence of the development of VTE. A causative role of MP-TF activity in the development of VTE can therefore not be established from our study. This should be assessed in larger studies, in which MP-TF activity is measured more frequently during induction treatment of MM.

The results of our study may have implications for prophylactic antithrombotic treatment of MM patients to prevent VTE during chemotherapy. So far no consensus on the optimal prophylactic antithrombotic regimen has been reached (2). Nowadays MM patients receive no prophylaxis, LMWH, fixed low-dose warfarin

or aspirin as prophylaxis (2, 35-36). The observation that MM patients have increased levels of MP-TF activity may suggest that antithrombotic agents targeted at inhibition of TF-initiated secondary hemostasis by LMWH or vitamin K antagonists is preferable to aspirin.

Our patients were treated with multi-agent chemotherapy and after three courses the MP-TF activity levels decreased irrespective of the therapeutic regimen (VAD or TAD or PAD). Chemotherapy in combination with anti-angiogenic drugs in MM is associated with the highest risk of thrombo-embolic complications. Our results indicate that this high risk in the TAD treated patients cannot be attributed to an increase of MP-TF activity (37).

In conclusion, MP-TF activity levels are increased in patients with MM and decrease significantly after induction chemotherapy. MP-TF activity levels after chemotherapy remained high in patients developing VTE. Whether MP-TF activity levels have a pathogenetic role in VTE in MM patients remains to be established.

Acknowledgment

This work was supported by the Dutch Cancer Society (KWF UL 2006-3618).

References

(1) Zangari M, Elice F, Fink L, Tricot G. Thrombosis in multiple myeloma. Expert Rev Anticancer Ther. 2007 Mar;7(3):307-315.

(2) Palumbo A, Rajkumar SV, Dimopoulos MA, Richardson PG, San Miguel J, Barlogie B, et al. Prevention of thalidomide- and lenalidomide-associated thrombosis in myeloma. Leukemia. 2008 Feb;22(2):414-423.

(3) Auwerda JJ, Sonneveld P, de Maat MP, Leebeek FW. Prothrombotic coagulation abnormalities in patients with newly diagnosed multiple myeloma. Haematologica. 2007 Feb;92(2):279-280.

(4) Minnema MC, Fijnheer R, De Groot PG, Lokhorst HM. Extremely high levels of von Willebrand factor antigen and of procoagulant factor VIII found in multiple myeloma patients are associated with activity status but not with thalidomide treatment. J Thromb Haemost. 2003 Mar;1(3):445-449.

(5) Elice F, Fink L, Tricot G, Barlogie B, Zangari M. Acquired resistance to activated protein C (aAPCR) in multiple myeloma is a transitory abnormality associated with an increased risk of venous thromboembolism. Br J Haematol. 2006 Aug;134(4):399-405.

(6) van Marion AM, Auwerda JJ, Minnema MC, van Oosterom R, Adelmeijer J, de Groot PG, et al. Hypofibrinolysis during induction treatment of multiple myeloma may increase the risk of venous thrombosis. Thromb Haemost. 2005 Dec;94(6):1341-1343.

(7) Jimenez VHs, Dominguez VJs. Acquired activated protein C resistance and thrombosis in multiple myeloma patients. Thromb J. 2006 Aug 21;4(1):11.

(8) Giesen PL, Rauch U, Bohrmann B, Kling D, Roque M, Fallon JT, et al. Blood-borne tissue factor: another view of thrombosis. Proc Natl Acad Sci U S A. 1999 Mar 2;96(5):2311-2315.

(9) Morel O, Toti F, Hugel B, Freyssinet JM. Cellular microparticles: a disseminated storage pool of bioactive vascular effectors. Curr Opin Hematol. 2004 May;11(3):156-164.

(10) Kakkar AK, Lemoine NR, Scully MF, Tebbutt S, Williamson RC. Tissue factor expression correlates with histological grade in human pancreatic cancer. Br J Surg. 1995 Aug;82(8):1101-1104.

(11) Uno K, Homma S, Satoh T, Nakanishi K, Abe D, Matsumoto K, et al. Tissue factor expression as a possible determinant of thromboembolism in ovarian cancer. Br J Cancer. 2007 Jan 29;96(2):290-295.

(12) Wojtukiewicz MZ, Sierko E, Klement P, Rak J. The hemostatic system and angiogenesis in malignancy. Neoplasia. 2001 Sep-Oct;3(5):371-384.

(13) Khorana AA, Ahrendt SA, Ryan CK, Francis CW, Hruban RH, Hu YC, et al. Tissue factor expression, angiogenesis, and thrombosis in pancreatic cancer. Clin Cancer Res. 2007 May 15;13(10):2870-2875.

(14) Tesselaar ME, Romijn FP, Van Der Linden IK, Prins FA, Bertina RM, Osanto S. Microparticle-associated tissue factor activity: a link between cancer and thrombosis? J Thromb Haemost. 2007 Mar;5(3):520-527.

(15) Manly DA, Wang J, Glover SL, Kasthuri R, Liebman HA, Key NS, et al. Increased microparticle tissue factor activity in cancer patients with Venous Thromboembolism. Thromb Res. 2010 Jun;125(6):511-512.

(16) Zwicker JI, Liebman HA, Neuberg D, Lacroix R, Bauer KA, Furie BC, et al. Tumor-derived tissue factor-bearing microparticles are associated with venous thromboembolic events in malignancy. Clin Cancer Res. 2009 Nov 15;15(22):6830-6840.

(17) Toth B, Liebhardt S, Steinig K, Ditsch N, Rank A, Bauerfeind I, et al. Platelet-derived microparticles and coagulation activation in breast cancer patients. Thromb Haemost. 2008 Oct;100(4):663-669.

(18) Zwicker JI. Predictive value of tissue factor bearing microparticles in cancer associated thrombosis. Thromb Res. 2010 Apr;125 Suppl 2:S89-91.

(19) Khorana AA, Francis CW, Menzies KE, Wang JG, Hyrien O, Hathcock J, et al. Plasma tissue factor may be predictive of venous thromboembolism in pancreatic cancer. J Thromb Haemost. 2008 Nov;6(11):1983-1985.

(20) Tesselaar ME, Osanto S. Risk of venous thromboembolism in lung cancer. Curr Opin Pulm Med. 2007 Sep;13(5):362-367.

(21) Hron G, Kollars M, Weber H, Sagaster V, Quehenberger P, Eichinger S, et al. Tissue factor-positive microparticles: cellular origin and association with coagulation activation in patients with colorectal cancer. Thromb Haemost. 2007 Jan;97(1):119-123.

(22) Kyle RA. Diagnostic criteria of multiple myeloma. Hematol Oncol Clin North Am. 1992 Apr;6(2):347-358.

(23) Greipp PR, San Miguel J, Durie BG, Crowley JJ, Barlogie B, Blade J, et al. International staging system for multiple myeloma. J Clin Oncol. 2005 May 20;23(15):3412-3420.

(24) Durie BG, Salmon SE. Cellular kinetics staging, and immunoglobulin synthesis in multiple myeloma. Annu Rev Med. 1975;26:283-288.

(25) Vanwijk MJ, Svedas E, Boer K, Nieuwland R, Vanbavel E, Kublickiene KR. Isolated microparticles, but not whole plasma, from women with preeclampsia impair endothelium-dependent relaxation in isolated myometrial arteries from healthy pregnant women. Am J Obstet Gynecol. 2002 Dec;187(6):1686-1693.

(26) Rickles FR, Patierno S, Fernandez PM. Tissue factor, thrombin, and cancer. Chest. 2003 Sep;124(3 Suppl):58S-68S.

(27) Mueller BM, Reisfeld RA, Edgington TS, Ruf W. Expression of tissue factor by melanoma cells promotes efficient hematogenous metastasis. Proc Natl Acad Sci U S A. 1992 Dec 15;89(24):11832-11836.

(28) Kakkar AK, DeRuvo N, Chinswangwatanakul V, Tebbutt S, Williamson RC. Extrinsic-pathway activation in cancer with high factor VIIa and tissue factor. Lancet. 1995 Oct 14;346(8981):1004-1005.

(29) Sase T, Wada H, Yamaguchi M, Ogawa S, Kamikura Y, Nishikawa M, et al. Haemostatic abnormalities and thrombotic disorders in malignant lymphoma. Thromb Haemost. 2005 Jan;93(1):153-159.

(30) Sase T, Wada H, Kamikura Y, Kaneko T, Abe Y, Nishioka J, et al. Tissue factor messenger RNA levels in leukocytes compared with tissue factor antigens in plasma from patients in hypercoagulable state caused by various diseases. Thromb Haemost. 2004 Jul;92(1):132-139.

(31) Negaard HF, Iversen PO, Ostenstad B, Iversen N, Holme PA, Sandset PM. Hypercoagulability in patients with haematological neoplasia: No apparent initiation by tissue factor. Thromb Haemost. 2008 Jun;99(6):1040-1048.

(32) Shimizu K, Itoh J. A possible link between Trousseau's syndrome and tissue factor producing plasma cells. Am J Hematol. 2009 Jun;84(6):382-385.

(33) Key NS, Chantrathammachart P, Moody PW, Chang JY. Membrane microparticles in VTE and cancer. Thromb Res. 2010 Apr;125 Suppl 2:S80-83.

(34) Palumbo A, Bringhen S, Caravita T, Merla E, Capparella V, Callea V, et al. Oral melphalan and prednisone chemotherapy plus thalidomide compared with melphalan and prednisone alone in elderly patients with multiple myeloma: randomised controlled trial. Lancet. 2006 Mar 11;367(9513):825-831.

(35) Zangari M, Barlogie B, Anaissie E, Saghafifar F, Eddlemon P, Jacobson J, et al. Deep vein thrombosis in patients with multiple myeloma treated with thalidomide and chemotherapy: effects of prophylactic and therapeutic anticoagulation. Br J Haematol. 2004 Sep;126(5):715-721.

(36) Hussein MA. Thromboembolism risk reduction in multiple myeloma patients treated with immunomodulatory drug combinations. Thromb Haemost. 2006 Jun;95(6):924-930.

(37) Zangari M, Barlogie B, Thertulien R, Jacobson J, Eddleman P, Fink L, et al. Thalidomide and deep vein thrombosis in multiple myeloma: risk factors and effect on survival. Clin Lymphoma. 2003 Jun;4(1):32-35.

CHAPTER 9

Summary and General Discussion

Background

Although the intriguing association between cancer and thrombosis has been recognized since the 19th century, the mechanism(s) underlying this association have not been revealed yet. In the past years it has been suggested that microparticles (MPs; also known as microvesicles) derived from various types of cells and formed by budding of cell membranes upon activation and apoptosis may play a role in cancer-associated thrombosis. These MPs still bear antigens from their parental cells (blood cells, endothelial cells, and most likely also tumour cells). In addition they carry the negatively charged phosphatidylserine (PS) on their membrane surface as the result of membrane remodelling during their formation (1;2). Interestingly, MPs bearing tissue factor (TF), the major initiator of blood coagulation, are increased in plasma of patients with certain types of cancer (3-6). Unfortunately, the growing interest to study the role of MPs in health and disease is limited by the lack of well standardized pre-analytical and analytical procedures resulting in a wide variation in the results reported by different research groups (1;2).

The aim of the studies described in this thesis was to develop novel methodology for the sensitive detection and accurate quantification of (subsets of) MPs in their native state and for the analysis of the cellular origin of MPs bearing active TF. In addition, a possible association between MPs bearing active TF and the development of venous thrombosis (VTE) was investigated in patients with multiple myeloma.

Measurement of microparticles

Important factors

Several pre-analytical conditions such as blood collection, centrifugation used to prepare plasma/MPs, and storage (including freezing-thawing) of plasma may influence the outcome of the measurement of MPs. In Chapter 2 of this thesis we discussed that during blood collection, it is necessary to prevent *ex vivo* activation of blood which may lead to inadvertent production of erythrocyte MPs (ErMPs) or platelet MPs (PMPs). We recommend that blood should be drawn by using a large diameter needle, for example a 21-G needle, and that prolonged placement of a tourniquet during venepuncture should be avoided.

Plasma for MP measurements is usually prepared from blood collected in 1/10 volume of sodium citrate (0.105 or 0.129 mol/L). The choice of this anticoagulant is based on international guidelines for routine haematology testing but might be less

optimal for MP measurements. Therefore, more information is needed on the stability of MPs in blood collected in other anticoagulants such as ethylenediaminetetraacetic acid (EDTA) and citrate theophylline adenosine dipyridamole (CTAD) in comparison to that in citrate. Furthermore, the entire process from blood collection until plasma preparation should be rapid and gentle to avoid *ex vivo* activation of blood cells in the collection tube. The removal of platelets from plasma by centrifugation is crucial, but at the same time the centrifugal force used should not trigger inadvertent formation of PMPs.

Preferably, MP measurements should be performed directly in fresh plasma to reduce MP loss and to preserve MP characteristics. However, in multi-centre studies and prospective trials it is often inevitable to freeze and store the plasma samples before performing the analysis. Unfortunately, validated protocols are not yet available for freezing and thawing of plasma to be used for MP analysis. In Chapter 2 we recommend that when frozen-thawed plasma is used for MP measurements, especially PMP and annexin V-positive MP counts should be interpreted with caution.

As mentioned in the general introduction of this thesis, MPs vary in size in the submicron range. Therefore, a method which enables the detection of MPs within this size range is needed to provide an accurate measurement of total MPs in the sample. Current flow cytometers are not able to sensitively detect MPs smaller than 0.5 µm (7). Although there are advances made in developing new generation flow cytometers (5;8), they have not been tested extensively for routine measurements of MPs. Nevertheless, when flow cytometry is chosen as a method for quantification of MPs, some analytical conditions should be standardized. Recently, the Vascular Biology group of the Scientific and Standardization Committee (SSC) of the International Society on Thrombosis and Haemostasis (ISTH) proposed to standardize the enumeration of PMPs larger than 0.5 µm by using calibrated size standard beads (Megamix beads) to adjust the instrument setting and increase the resolution of the flow cytometer (9).

Other methods used to study plasma MPs are electron microscopy, capture-based assays and functional assays of isolated MPs. In Chapter 2 we discussed the advantages and disadvantages of these methods. In general, they can be used to study plasma MPs as long as there is standardization of protocols, including the use of appropriate reagents and reference materials, to improve intra- and inter-laboratory reproducibility. We also discussed some novel methods to measure MPs including proteomic analysis, impedance-based flow cytometry, atomic force microscopy (AFM), nanoparticle tracking analysis (NTA), and dynamic light scattering (DLS). At this moment, these methods are not easily applicable in the

clinic since they are time-consuming and labour-intensive. In addition, none of these methods gives information on the functional properties of MPs.

Atomic force microscopy

In Chapter 3 we report the development of a novel method to measure MPs by using AFM. This method is based on the capture of MPs by anti-human CD41 monoclonal antibody (MoAb) coated on a modified mica surface. AFM operated in fluid/liquid tapping mode is used to detect MPs attached to the anti-CD41-coated surface. The advantages of this method are that forces as small as a few picoNewton can be sensitively detected and that sample properties are preserved. In this study, we observed that the binding of MPs to anti-CD41-coated mica seemed to be specific, as a markedly lower number of MPs bound to IgG1 isotype control-coated mica. Also, a linear relationship was obtained between the number of CD41-positive MPs per 100 μm^2 surface and the MP concentration which saturated at a concentration of ~500 MPs per 100 μm^2 surface. We quantified the number of CD41-positive MPs isolated from double-centrifuged fresh platelet-poor plasma (PPP) of 7 blood donors and 3 cancer patients both by AFM and flow cytometry. We found that the numbers of CD41-positive MPs measured by AFM were 1,000-fold higher than those measured by flow cytometry (3-702 x 10^9/L plasma vs. 11-626 x 10^6/L plasma). The MPs detected by AFM have diameters (d_{sph}) ranging from 10-475 nm with a peak at 67.5 nm, which is clearly far below the detection limit of conventional flow cytometry.

We also investigated whether the AFM method can be used to detect TF-bearing MPs (Chapter 4). To this purpose, we coated modified mica with FITC-labelled anti-human TF MoAb to capture MPs isolated from the supernatant of cultured MDA-MB231 cells stimulated with calcium ionophore. TF-positive MPs with diameters (d_{sph}) ranging from 6-296 nm (median: 40.4 nm; mean: 46.4 ± 26.0 nm) were successfully captured on FITC-labelled anti-TF-coated surface. Only few MPs were captured on the mica surface coated with FITC-labelled mouse IgG1 isotype control MoAb. We also found that the numbers of TF-positive MPs measured by AFM were 2,000-fold higher than those measured by flow cytometry in the same sample (8 x 10^6 per µL supernatant vs. 4 x 10^3 per µL supernatant).

To allow the detection of MPs directly in plasma, the use of a combination of microfluidics and AFM was investigated (Chapter 5). Tenfold-diluted EDTA PPP was flown through a microfluidic channel with a controlled pressure driven laminar flow to allow direct contact with anti-human CD41 antibody-coated mica. MPs bearing CD41 antigen were captured on this surface and subsequently detected by AFM operated in fluid tapping mode. The majority of the captured MPs have

diameters (d_{sph}) of 45 nm (range: 30-90 nm), similar to prior results obtained with MPs immediately isolated from fresh PPP. Apparently, the high-speed centrifugation needed to isolate MPs did not influence the size distribution of MPs. Use of the microfluidic system also increased the efficiency of capturing MPs. We applied this microfluidic system to count PMPs in plasma from healthy donors and compared it with a drop method. We detected considerably more CD41-positive MPs per 100 μm^2 surface when plasma was run through the microfludic system than when measured by the drop method. Our preliminary data also showed that there was a linear dose-response curve between the number of CD41-positive MPs per 100 μm^2 surface and the MP concentration.

In conclusion, AFM operated in fluid tapping mode can sensitively detect and accurately quantify subsets of MPs by using specific MoAbs. In combination with microfluidics MPs can be directly measured in plasma, thus, reducing time between venepuncture and MP measurement and also preventing MP loss because of washing steps in the isolation procedure. Importantly, as this method relies on the use of an antibody for the detection of MPs, a specific and high-affinity antibody is required to capture a specific MP subset on the mica surface. Furthermore, to assess the precise number of MPs in a given sample, the availability of an external standard (e.g. MPs with a known concentration) will be essential.

Cryo-electron microscopy

Conventional electron microscopy (EM) has been used to study the morphology of isolated MPs. However, the sample preparation and imaging techniques in conventional EM require dehydration, chemical fixation, and staining of specimens and are, therefore, less suitable to study the morphology of MPs directly in plasma. We investigated whether cyro-EM can be used to study the size and morphology of submicron particles (MPs and exosomes), and also to estimate the number of these particles in a fresh plasma sample without the use of staining or chemical fixation procedures. We used fresh plasma (platelet-rich plasma/PRP, PPP, platelet-free plasma/PFP), isolated MPs, and also (thrombin activated-) isolated platelets. These samples were directly applied onto an EM grid and vitrified for cyro-EM measurement (Chapter 6).

In Chapter 6 we observed that platelets were more activated in fresh citrate PRP than in EDTA PRP, although clearly less than in samples of thrombin-activated platelets. Therefore, to reduce *in vitro* activation of platelets and PMP formation, blood collection in EDTA is recommended for the study of plasma MPs. Most of the submicron particles found in plasma of healthy volunteers were spherical electron dense particles resembling lipoprotein particles. Low numbers of electron lucent

particles with a discernable lipid bilayer (lipid vesicles) were also found. These could be MPs, exosomes or both. Similar lipid vesicles were found in samples of thrombin-activated isolated platelets and isolated MPs. All types of particles have about the same size distribution (median: 30 nm; range: 25-260 nm). Because MPs form only a minority of all submicron particles present in fresh plasma, we have to consider the limitations of techniques used to measure MPs directly in plasma. Finding ways to label MPs and/or exosomes directly in plasma will be essential for further studies of these particles by for instance NTA and cryo-EM.

Immuno-magnetic beads capture

There is not yet a method which provides information on the cellular origin of the plasma MPs carrying active TF. In Chapter 7 we report on the development of an immuno-magnetic beads method to capture a defined subset of MPs from plasma by using a specific biotinylated antibody and streptavidin magnetic beads.

This method was optimized for the capture of PMPs from plasma of healthy volunteers. Plasma was incubated with biotinylated anti-human CD41 MoAb before streptavidin magnetic beads were added. After application of this mixture to the column, positive (containing the selected subset of MPs) and negative (containing the depleted plasma) fractions were collected and used directly for the isolation and analysis of MPs for specific antigens and TF activity.

By using flow cytometry we showed that biotinylated anti-human CD41 MoAb specifically binds and saturates the surface antigen CD41 of PMPs. The streptavidin magnetic beads did not interfere with the binding of anti-CD41 and anti-CD61 antibodies to PMPs. After separation, there were no CD41-positive MPs and only few CD61-positive MPs in the negative fraction, indicating that almost all PMPs (CD41-positive MPs) were captured. This capture was CD41-specific as most of CD41/CD61-positive MPs were recovered in the negative fraction of the biotinylated IgG1-beads separation.

Using biotinylated anti-CD14 MoAb at the same concentration as anti-CD41 MoAb, CD14-positive MPs were captured from normal plasma spiked with MPs isolated from the supernatant of LPS-stimulated isolated monocytes (MoMPs). TF activity was found both in the positive and negative fractions indicating that both CD14-positive and -negative MoMPs have active TF. This seems in agreement with our finding that not all active TF carrying MoMPs isolated from the supernatant of LPS stimulated monocytes were CD14-positive.

In the future the beads capture method can be used to investigate the source of MPs carrying active TF in plasma of patients with cancer by using cell- or other tumour-specific antibodies such as anti-MUC1 (breast and pancreatic cancer cells) (4;5), anti-FasL (melanoma cells) (10), anti-EGFRvIII (glioblastoma cells) (11), and anti-CXCR-4 (leukaemic cells) (12).

MP-associated TF activity in patients with multiple myeloma

For the measurement of MP associated tissue factor activity (MP-TF activity) freshly isolated MPs are supplemented with excess FVII(a) and FX in the presence of calcium, after which the formation of FXa is measured with a specific chromogenic substrate using either a one-stage (4;6;13) or two-stage approach (14;15). These two different approaches were discussed in detail in Chapter 2 of this thesis. To asses MP-TF activity in multiple myeloma (MM) patients, we used the one-stage approach (Chapter 8).

Chemotherapy in combination with anti-angiogenic drugs in multiple myeloma is associated with a high risk of thrombo-embolic complications (16;17). We measured MP-TF activity in MPs isolated from PFP of 122 patients with newly diagnosed MM before and after chemotherapy to investigate whether MP-TF activity is associated with VTE. MP-TF activity levels of untreated patients were significantly higher than those in healthy volunteers [17.6 fM FXa/min (IQR 8.6-33.2) versus 4.1 fM FXa/min (IQR 2.3-6.6), P<0.001]. None of the patient characteristics or laboratory measurements (sex, age, disease stage, beta-2 microglobulin, albumin, calcium, haemoglobin, platelets) correlated with the MP-TF activity levels.

MP-TF activity prior to the start of treatment was not different between patients who developed a VTE during follow-up (n=15) and those who did not (n=107). In 75 patients in whom plasma was obtained before and after chemotherapy, MP-TF activity decreased significantly (from 17.4 [10.2-32.8] to 12.0 [7.0-18.5] fM Xa/min, P=0.006). This reduction was observed in all ISS stages of disease suggesting that the tumour load is not associated with MP-TF activity levels. The MP-TF activity levels also decreased irrespective of the therapeutic regimen [vincristine, adriamycin, and dexamethasone (VAD), thalidomide, adriamycin, and dexamethasone (TAD), or bortezomib, adriamycin, and dexamethasone (PAD)]. MP-TF activity remained, however, elevated in patients who developed VTE (15.1 [10.3-25.2]), in contrast to patients not developing VTE (11.4 [7.0-25.2], P<0.001).

In future studies MP-TF activity should be assessed more frequently during induction treatment of MM to investigate whether MP-TF activity has a pathogenetic role in VTE in MM patients.

General Discussion

Thus far there is no general consensus on the size and number of MPs due to discrepancies between the results of MP measurements reported in the literature. We are aware that these discrepancies are not only caused by differences between the methods used to measure MPs. Pre-analytical procedures such as blood collection, plasma/MPs preparation, and storage are some of the important factors which might influence the number, morphology and characteristics of MPs. The use of EDTA instead of citrate as anticoagulant for blood collection to reduce *in vitro* activation of platelets and PMP formation (Chapter 6) is preferred for the study of plasma MPs. We also have an indication that the high-speed centrifugation used to isolate MPs has no effect on the size distribution of MPs (Chapter 5). Eventually, it is essential to set up guidelines for these pre-analytical procedures to improve intra- and inter-laboratory reproducibility.

In the past, MPs were defined by having a size distribution in the micrometer range, whereas now we found them to be in the nanometer range (Chapter 3, 4, 5, and 6). This is explained by the technical limitations of the methods previously used to characterize MPs. For example, methods such as flow cytometry with a detection threshold of 0.5 µm and conventional EM for which dehydration, chemical fixation, and staining of specimens are needed for sample preparation, are less suitable for detection and characterization of MPs. Furthermore, there are no suitable reference materials (standards) to calibrate and adjust the settings of the methods for MP analysis (18). Currently, new methods such as AFM, NTA, and cryo-EM allow detection and characterization of MPs in the nanometer range and in their physiological state. However, these methods are not yet suitable for use in the clinic as they are low throughput, labour-intensive and still need to be optimized and validated (e.g. accuracy, precision, specificity, detection limit and quantification, linearity and range, robustness). Therefore, improvements are needed, for example by using automated sample handling systems, standardized reagents, reference materials for calibration and settings, and an external standard to obtain absolute numbers of MPs. Ultimately, a small MP measurement device which uses just a pinprick of blood and provides results in less than 30 minutes (lab-on-a-chip) would be desirable for a routine test.

There is evidence that MP-TF activity is increased in cancer patients who develop (cancer-associated) VTE (4;6). Further investigations are needed to learn whether

MPs bearing active TF in cancer patients are indeed the cause of thrombosis. Furthermore, to understand the mechanism(s) of the association between cancer and thrombosis, it is important to identify whether MPs bearing active TF come from the cancer cell itself or not; in the latter case it is important to identify the cell of origin (monocytes, endothelial cells, platelets) and the mechanism by which the active TF is produced.

Finally, further research is needed to investigate how MPs are precisely formed. According to a widely accepted hypothesis MPs are shed by cells as a result of loss of membrane phospholipid asymmetry during processes such as activation and apoptosis, exposing PS on the outer cell surface. This hypothesis is supported by the rare bleeding disorder, Scott syndrome. This syndrome is characterized by a decreased scramblase activity which results in reduced expression of PS and reduced MPs shedding (1;2). Interestingly, the existence of MPs that do not expose PS challenges the hypothesis of MP formation (19-22). It remains a matter of debate whether the existence of PS-negative MPs is the result of the limitations of the current methodology. Annexin V is widely used as a probe of PS exposure in methods to detect and quantify MPs such as flow cytometry and annexin V capture-based assays. However, the binding of annexin V to MPs depends on the calcium concentration and the membrane PS content (23;24). Another possible explanation for the finding of PS negative MPs might be that they are formed by multiple fusion events between plasma membrane components with cell debris or small endosomal secreted vesicles (exosomes) (25). Alternatively, MPs might be released from the plasma membrane as a result of destabilization of the actin cytoskeleton via αIIbβ3 signalling which does not require rearrangement of phospholipids distribution (26).

In conclusion, MPs are no longer regarded as cellular debris or experimental artefacts, but in fact MPs may participate in processes of coagulation, inflammation and tumorigenesis. It is of interest to investigate from which cells MPs are formed, why they are formed and how they interact with other cells in the body. Therefore, standardisation of pre-analytical and analytical procedures for the measurement of MPs is urgently needed to understand their presence and to elucidate their physiological function and role in diseases. In the future the measurement of MPs will contribute to the development of MPs as diagnostic and perhaps predictive (bio)marker in various diseases.

References

(1) Piccin A, Murphy WG, Smith OP. Circulating microparticles: pathophysiology and clinical implications. Blood Rev 2007;21:157-171.

(2) Burnier L, Fontana P, Kwak BR, Angelillo-Scherrer A. Cell-derived microparticles in haemostasis and vascular medicine. Thromb Haemost 2009;101:439-451.

(3) Hron G, Kollars M, Weber H, Sagaster V, Quehenberger P, Eichinger S, et al. Tissue factor-positive microparticles: Cellular origin and association with coagulation activation in patients with colorectal cancer. Thromb Haemost 2007;97:119-123.

(4) Tesselaar ME, Romijn FP, van der Linden IK, Prins FA, Bertina RM, Osanto S. Microparticle-associated tissue factor activity: a link between cancer and thrombosis? J Thromb Haemost 2007;5:520-527.

(5) Zwicker JI, Liebman HA, Neuberg D, Lacroix R, Bauer KA, Furie BC, et al. Tumor-derived tissue factor-bearing microparticles are associated with venous thromboembolic events in malignancy. Clin Cancer Res 2009;15:6830-6840.

(6) Tesselaar ME, Romijn FP, van dL, I, Bertina RM, Osanto S. Microparticle-associated tissue factor activity in cancer patients with and without thrombosis. J Thromb Haemost 2009;7:1421-1423.

(7) Furie B, Furie BC. Cancer-associated thrombosis. Blood Cells Mol Dis 2006;36:177-181.

(8) Lacroix R, Robert S, Poncelet P, Dignat-George F. Overcoming limitations of microparticle measurement by flow cytometry. Semin Thromb Hemost 2010;36:807-818.

(9) Lacroix R, Robert S, Poncelet P, Kasthuri RS, Key NS, Dignat-George F. Standardization of platelet-derived microparticle enumeration by flow cytometry using calibrated beads: results of ISTH SSC collaborative workshop. J Thromb Haemost 2010;8:2571-2574.

(10) Andreola G, Rivoltini L, Castelli C, Huber V, Perego P, Deho P, et al. Induction of lymphocyte apoptosis by tumor cell secretion of FasL-bearing microvesicles. J Exp Med 2002;195:1303-1316.

(11) Al Nedawi K, Meehan B, Micallef J, Lhotak V, May L, Guha A, et al. Intercellular transfer of the oncogenic receptor EGFRvIII by microvesicles derived from tumour cells. Nat Cell Biol 2008;10:619-624.

(12) Kalinkovich A, Tavor S, Avigdor A, Kahn J, Brill A, Petit I, et al. Functional CXCR4-expressing microparticles and SDF-1 correlate with circulating acute myelogenous leukemia cells. Cancer Res 2006;66:11013-11020.

(13) Garcia RP, Eikenboom HC, Tesselaar ME, Huisman MV, Nijkeuter M, Osanto S, et al. Plasma levels of microparticle-associated tissue factor activity in patients with clinically suspected pulmonary embolism. Thromb Res 2010;126:345-349.

(14) Tilley RE, Holscher T, Belani R, Nieva J, Mackman N. Tissue factor activity is increased in a combined platelet and microparticle sample from cancer patients. Thromb Res 2008;122:604-609.

(15) Manly DA, Wang J, Glover SL, Kasthuri R, Liebman HA, Key NS, et al. Increased microparticle tissue factor activity in cancer patients with Venous Thromboembolism. Thromb Res 2010;125:511-512.

(16) Zangari M, Saghafifar F, Mehta P, Barlogie B, Fink L, Tricot G. The blood coagulation mechanism in multiple myeloma. Semin Thromb Hemost 2003;29:275-282.

(17) Zangari M, Elice F, Fink L, Tricot G. Thrombosis in multiple myeloma. Expert Rev Anticancer Ther 2007;7:307-315.

(18) Chandler WL, Yeung W, Tait JF. A new microparticle size calibration standard for use in measuring smaller microparticles using a new flow cytometer. J Thromb Haemost. 2011 Jun;9(6):1216-1224.

(19) Jimenez JJ, Jy W, Mauro LM, Soderland C, Horstman LL, Ahn YS. Endothelial cells release phenotypically and quantitatively distinct microparticles in activation and apoptosis. Thromb Res 2003;109:175-180.

(20) Aras O, Shet A, Bach RR, Hysjulien JL, Slungaard A, Hebbel RP, et al. Induction of microparticle- and cell-associated intravascular tissue factor in human endotoxemia. Blood 2004;103:4545-4553.

(21) Perez-Pujol S, Marker PH, Key NS. Platelet microparticles are heterogeneous and highly dependent on the activation mechanism: studies using a new digital flow cytometer. Cytometry A 2007;71:38-45.

(22) Bernimoulin M, Waters EK, Foy M, Steele BM, Sullivan M, Falet H, et al. Differential stimulation of monocytic cells results in distinct populations of microparticles. J Thromb Haemost 2009;7:1019-1028.

(23) Tait JF, Gibson D. Phospholipid binding of annexin V: effects of calcium and membrane phosphatidylserine content. Arch Biochem Biophys 1992;298:187-191.

(24) Connor DE, Exner T, Ma DD, Joseph JE. The majority of circulating platelet-derived microparticles fail to bind annexin V, lack phospholipid-dependent procoagulant activity and demonstrate greater expression of glycoprotein Ib. Thromb Haemost 2010;103:1044-1052.

(25) Cocucci E, Racchetti G, Meldolesi J. Shedding microvesicles: artefacts no more. Trends Cell Biol 2009;19:43-51.

(26) Cauwenberghs S, Feijge MA, Harper AG, Sage SO, Curvers J, Heemskerk JW. Shedding of procoagulant microparticles from unstimulated platelets by integrin-mediated destabilization of actin cytoskeleton. FEBS Lett 2006;580:5313-5320.

Nederlandse samenvatting

Achtergrond

Hoewel het intrigerende verband tussen kanker en trombose sinds de 19de eeuw bekend is, is het mechanisme dat deze samenhang verklaart nog niet duidelijk. Micropartikels (MPs; ook wel microvesicles genoemd) kunnen ontstaan na activering van de cel door afsnoering van de celmembraan of na apoptosis (geprogrammeerde zelfdood van de cel) en kunnen afkomstig zijn van diverse soorten cellen. Sinds enige jaren denkt men dat MPs een rol zouden kunnen spelen bij het ontstaan van kanker-geassociëerde trombose.

MPs dragen nog kenmerken (antigenen) van de cellen waaruit ze gevormd werden, bloedcellen, vaatendotheelcellen, en vermoedelijk ook tumorcellen. Daarnaast bevatten ze op hun buitenmembraan negatief geladen fosfolipiden (fosfatidylserine, PS) ten gevolge van membraan remodelling tijdens hun vorming. Interessant is dat in plasma van patiënten met bepaalde soorten kanker het aantal MPs, dat actief tissue factor (TF, de belangrijkste initiator van de bloedstolling) bevat, sterk verhoogd blijkt te zijn. Helaas wordt de studie van de rol van MPs bij ontstaan en progressie van ziekte ernstig gehinderd door het ontbreken van gestandaardiseerde pre-analytische en analytische procedures voor het meten van MPs, hetgeen resulteert in een grote variatie in de resultaten die door verschillende onderzoeksteams worden gerapporteerd.

Het doel van het onderzoek dat in dit proefschrift wordt beschreven, was om nieuwe methoden te ontwikkelen voor het nauwkeurig kwantificeren en karakteriseren van MPs en hun deelpopulaties, en wel zoveel mogelijk in hun oorspronkelijke staat. De tot voor kort gebruikte technieken, waarmee de concentratie van MPs werd gemeten, zijn geen van alle geschikt om deeltjes met afmetingen in het nanometer gebied te meten. Daarnaast hebben we geprobeerd een methode te ontwikkelen om de cellulaire oorsprong van MPs met op hun membraan functioneel TF, vast te stellen. Tenslotte werd een mogelijk verband onderzocht tussen MPs die funtioneel TF op het oppervlak hebben en het optreden van veneuze trombo-embolie (VTE) in patiënten die behandeld worden voor de kwaadaardige ziekte multipel myeloom.

Meting van micropartikels

Belangrijke factoren

Verschillende pre-analytische omstandigheden zoals bloedafname, centrifugeren tijdens de bereiding van plasma en MPs, en opslag van plasma (inclusief invriezen-ontdooien), kunnen het resultaat van de MP metingen beïnvloeden. In Hoofdstuk 2 van dit proefschrift wordt besproken dat het noodzakelijk is om *ex vivo*-activering van bloedcellen te verhinderen tijdens afname en opwerken van bloed. Dit zou namelijk kunnen leiden tot de ongewenste vorming van MPs uit bloedcellen, met name uit bloedplaatjes (PMPs), maar wellicht ook uit andere bloedcellen zoals de erytrocyt (ErMPs). Om activatie van bloedcellen buiten het lichaam zoveel mogelijk tegen te gaan, is het van belang bloed af te nemen met een naald met een grote diameter, bijvoorbeeld een 21-G naald, en tijdens de venapunctie langdurig stuwen met een tourniquet te vermijden.

Plasma voor MP metingen wordt gewoonlijk bereid door bloed tijdens afname te verzamelen in, en te mengen met, 1/10 volume natriumcitraat (0.105 of 0.129 mol/L). De keuze van dit antistollingsmiddel is gebaseerd op internationale richtlijnen voor routine bepalingen in de hematologie, maar dit kan voor MP metingen minder optimaal zijn. Daarom is het nodig de stabiliteit van MPs in bloed verzameld in andere antistollingsmiddelen zoals ethylenediaminetetra-azijn zuur (EDTA) en citraat theofylline adenosine dipyridamole (CTAD) te vergelijken met de stabiliteit van MPs in bloed afgenomen op natriumcitraat. Voorts moet het volledige proces van bloedafname tot plasmabereiding snel plaatsvinden om *ex vivo*-activering van bloedcellen in de verzamelbuis te voorkomen. De verwijdering van bloedplaatjes uit plasma door centrifugatie is essentieel, maar tegelijkertijd kan het centrifugeren tot ongewenste vorming van MPs uit bloedplaatjes (PMPs) aanleiding geven.

Om MP kenmerken zo goed mogelijk te behouden zouden de MP metingen bij voorkeur direct in vers bereid plasma moeten worden uitgevoerd. Het is echter vaak niet praktisch uitvoerbaar om een meting direct uit te voeren na afname van het bloed. Plasmamonsters moeten dan worden ingevroren en bewaard. Dit teneinde in een later stadium plasmamonsters van verschillende individuen, afgenomen op verschillende tijdstippen, tegelijk te meten, zodat monsters onderling vergeleken kunnen worden. Helaas zijn er nog geen gestandaardiseerde protocollen beschikbaar voor het invriezen en ontdooien van plasma voor het meten van MPs. In Hoofdstuk 2 adviseren wij, dat wanneer MP metingen worden gedaan in ingevroren en vervolgens ontdooid plasma, vooral de aantallen PMPs

en annexin V positieve MPs met terughoudendheid moeten worden geïnterpreteerd.

Zoals vermeld in de introductie van dit proefschrift, variëren MPs in grootte in het submicrongebied. Daarom is een methode nodig, die MPs met nanometer afmetingen nauwkeurig kan meten. De huidige flowcytometers kunnen echter MPs kleiner dan 0.5 µm niet nauwkeurig detecteren. Er zijn wel nieuwe typen flowcytometers in ontwikkeling, die ook deeltjes die iets kleiner zijn dan 0.5 micron nauwkeurig kunnen meten, maar het betrouwbare meetgebied zal niet liggen onder de 0.3 µm. Ook zijn deze nieuwere flowcytometers nog niet uitgebreid getest voor het routinematig meten van aantallen MPs. Wanneer desalniettemin flowcytometrie gebruikt blijft worden voor MP tellingen, zullen een aantal analytische omstandigheden moeten worden gestandaardiseerd. Onlangs stelde de Vascular Biology groep van de Scientific and Standardization Committee (SSC) van de International Society on Thrombosis and Haemostasis (ISTH) voor om het meten van PMPs groter dan 0.5 µm te standaardiseren door bolletjes met een gekalibreerde grootte (Megamix) te gebruiken om de instelling van de flowcytometer aan te passen en de resolutie te verhogen.

Andere methoden, die gebruikt worden om plasma MPs te bestuderen, zijn elektronenmicroscopie, capture-based analyses en functionele analyses van geïsoleerde MPs. In Hoofdstuk 2 bespreken wij de voor- en nadelen van deze methoden. In het algemeen kunnen ze gebruikt worden om metingen aan plasma MPs te doen mits ze gebruik maken van gestandaardiseerde protocollen, inclusief het gebruik van geschikte reagentia en referentiematerialen. Deze zijn nodig om de reproduceerbaarheid van de bepaling zoals verricht in verschillende laboratoria te vergroten. Wij bespreken in Hoofdstuk 2 ook enkele nieuwe methoden om MPs te meten zoals proteoom analyse, impedance-based flowcytometrie, atoomkrachtmicroscopie (AFM), nanoparticle tracking analysis (NTA), en dynamic light scattering (DLS). Op dit ogenblik zijn deze methoden niet eenvoudig toepasbaar in het laboratorium omdat ze tijdrovend en arbeidsintensief zijn. Ook geeft geen van deze methoden informatie over de functionele eigenschappen van MPs.

De atoomkrachtmicroscopie

In Hoofdstuk 3 beschrijven wij de ontwikkeling van een geheel nieuwe methode om MPs afkomstig uit bloed te meten door gebruik te maken van een atoomkrachtmicroscoop (AFM) of tastmicroscoop. Eerst hebben we een methode ontwikkeld om MPs met een specifiek antilichaam te binden aan een zeer zuiver en glad mica-oppervlak. De AFM werd vervolgens gebruikt om met de zogenaamde

vloeistof tapping mode de MPs te detecteren die specifiek aan anti-CD41-gecoat mica waren gebonden. We meten met deze techniek dus alleen MPs die zelf het antigeen CD41 (een bloedplaatjes antigeen) bevatten. Voordelen van deze methode zijn dat zelfs krachten van een paar picoNewton zeer gevoelig kunnen worden gedetecteerd en dat de eigenschappen van de micropartikels worden behouden. In Hoofdstuk 3 toonden we aan dat de binding van MPs aan anti-CD41-gecoat mica specifiek was. Er werden duidelijk geringere aantallen MPs gemeten op mica gecoat met een IgG1 isotype controle. Ook werd een lineair verband gevonden tussen het aantal CD41-positieve MPs, dat per 100 μm^2 mica gebonden werd, en de MP concentratie in het monster. Wij maten het aantal CD41-positieve MPs in uit vers, dubbel-gecentrifugeerd plaatjes-arm plasma (PPP) geïsoleerde MPs van 7 bloeddonoren en 3 kankerpatiënten met zowel AFM als flowcytometrie. Wij vonden dat de aantallen CD41-positieve MPs, die met AFM worden gemeten, 1.000-maal hoger waren dan de aantallen gemeten met flowcytometrie (3-702 x 10^9/L plasma versus 11-626 x 10^6/L plasma). De MPs die met AFM werden gedetecteerd hebben diameters (d_{sph}) van 10-475 nm met een piek bij 67.5 nm, die duidelijk ver onder de detectiegrens van conventionele flowcytometrie ligt.

We hebben ook onderzocht of de AFM kon worden gebruikt voor de detectie van TF-positieve MPs (Hoofdstuk 4). Daartoe werd gemodificeerd mica met FITC-gelabeld anti-humaan TF MoAb gecoat. TF-positieve MPs werden geïsoleerd uit het supernatant van gekweekte MDA-MB231 borstkankercellen, die met calcium ionofore waren gestimuleerd. TF-positieve MPs met diameters (d_{sph}) van 6 tot 296 nm (mediaan: 40,4 nm met een gemiddelde van 46,4 ± 26,0 nm) werden met succes gebonden en gedetecteerd op een FITC-gelabeld anti-TF-gecoat oppervlak. Slechts enkele MPs werden gebonden op een mica oppervlak, dat was gecoat met FITC-gelabeld muis lgG1 isotypecontrole. We vonden ook dat het aantal TF-positieve MPs gemeten met de AFM 2.000-maal hoger was dan dat gemeten met flowcytometrie in hetzelfde monster (8 x 10^6 per µL supernatant vs 4 x 10^3 per µL supernatant).

Om MPs direct in plasma te kunnen detecteren is een geheel nieuwe meetopstelling gemaakt, waarbij we gebruik hebben gemaakt van een combinatie van microfluidics en AFM (Hoofdstuk 5). Tienvoudig verdund-EDTA PPP werd door een capillair (een heel dun kanaal) van een microfluïdic chip geinjecteerd onder een gecontroleerde constante druk. Deze veroorzaakt een laminaire stroming die nodig is om direct contact tussen het anti-humaan CD41 antilichaam-gecoate mica en MPs te bewerkstelligen. MPs met CD41 antigeen werden gebonden op dit oppervlak en vervolgens gedetecteerd door middel van AFM in vloeistof tapping mode. De meerderheid van de gebonden MPs bleken een diameter (d_{sph}) van 45 nm (bereik: 30-90 nm) te hebben, hetgeen goed overeenkomt met wat wij eerder

vonden met MPs onmiddellijk geïsoleerd uit vers PPP. Blijkbaar heeft de hoge-snelheid centrifugatie, die nodig is om MPs te isoleren, geen invloed op de grootteverdeling van de MPs. Gebruik van microfluidics bleek ook de efficiëntie waarmee MPs op het mica oppervlak werden gebonden, te verhogen. We gebruikten de microfluidics om PMPs aanwezig in het plasma van gezonde donoren te tellen en we vergeleken de resultaten met die verkregen met de zogenaamde druppelmethode. We constateerden dat aanzienlijk meer CD41-positieve MPs per 100 μm^2 oppervlak gebonden werden, wanneer het plasma werd gemeten met microfluidics dan wanneer deze gemeten werd met een druppelmethode. Uit onze voorlopige gegevens bleek ook dat er een lineair verband bestond tussen het aantal CD41-positieve MPs per 100 μm^2 oppervlak en de MP concentratie in het monster.

Tot slot, door gebruik te maken van een specifiek MoAb en AFM in vloeistof tapping mode zijn wij in staat om een deelpopulatie van MPs met grote gevoeligheid te detecteren en nauwkeurig te kwantificeren. In combinatie met microfluidics kunnen MPs ook direct worden gemeten in plasma. Dit verkort de tijd tussen venapunctie en MP meting en het voorkomt ook verlies van MPs in de wasstappen, die nodig zijn tijdens de isolatie van MPs. Omdat deze methode afhankelijk is van het gebruik van antilichamen, die een specifieke subpopulatie van MPs kunnen binden, zijn specifieke antilichamen nodig met een hoge affiniteit voor het geselecteerde antigeen. Bovendien, om in de toekomst het precieze aantal MPs te kunnen bepalen in een monster, zal de beschikbaarheid van een externe standaard (bijv. MPs met een bekende concentratie) van essentieel belang worden.

Cryo-elektronenmicroscopie

Conventionele elektronenmicroscopie (EM) werd eerder gebruikt om de morfologie van geïsoleerde MPs te bestuderen. In de conventionele EM is voor de monstervoorbereiding en beeldvormende technieken uitdroging, chemische fixatie en kleuring van het preparaat nodig. Daarom is conventionele EM minder geschikt om de morfologie van MPs direct in plasma te bestuderen. We hebben in Hoofdstuk 6 onderzocht of Cyro-EM kan worden gebruikt om de grootte en de morfologie van submicrondeeltjes (MPs en exosomen) in plasma te bestuderen, en ook om het aantal van deze deeltjes in een vers plasmamonster te schatten zonder gebruik te maken van kleuringen of chemische fixatie procedures. We gebruikten vers plasma (bloedplaatjes-rijk plasma/PRP, bloedplaatjes arm plasma/PPP, bloedplaatjes-vrij plasma/PFP), geïsoleerde MPs, en ook (trombine geactiveerde-) geïsoleerde bloedplaatjes. Deze monsters werden direct op een EM grid ingevroren voor Cyro-EM metingen.

In Hoofdstuk 6 hebben we vastgesteld, dat bloedplaatjes in vers citraat PRP meer geactiveerd waren dan in EDTA PRP, maar duidelijk minder dan in monsters van trombine-geactiveerde bloedplaatjes. Om *in vitro*-activatie van bloedplaatjes en vorming van PMP te verminderen wordt daarom voor de studie van plasma MPs bloedafname in EDTA aanbevolen. Het merendeel van de submicrondeeltjes aangetroffen in plasma van gezonde vrijwilligers bestond uit bolvormige elektronen-dichte deeltjes, die op lipoproteïne deeltjes lijken. Lage aantallen van elektronen-arme deeltjes met een waarneembare lipide dubbellaag (lipide vesikels) werden ook gevonden. De laatste kunnen MPs zijn, exosomen of beide. Soortgelijke lipide vesikels werden gevonden in monsters van trombine-geactiveerde geïsoleerde bloedplaatjes en geïsoleerde MPs. Alle soorten deeltjes hebben ongeveer dezelfde grootteverdeling (mediaan: 30 nm, bereik: 25-260 nm). Omdat MPs slechts een minderheid vormen van alle submicrondeeltjes, die in vers plasma aanwezig zijn, moeten we de beperkingen overwegen van de technieken die gebruikt worden om MPs direct in plasma te meten. Het vinden van manieren om MPs en / of exosomen direct in plasma te kleuren met behulp van specifieke gelabelde antilichamen is van essentieel belang voor de verdere studies van deze deeltjes met technieken als NTA en cryo-EM.

Immuno-magnetische beads

Er is nog geen methode, die informatie geeft over de cellulaire oorsprong van de MPs met actief TF, die uit plasma geïsoleerd kunnen worden. In Hoofdstuk 7 hebben we gerapporteerd over de ontwikkeling van een methode die gebruik maakt van een specifiek gebiotinyleerd antilichaam en magnetische streptavidine beads om een bepaalde populatie van MPs uit het plasma te isoleren.

Deze methode werd geoptimaliseerd voor het isoleren van PMPs uit plasma van gezonde vrijwilligers. Plasma werd met gebiotinyleerd anti-humaan CD41 MoAb geïncubeerd voordat streptavidine magnetische beads werden toegevoegd. Na het aanbrengen van dit mengsel op een kolom van magnetische streptavidine beads, werden positieve (met daarin de geselecteerde subset van MPs) en negatieve (met daarin het gedepleteerde plasma) fracties verzameld en direct gebruikt voor de isolatie en analyse van MPs voor specifieke antigenen en TF activiteit.

Met behulp van flowcytometrie laten we zien dat gebiotinyleerd anti-humaan CD41 MoAb specifiek het antigeen CD41 van PMPs verzadigt. De magnetische streptavidine beads interfereren niet met de binding van anti-CD41 en anti-CD61 antilichamen aan PMPs. Na de scheiding waren er geen CD41-positieve MPs en slechts enkele CD61-positieve MPs in de negatieve fractie, waaruit blijkt dat bijna

alle PMPs (CD41-positieve MPs) werden gebonden door de beads. De binding was CD41-specifiek, want de meeste CD41/CD61-positive MPs werden in de negatieve fractie gevonden, indien gebiotinyleerd IgG1 MoAb werd gebruikt in plaats van gebiotinyleerd anti-CD41 MoAb.

Met behulp van gebiotinyleerd anti-CD14 MoAb en magnetische streptavidine beads werden CD14-positieve MPs gevangen uit normaal plasma, dat verrijkt was met MPs geïsoleerd uit het supernatant van LPS-gestimuleerde geïsoleerde monocyten (MoMPs). TF-activiteit werd zowel in de positieve als negatieve fracties gevonden. Dit geeft aan dat zowel de CD14-positieve als negatieve MoMPs actief TF hebben. Dit lijkt in overeenstemming met onze bevinding dat niet alle MoMPs met actief TF, die geïsoleerd werden uit het supernatant van LPS gestimuleerde monocyten, CD14-positief waren.

In de toekomst zal de beads capture methode gebruikt kunnen worden om de oorsprong van MPs met actief TF in het plasma van patiënten met kanker te onderzoeken. Hierbij zal gebruik gemaakt moeten worden van celspecifieke of tumorspecifieke antilichamen, zoals anti-MUC1 (borst-en pancreaskanker cellen), anti-FasL (melanoom cellen), anti-EGFRvIII (glioblastoma cellen) en anti-CXCR-4 (leukemische cellen).

MP-geassocieerde TF activiteit in patiënten met multipel myeloom

Voor het meten van MP-geassocieerde tissue factor activiteit (MP-TF activiteit) werden vers geïsoleerde MPs geïncubeerd met een overmaat FVII(a) en FX in de aanwezigheid van calcium, waarna de vorming van FXa met een specifiek chromogeen substraat kon worden gemeten in een eenstaps of tweestaps bepaling. Deze bepalingen werden in detail in Hoofdstuk 2 van dit proefschrift besproken. Voor de meting van MP-TF activiteit in multipel myeloom (MM) patiënten hebben we de eenstaps bepaling gebruikt. (Hoofdstuk 8).

Chemotherapie in combinatie met anti-angiogene geneesmiddelen bij multipel myeloom is geassocieerd met een hoog risico op trombo-embolische complicaties. We hebben MP-TF activiteit gemeten in MPs geïsoleerd uit PFP van 122 patiënten met MM voor en na de chemotherapie en onderzochten of de MP-TF activiteit geassocieerd is met VTE. MP-TF activiteit van niet-behandelde patiënten was significant hoger dan die van gezonde vrijwilligers [17,6 fM FXa / min (IQR 8,6-33,2) versus 4,1 fM FXa / min (IQR 2,3 tot 6,6), P <0,001]. Geen van de patiëntkenmerken (geslacht, leeftijd, ziekte stadium) of laboratoriummetingen (beta-2 microglobuline, albumine, calcium, hemoglobine, bloedplaatjes) bleek gecorreleerd met de MP-TF activiteit.

Voor de start van de behandeling was er geen verschil in MP-TF-activiteit tussen patiënten die tijdens de follow-up wel een VTE ontwikkelden (n = 15) en degenen die geen VTE ontwikkelden (n = 107). Bij 75 patiënten van wie plasma beschikbaar was van voor en na de chemotherapie, daalde de MP-TF-activiteit aanzienlijk na chemotherapie (van 17,4 [10,2-32,8] tot 12,0 [7,0-18,5] fM Xa / min, P = 0,006). Deze daling werd in alle ISS stadia van de ziekte waargenomen. Dit suggereert dat de tumormassa niet met MP-TF activiteit is geassocieerd. De MP-TF activiteit verminderde ook onafhankelijk van het therapeutische regime [vincristine, adriamycine en dexamethason (VAD); thalidomide, adriamycine en dexamethason (TAD); of bortezomib, adriamycine en dexamethason (PAD)]. MP-TF activiteit bleef echter na chemotherapie verhoogd bij patiënten die VTE hadden ontwikkeld (15,1 [10,3-25,2]), in tegenstelling tot patiënten die geen VTE hadden ontwikkeld (11,4 [7,0-25,2], p <0,001).

In toekomstige studies moet MP-TF activiteit vaker gemeten worden tijdens de inductietherapie van MM om te leren of MP-TF activiteit een pathogenetische rol speelt bij het ontstaan van VTE bij MM patiënten.

Discussie

Tot nu toe is er geen consensus over de grootte en het aantal MPs in plasma. Dit komt doordat de in de literatuur gerapporteerde resultaten van MP metingen sterk verschillen. Wij zijn ons ervan bewust dat deze verschillen niet alleen veroorzaakt worden door verschillen tussen de tot dusver gebruikte methoden om MPs te meten. Pre-analytische procedures zoals bloedafname, plasma/MP bereidingen en de opslag van plasma zijn ook belangrijke factoren, die het aantal, de morfologie en andere kenmerken van MPs, zouden kunnen beïnvloeden. Het gebruik van EDTA in plaats van citraat voor de bloedafname kan *in vitro*-activatie van bloedplaatjes en vorming van PMP verminderen (Hoofdstuk 6) en heeft daarom de voorkeur voor de studie van plasma MPs. We hebben ook een aanwijzing dat de hoge-snelheid centrifugatie die gebruikt wordt om de MPs te isoleren geen belangrijk effect heeft op de grootteverdeling van de MPs (Hoofdstuk 5). Uiteindelijk is het belangrijk richtlijnen voor de pre-analytische procedures op te stellen om de intra- en inter-laboratorium reproduceerbaarheid te verbeteren.

In het verleden werden MPs gevonden in het micrometergebied, terwijl we ze nu vinden in het nanometergebied (Hoofdstuk 3, 4, 5 en 6). Dit wordt verklaard door de technische beperkingen van de methoden, die eerder gebruikt werden om MPs te karakteriseren. Bijvoorbeeld, methoden zoals flowcytometrie met een detectiegrens van 0,5 micrometer en conventionele EM waarvoor uitdroging, chemische fixatie en kleuring van monsters nodig is, zijn minder geschikt voor de

detectie en karakterisering van MPs. Verder zijn er geen geschikte referentiematerialen (standaarden) om de instellingen van de verschillende methoden voor de analyse van MPs te kalibreren. Op dit moment maken nieuwe methoden, zoals AFM, NTA, en cryo-EM het mogelijk MPs in het nanometergebied in hun fysiologische toestand te detecteren en te karakteriseren. Maar deze methoden zijn nog niet geschikt voor gebruik in de kliniek omdat ze tijdrovend en arbeidsintensief zijn en nog moeten worden geoptimaliseerd en gevalideerd met betrekking tot hun nauwkeurigheid, specificiteit, detectielimiet en kwantificering, lineariteit en bereik, en robuustheid. Daarvoor zijn verbeteringen nodig zoals bijvoorbeeld geautomatiseerde monsterbehandelingsystemen, gestandaardiseerde reagentia, referentiematerialen voor de kalibratie van apparatuur instellingen en een externe standaard om absolute aantallen MPs te kunnen rapporteren. Uiteindelijk zou een klein MP meetapparaat wenselijk zijn dat slechts gebruik maakt van een speldenprik bloed en voor een routine test resultaten levert in minder dan 30 minuten (lab-on-a-chip).

Er is bewijs dat MP-TF-activiteit is verhoogd bij patiënten met kanker die VTE ontwikkelen (kanker-geassocieerde VTE). Verder onderzoek is nodig om te leren of een verhoogde MP-TF-activiteit bij patiënten met kanker daadwerkelijk de oorzaak is van trombose. Om het onderliggend mechanisme van het verband tussen kanker en trombose te begrijpen, is het bovendien belangrijk om vast te stellen of TF-dragende MPs afkomstig zijn uit de kankercel zelf of niet. In het laatste geval is het belangrijk om de cel van oorsprong (monocyten, endotheelcellen, bloedplaatjes) en het mechanisme waarmee de actieve TF wordt geproduceerd te onderzoeken.

Uiteindelijk is nader onderzoek nodig om te onderzoeken hoe MPs precies worden gevormd. Volgens een algemeen aanvaarde hypothese vormen cellen MPs ten gevolge van het verlies van membraanfosfolipiden-asymmetrie tijdens processen als activering en apoptose, waarbij PS beschikbaar komt op de buitenkant van het celoppervlak. Deze hypothese wordt ondersteund door de zeldzame bloedaandoening, Scott syndroom. Dit syndroom wordt gekenmerkt door een verminderde activiteit van het enzym scramblase hetgeen resulteert in een verminderde expressie van PS en verminderde vorming van MPs. Interessant is dat de aanwezigheid van MPs die geen PS-expressie hebben de hypothese van MP vorming lijkt tegen te spreken. De vraag blijft of het bestaan van PS-negatieve MPs het gevolg is van de beperkingen van de huidige meetmethoden. Annexine V wordt op grote schaal gebruikt voor de meting van PS-expressie in flowcytometrie en capture-gebaseerde testen. Echter, de binding van annexine V aan MPs is afhankelijk van de calciumconcentratie en de PS dichtheid op de membraam. Een andere mogelijke verklaring voor het vinden van PS-negatieve MPs zou kunnen zijn dat ze gevormd worden door fusies van plasmamembraancomponenten met

celresten of kleine uitgescheiden endosomale blaasjes (exosomen). Ook is het mogelijk, dat MPs worden afgestoten door de plasmamembraan ten gevolge van destabilisatie van het actine-cytoskelet via αIIbβ3 signalering, waarvoor geen verlies van membraamfosfolipiden-assymmetrie nodig is.

Tot slot, MPs worden niet langer beschouwd als cellulaire brokstukken of experimentele artefacten. In feite kunnen MPs deelnemen aan processen van stolling, ontstekingen en tumorvorming. Het is van belang om te onderzoeken uit welke cellen MPs worden gevormd, waarom ze worden gevormd en hoe ze met andere cellen in het lichaam communiceren. Standaardisering van pre-analytische en analytische procedures voor de meting van MPs is dringend nodig om hun aanwezigheid in bloed te begrijpen en om hun fysiologische functie en rol in ziektes toe te lichten. De toekomst zal leren of MP metingen gebruikt kunnen worden als diagnostische en misschien voorspellende (bio)marker in verschillende ziekten.

Curriculum vitae

Yuana was born in 1976, in Jakarta, Indonesia. In 1994, she was graduated from Christian I High School in Jakarta. In the same year, she continued her study at the Department of Food Technology in Bogor Agricultural University in Bogor, Indonesia and obtained her Bachelor of Science degree in 1998. In 1999, she started her study at the Department of Pharmacognosy, Institute of Biology at Leiden University in Leiden, The Netherlands and obtained her Master of Science degree in Biodiversity and Natural Products in 2001. From 2003, she was appointed at the Department of Medical Oncology in the Free University Medical Center in Amsterdam, where she worked on a project of circulating endothelial cells as markers for anti-angiogenic therapy. In 2006, she started her PhD thesis on the role of blood microparticles in cancer associated-thrombosis at the Department of Clinical Oncology in Leiden University Medical Center in Leiden under the supervision of Prof. Dr. S. Osanto and Prof. Dr. R.M. Bertina. The research was funded by a grant of the Dutch Cancer Society ("Microparticles, the missing link between Cancer and Thrombosis?") and experiments were conducted in the Einthoven Laboratory for Experimental Vascular Medicine, of the Leiden University Medical Center. Much of the work was done in close collaboration with the Department of Molecular Cell Biology, Section Electron Microscopy, of the Leiden University Medical Center, the Department of Biophysical Structural Chemistry, Leiden Institute for Chemistry and the Leiden Institute of Physics, of the Leiden University. One of her research highlights is the development of a novel method to detect blood microparticles by using atomic force microscopy (supervised by Prof. Dr. T.H. Oosterkamp and her promotores). She received a Young Investigator Award for this work at the 2009 International Society of Thrombosis and Haemostasis (ISTH) congress in Boston. She participated in the ISTH Scientific Subcommittee collaborative workshop on standardization of platelet-derived microparticle enumeration by flow cytometry with calibrated beads.

List of publications

Yuana Y, Kuil ME, Oosterkamp TH, Bertina RM, Osanto S. Atomic force microscopy and the detection of nanosized blood microparticles. In: Nanomedicine and the Cardiovascular System. Science Publishers 2011.

Auwerda JJ, **Yuana Y**, Osanto S, de Maat MP, Sonneveld P, Bertina RM, Leebeek FW. Microparticle-associated tissue factor activity and venous thrombosis in multiple myeloma. Thromb Haemost 2011;105(1):14-20.

Yuana Y, Bertina RM, Osanto S. Pre-analytical and analytical issues in the analysis of blood microparticles. Thromb Haemost 2010;105(3):396-408.

Yuana Y, Oosterkamp TH, Bahatyrova S, Ashcroft B, Garcia RP, Bertina RM, Osanto S. Atomic force microscopy: a novel approach to the detection of nanosized blood microparticles. J Thromb Haemost 2010;8(2):315-23.

Vroling L, **Yuana Y**, Schuurhuis GJ, van Hinsbergh VW, Gundy C, de Haas R, van Cruijsen H, Boven E, Hoekman K, Broxterman HJ. VEGFR2 expressing circulating (progenitor) cell populations in volunteers and cancer patients. Thromb Haemost. 2007;98(2):440-50.

Fontijn D, Duyndam MC, van Berkel MP, **Yuana Y**, Shapiro LH, Pinedo HM, Broxterman HJ, Boven E. CD13/Aminopeptidase N overexpression by basic fibroblast growth factor mediates enhanced invasiveness of 1F6 human melanoma cells. Br J Cancer. 2006;94(11):1627-36.

Hansma AH, Broxterman HJ, van der Horst I, **Yuana Y**, Boven E, Giaccone G, Pinedo HM, Hoekman K. Recombinant human endostatin administered as a 28-day continuous intravenous infusion, followed by daily subcutaneous injections: a phase I and pharmacokinetic study in patients with advanced cancer. Ann Oncol. 2005;16(10):1695-701.

Acknowledgments

The results produced in this thesis are a reflection of a good collaboration between researchers with various expertise. Especially I would like to thank Tjerk Oosterkamp and Svetlana Bahatryrova who guided me through the knowledge of AFM. Also I thank Brian Ashcroft, Maarten van Es, and Frederica Galli who gave their excellent technical support during my research in the laboratory of Leiden Institute of Physics. I would like to thank Jan de Sonneville and Maxim Kuil for their innovative contribution in designing the microfluidic chip. My enthusiastic students, Nicole de Groot and Wendy Damman, I like to thank you both for your assistance in setting up some of the experimental methods used in my project. I thank all the nurses in the Oncology poli, especially Jeanne van Stijn for helping me in patients-related research.

I have enjoyed my time working in the Clinical Oncology Laboratory. The members of the laboratory were always helpful, especially Lien who works behind the scene and keeps the laboratory up and running. I really thank you all for all fun in lab-weekends/outings and talks in coffee/lunch breaks. I thank colleagues in the Einthoven laboratory for their warm welcome when I had to move my research activities from the laboratory on the 5^{th} floor to the 2^{nd} floor. I especially enjoyed the time during meetings and congresses with you all. Patricia, Begum, Bernadine, and Chun Yu, in the last couple years of my project we shared good moments in the office room on the 7^{th} floor and also helped each other in difficult times. Thank you for all fun talks and outings.

Finally, I would like to thank Patricia and Mark to become my paranimfs. Patricia, for all the hard work we did for more than 4 years in this project, I also wish you all the best for pursuing your dream and moving forward in a more challenging career. Mark, 9 years ago I was one of your paranimfs. It is really special to have you sitting now next to me during the defense of my thesis. After this, we and our newly born child, Oliver, will continue our exciting journey together.